

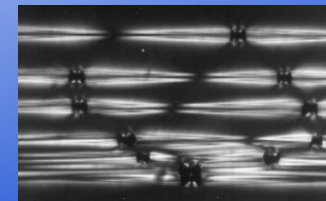
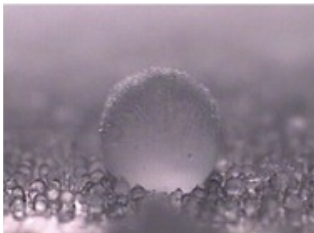
# 주요공학연구 요약

## Interfacial Evaluation of Carbon Based Nano and Micro-Composites using Electro-Micromechanical Tests and their Practical Applications

박 종 만 대표  
(Joung-Man Park)

*PC&IL*

Gyeongsang National University  
Department of Materials Engineering and Convergence  
Technology



# Acknowledgements

❖ **Agency for Defense Development (ADD)** (2012-2014), Korea.



국방과학연구소  
AGENCY FOR DEFENSE DEVELOPMENT

❖ **National Research Foundation (KRF)** (2013-2016) (2016-2022)



한국연구재단  
National Research Foundation of Korea

❖ **Korea Institute of Materials Science (KIMS)** (2012-2014)



재료연구소  
Korea Institute of Materials Science

❖ **Korea Institute for the Advancement of Technology (KIAT)** (2012-2015)



한국산업기술진흥원  
Korea Institute for Advancement of Technology

❖ **Defense Acquisition Program Administration (DAPA)** (2013-2018)



Defense Acquisition  
Program Administration

❖ **Hyundai Automobiles group** (2011-2013)



HYUNDAI

❖ **Doosan Heavy Industries & Construction** (2014-2015)



❖ **TB Carbon** (2012-2015)



티비카본

❖ **Hankuk Carbon** (2014-2015)



한국카본  
HANKUK CARBON

❖ **Dongsung TCS** (2013-2018)



Dongsung  
TCS  
Total Composite  
Solution

❖ **Small & Medium Business Administration** (2016-2017)



중소기업청  
Small & Medium Business  
Administration



송월 테크놀로지

❖ **Korea Institute of Energy Technology Evaluation and Planning** (2017-2019)



한국에너지기술평가원  
KOREA INSTITUTE OF ENERGY TECHNOLOGY  
EVALUATION AND PLANNING



❖ **Korea Aerospace Inc. (KAI)** (2005-2006)

❖ **Dept of Mechanical Engineering, The University of Utah**  
for **Distinguished Professor Lawrence K. DeVries**

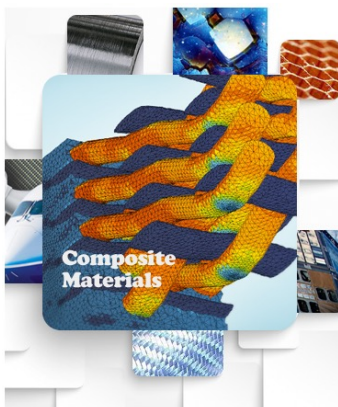


THE  
UNIVERSITY  
OF UTAH





# KSCM (Korea Society of Composite Materials)



The Korean Society for Composite Materials (KSCM), founded in 1988, is a not-for-profit membership organization that has established itself as the primary society in Korea for providing a forum for researchers, educators, manufacturers, engineers and students in the fields of composite materials and structures. KSCM currently has more than 1,700 active members.



2016. 1. 1~2016. 12. 31

Joung-Man Park

- Gyeongsang National University
- Vice President, Korea Society of Adhesion and Interface (KSAI)
- Vice President, SAMPE Korea
- Adjunct Professor, The University of Utah, Dept. of Mechanical Engineering

## ICCE 24 (24<sup>th</sup> International Conference on Composites /Nano-Engineering)



## ACCM 10 (The 10<sup>th</sup> Asian-Australasian Conference on Composites Materials)-550 attended



## Korea-Japan Joint Symposium on Composite Materials



Korean Society for Composite Materials

一般社団法人

日本複合材料学会

Japan Society for Composite Materials

Cooperate

Korea journal

International journal



## 20주년 기념 한국접착및계면학회- 제주학회



‘접착및계면’ KCI 등재지 선정~ 2020년





## 한·중·일·독 SAMPE Korea Forum (2021. 9. 29) 서울양재 AT센타

www.miceforum.co.kr  
www.sampekorea.org

### SAMPE Korea Forum

“한·중·일·독 경량화 기술 고도화 포럼” 2021

**일시**  
2021년 9월 29일(수) 10:30~17:30  
September 29(Wed), 2021

**장소**  
서울 양재 aT센터. 3층 세계모름 III  
Seoul, Korea

**주최** sampe 한국첨단소재기술협회  
SAMPE Korea, 마이스포럼

**후원** KUKINDO, BAE, 한국탄소나노산업협회, 프라운호퍼 ICT 한국분원  
국도화학, 데크카본, 한국탄소나노산업협회, 프라운호퍼 ICT 한국분원

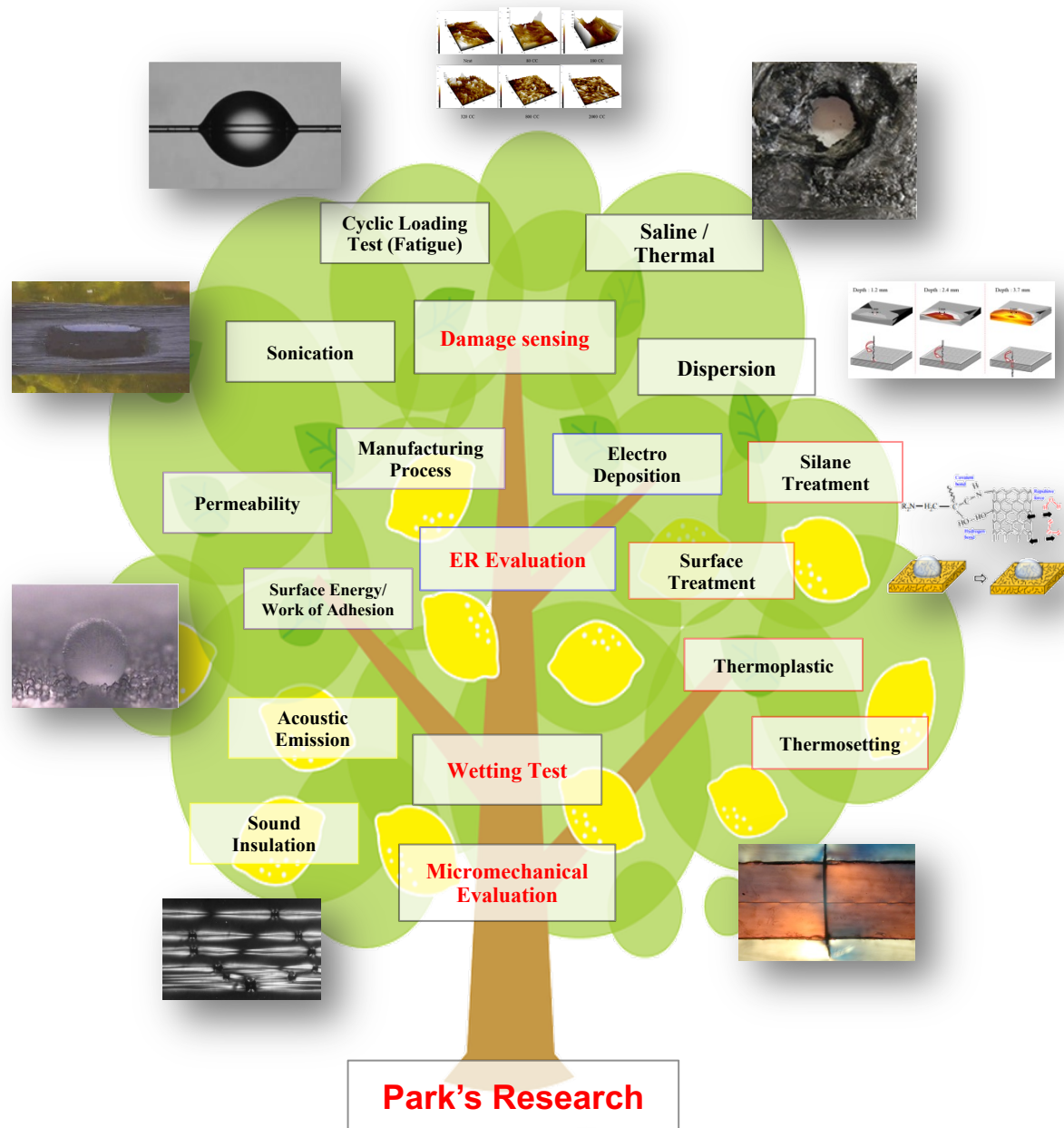
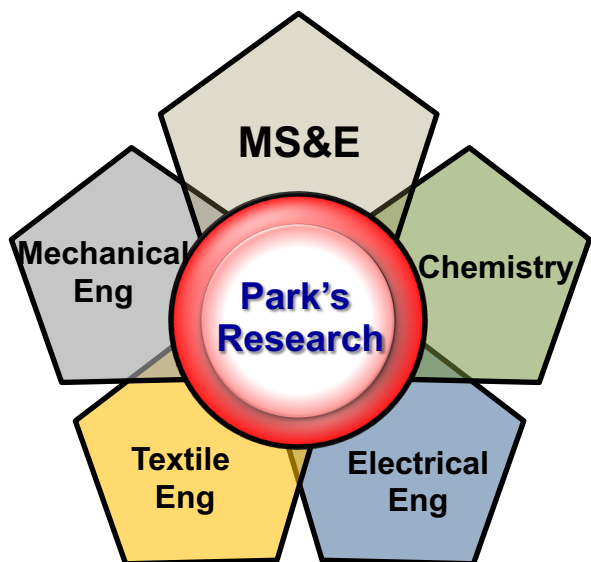


## 한국탄소나노산업협회 (KCANIA) – 한국첨단소재기술협회 (SAMPE Korea) MOU 체결 (2022.11.24)



## International Paper (2018-2022)

1. Innovative Effects on GFRP Inserted Epoxy Adhesives with the Different Thicknesses for Bonding Wind Turbine Blades of Two Parts, *Composites Part B, in review*.
2. Innovative Wicking and Interfacial Evaluation of Carbon Fiber (CF)/Epoxy Composites by CF tow Capillary Glass Tube Method (TCGTM) with Tripe-CF Fragmentation Test, *Composites Science and Technology, in review*.
3. Interfacial, electrical, and mechanical properties of MWCNT in polyurethane nanocomposite coating via 2D electrical resistance mapping for aircraft topcoat, *Progress in Organic Coatings*, Vol. 163, 106667 (2022-02).
4. Evaluation of interfacial, dispersion, and thermal properties of carbon Fiber/ABC added epoxy composites manufactured by VARTM and RFI methods, *Composites Part A*, Vol. 151, 106660 (2021-12).
5. Stretchable calix[4]arene-based gels by induction of water, *Journal of Applied Polymer Science*, Vol. 42, 51235 (2021-11).
6. Optimized epoxy foam interface of CFRP/Epoxy Foam/CFRP sandwich composites for improving compressive and impact properties, *Journal of Materials Research and Technology*, Vol. 11, pp. 62-71 (2021).
7. 2D Electrical Resistance (ER) Mapping to Detect Damage for Carbon Fiber Reinforced Polyamide Composites under Tensile and Flexure Loading, *Composites Science and Technology* (2021-01).
8. Manufacturing and qualitative properties of glass fiber/epoxy composite boards with added air bubbles for airborne and solid-borne sound insulation, *Composites Science and Technology*, Vol. 194, pp. 108166 (2020-07).
9. Evaluation of dispersion of MWCNT/cellulose composites sheet using electrical resistance 3D-mapping for strain sensing, *Functional Composites and Structures*, Vol. 2, pp. 025004 (2020-06).
10. A Review: Mechanical and Interfacial Properties of Composites after Diverse Types of Aging Using Micromechanical Evaluation, *Fibers and Polymers*, Vol.21, pp. 225-237 (2020-02).
11. Thermal transfer, interfacial, and mechanical properties of carbon fiber/polycarbonate-CNT composites using infrared thermography, *Polymer Testing*, Vol. 81, pp. 106247 (2020-01).
12. Interfacial and Mechanical Properties of Carbon Fiber Reinforced Polycarbonate (PC) Film and PC Fiber Impregnated Composites, *Fibers and Polymers* (2019-11).
13. Comparison of interfacial adhesion of hybrid materials of aluminum/carbon fiber reinforced epoxy composites with different surface roughness, *Composites Part B* (2019-08).
14. The evaluation of the interfacial and flame retardant properties of glass fiber/unsaturated polyester composites with ammonium dihydrogen phosphate, *Composites Part B* (2019-06).
15. Improvement of interlaminar properties of carbon fiber-reinforced epoxy composites using aluminum trihydroxide, *Carbon Letters* (2019-04).
16. Evaluation of surface roughness and frost retardancy of a glass fiber/unsaturated polyester composite, *Int'l urnal of Heat and Mass Transfer* (2019-03).
17. Damage sensing, mechanical and interfacial properties of resins suitable for new CFRP rope for elevator applications, *Composites Part B* (2019-01).
18. Advanced interfacial properties of glass fiber/dopamine-epoxy composites using a microdroplet pull-out test and acoustic emission, *Journal of Adhesion* (2019).
19. Evaluation of interfacial and mechanical properties of glass fiber and p-DCPD composites with surface treatment of glass fiber, *Composites Part B* (2018-12).
20. New Evaluation of Interfacial Properties and Damage Sensing on Carbon Fiber Reinforced Composites by VARTM using 3-Dimensional Electrical Resistance Mapping, *Composites Part B* (2018-11).
21. New evaluation of interfacial and mechanical properties of thermallytreated Pine/CFRP composites using electrical resistance measurement, *Composites Part B* (2018-10).
22. Interfacial Properties and Permeability of Three Patterned Glass Fiber/Epoxy Composites by VARTM, *Composites part B* (2018-09).
23. Evaluation of Interfacial and Mechanical Properties of Glass Fiber/Poly-Dicyclopentadiene Composites with Different Post Curing at Ambient and Low Temperatures, *Fibers and Polymers* (2018-09).
24. Investigation of Interfacial and Mechanical Properties of Various Thermally-Recycled Carbon Fibers/Recycled PET Composites, *Fibers and Polymers* (2018-08).
25. Evaluation of thermally-aged carbon fiber/epoxy composites using acoustic emission, electrical resistance and thermogram, *Composite Structures* (2018-07).
26. Interfacial and Wetting Properties between Glass Fiber and Epoxy Resins with Different Pot Lives. *Collides and Surface A* (2018-04).



# Contents

## Introduction:

How Micromechanical Testing Methods can be used for **evaluating the interface** of composite materials?

- Correlation between Micromechanical tests and Macromechanical tests

Part 1: Micromechanical tests & Acoustic Emission (AE)

Part 2: **Interfacial adhesion** with Wettability and Electrical Resistance (ER)

Part 3: Damage sensing of Nanocomposites by ER by **2D & 3D Mapping**

Part 4: **Practical Applications**: Transportation, Aerospace, Defense, Home appliance, Marine etc

Part 5: Recent Works – Aircraft top **coating, deicing** etc



# Introduction & Background

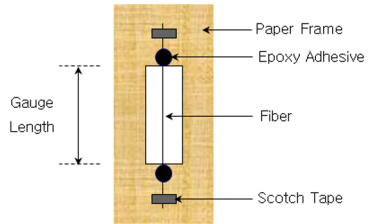
- **What is Micromechanical Testing Methods for interfacial evaluation of composite materials?**
- Any fibers and matrix system can be available for brittle, ductile, thermosetting, thermoplastic, even ceramic matrix under room and high and cryogenic temperatures under short or long terms.
- Fragmentation, microdroplet tests for micro-IFSS *versus* short beam test for macro-ILSS
- NDE using AE by emitting elastic wave coming from damage sources can be combined with micromechanical fragmentation test
- **Damage sensing** using conductive nano-fillers applicable to predict micro-failure of structural composites **by 2D or 3D ER**
- Biodegradable-, high temperature-, high toughness DCPD-, multifunctional-, nano-composites can be applicable for the tests.

# Part 1

## Micromechanical Testing methods & AE with Electrical Resistance (ER)

## ❖ Micro-mechanical test method

### Single-Fiber Tensile Test



❑ Gauge length: 2-100 mm

❑ Test speed: 0.5 mm/min

❑ Strength distribution depends on fiber volume

$$P(\sigma) = 1 - \exp \left[ -\frac{V}{V_o} \left( \frac{\sigma}{\alpha} \right)^\beta \right]$$

❑ Strength distribution depends on fiber length

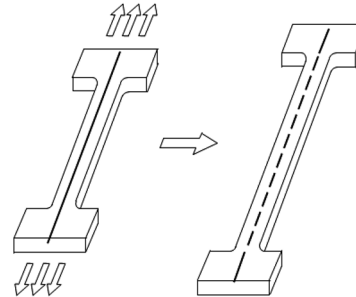
$$P(\sigma) = 1 - \exp \left[ -\frac{l}{l_o} \left( \frac{\sigma}{\alpha} \right)^\beta \right]$$

❑ Strength distribution depends on fiber length and fiber diameter

$$P(\sigma) = 1 - \exp \left[ -\frac{l}{l_o} \left( \frac{d}{d_o} \right)^\gamma \left( \frac{\sigma}{\alpha} \right)^\beta \right]$$

$V_o$ : reference volume  
 $V$ : fiber volume  
 $L_o$ : reference length  
 $\alpha$ : scale parameter  
 $\beta$ : shape parameter

### Interfacial Shear Strength (IFSS)



### Single Fiber Composite (SFC) Test

❑ Kelly - Tyson equation

$$\tau = \frac{\sigma_f \cdot d}{2l_c} \quad \left\{ \begin{array}{l} d: \text{Fiber diameter} \\ \sigma_f: \text{Fiber tensile strength at the critical fragment length, } l_c \end{array} \right\}$$

❑ Drzal equation

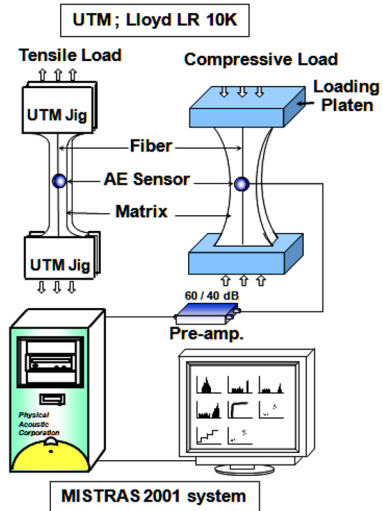
$$\tau = \frac{\sigma_f}{2\alpha} \cdot \Gamma(1 - 1/\beta)$$

$\Gamma$ : Gamma function  
 $\alpha, \beta$ : Scale and shape parameter of the Weibull distribution for the aspect ratio

❑ Weakest link rule

$$\frac{\sigma_f}{\sigma_0} = \left( \frac{l_c}{l_0} \right)^{1/\rho} \quad \left\{ \begin{array}{l} \sigma_0: \text{Fiber strength at gauge length, } l_c \\ \beta: \text{Shape parameter for fiber strength} \end{array} \right\}$$

### Acoustic Emission



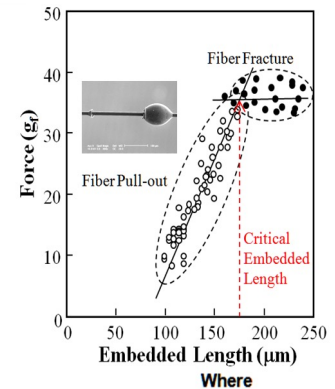
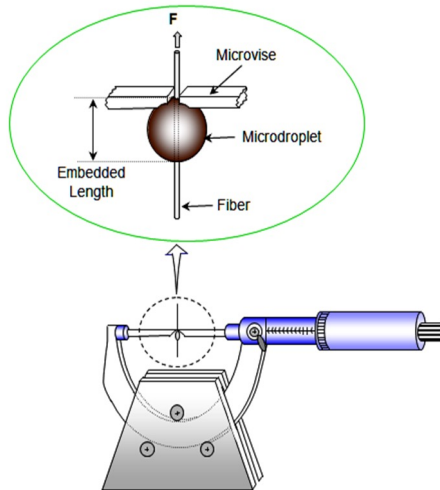
❑ MISTRAS 2001 System

- R15 sensor (Resonance type: 50-200 kHz)
- Pre-amplifier : 40, 60 dB
- Threshold : 35 dB

❑ UTM (Lloyd Ltd. LR 10K) System

- Load Cell : 10 kN
- Test speed : 0.5 mm/min.
- Tensile/Compressive load

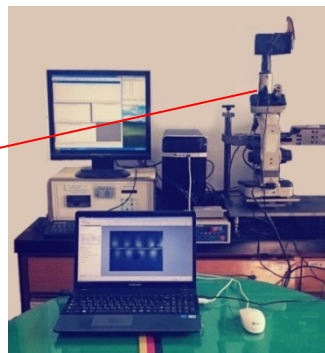
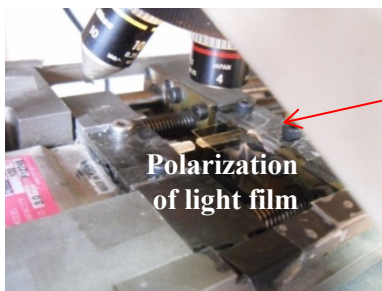
### Microdroplet Test



$$\tau_s = \frac{F_d}{\pi D_f L} \quad \left\{ \begin{array}{l} F_d: \text{Pull-out force} \\ D_f: \text{Fiber diameter} \\ L: \text{Embedded length} \end{array} \right\}$$

# IFSS tests (Microdroplet, Pullout/Fragmentation tests)

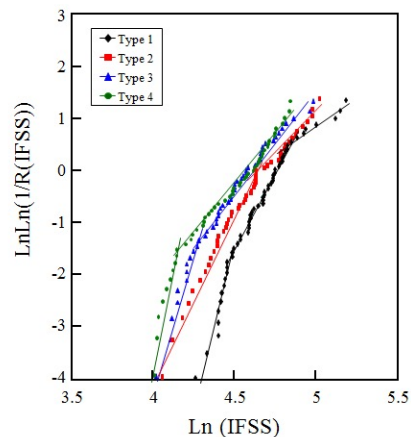
Fragmentation test



Observance real time



Polarized photos

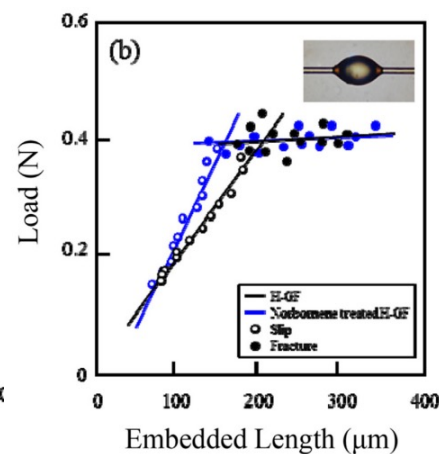
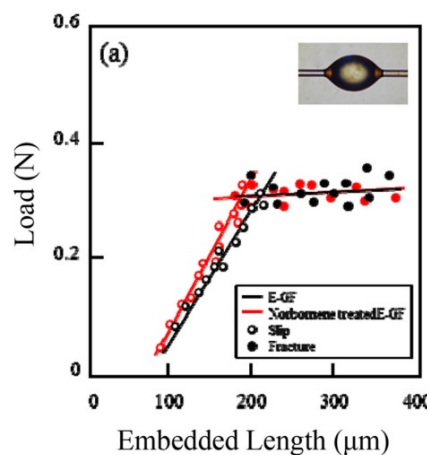


Weibull weakest link rule

$$\sigma_f = \sigma_0 \left( \frac{l_c}{l_0} \right)^{-\frac{1}{p}}$$

Drzal's equation (IFSS)

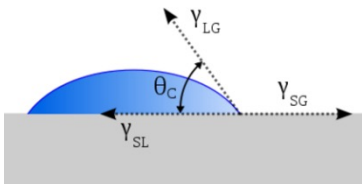
$$\tau = \frac{\sigma_f}{2\alpha} \Gamma \left[ 1 - \frac{1}{\beta} \right]$$



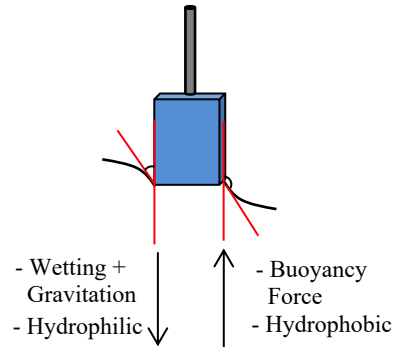
## ❖ Wetting test method

### Static/dynamic contact angles

-Static contact angle-



-Dynamic contact angle-



### Work of adhesion

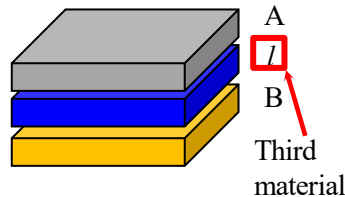
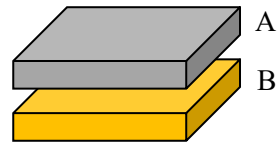
-Owens and Wendt equation-

$$W_a = 2(\gamma_A^d \gamma_B^d)^{1/2} + (\gamma_A^p \gamma_B^p)^{1/2}$$



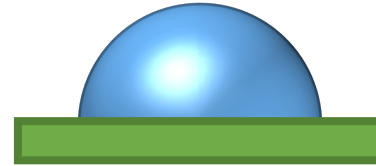
-Third material present-

$$W_a^l = \{\gamma_l - (\gamma_A^d \gamma_l^d)^{1/2} - (\gamma_A^p \gamma_l^p)^{1/2} - (\gamma_B^d \gamma_l^d)^{1/2} - (\gamma_B^p \gamma_l^p)^{1/2} + (\gamma_A^d \gamma_B^d)^{1/2} + (\gamma_A^p \gamma_B^p)^{1/2}\}$$



### Modeling of wetting equation

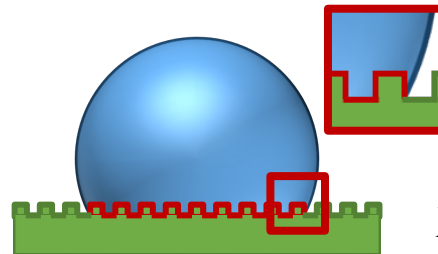
-Young's equation-



$$\gamma_{SG} = \gamma_{SL} + \gamma_{LG} \cdot \cos \theta$$

$\gamma$  are the surface tension coefficients of solid-gas (SG), solid-liquid (SL) and liquid-gas (LG) interfaces.

-Wenzel's equation (Advancing CA < 150°)-

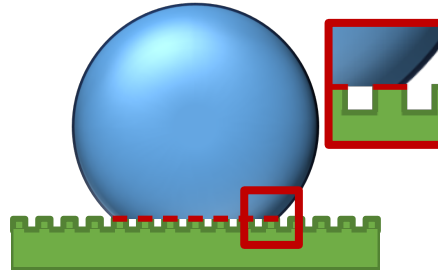


$$\cos \theta = r_w \cdot \cos(\theta_Y)$$

$$r_w = \frac{A_{CSA}}{A_{Proj}}$$

$\cos(\theta_A)$  is an apparent contact angle.  
 $r$  is proportional to the extension of surface area  
 $A_{CSA}$  is the contact surface.  
 $A_{proj}$  is the horizontal projection.

-Cassie-Baxter's equation (Advancing CA > 150°)-



$$\cos \theta_C = r_w f_{SL} \cos \theta_Y - 1 + f_{SL}$$

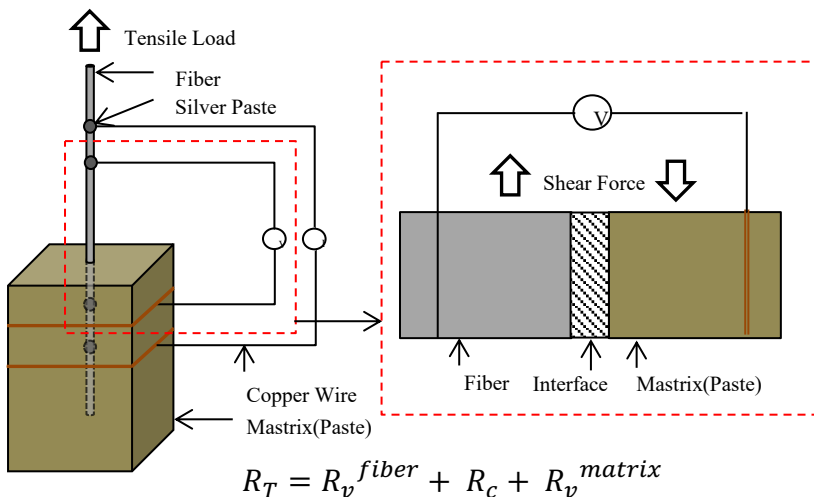
$f_{SL}$  is the fraction of the solid surface in contact with the liquid.

## ❖ Electro-mechanical test method

## ❖ What is acoustic emission (AE)?

### Electro-pullout test

*"Contact Resistance"*

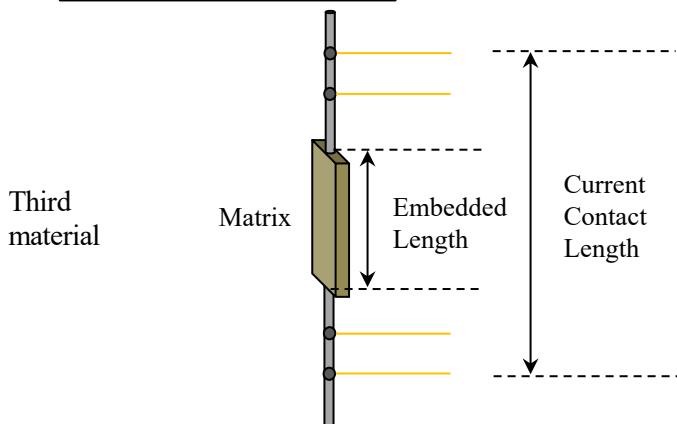


$R_v^{fiber}$  is negligible to be conductive fiber.

$R_v^{matrix}$  is also negligible to be small in volume resistivity.

### Cyclic loading test

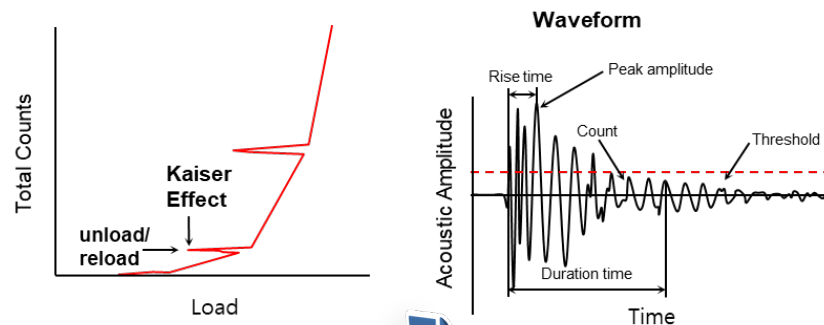
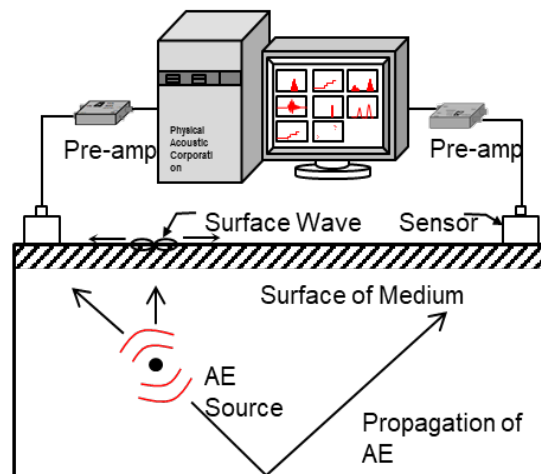
*"Interface effect"*



### Kaiser Effect

If the effect is present, there is an absence of detectable AE until previously applied stress levels are exceeded.

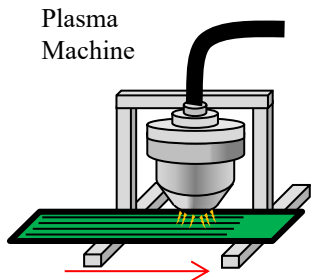
Propagation and Receiving AE waveforms



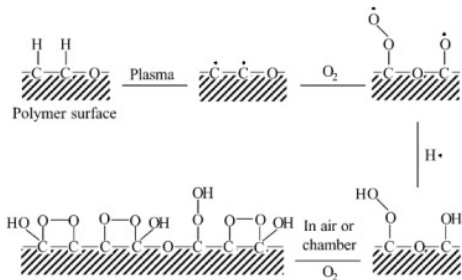


## ❖ Treatment/Dispersion methods

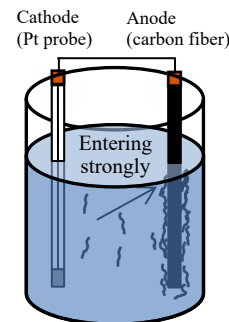
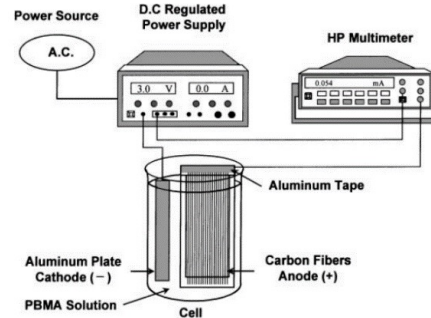
## Plasma treatment








*'Surface functional Introduction'*



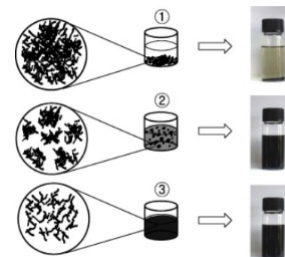
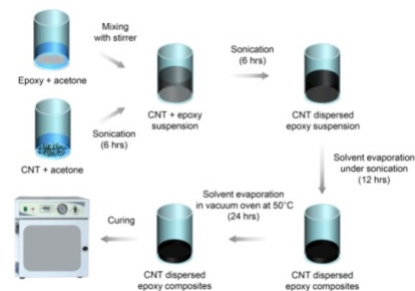
## Electrodeposition



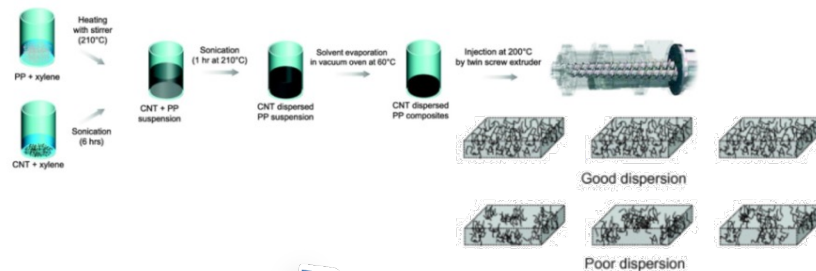
## Dispersion Equipment

Type	Product name (Model name)	Company	Picture	Feature
1	<b>Ultrasonic homogenizer</b> (UP200S)	Hielscher, Germany		24kHz Amplitude adjustable : 20~100% pulse adjustable : 0~100% Processing capability : 0.1~2000ml
2	<b>Ultrasonic processors, Vibra-Cell™</b> (VC 505)	Sonics & Materials, U.S.		20kHz Processing capability : 10~250ml
3	<b>T.K. Homo mixer mark II</b> (model 2.5)	Primix, Japan		500~12000RPM Maximum viscosity : 70Pa·S Processing capability : 3000ml
4	<b>Thinky mixer</b> (ARM-310)	Thinky, U.S.		Fixed : 2000RPM Step : 200~2000RPM Processing capability : 250ml · 250g (net) 250ml · 310g (gross)
5	<b>Overhead Stirrer</b> (HT 120T)	Daihan scientific Co. Ltd, Korea		50~1000RPM Maximum viscosity : 150Pa·s Processing capability : 60,000ml

## Sonication



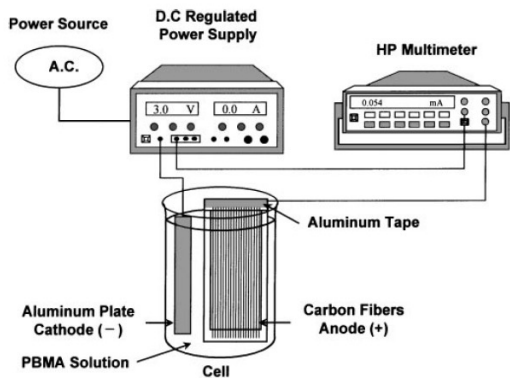
## Extrude



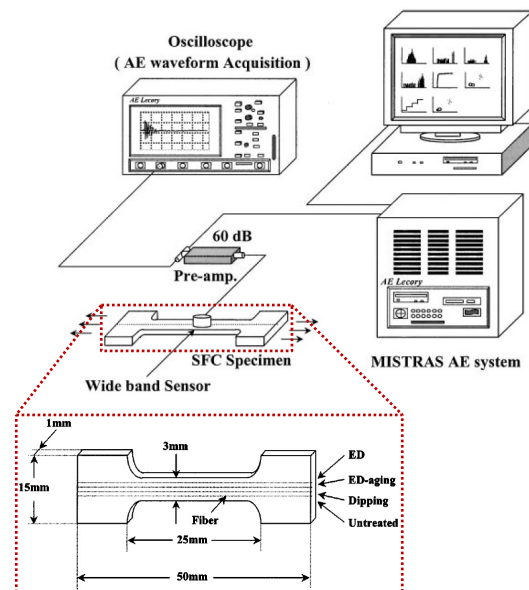
Cited 43th

Journal of Colloid and Interface Science 231, 114-128 (2000)

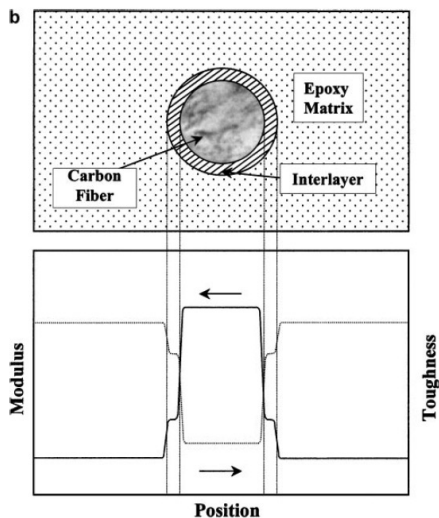
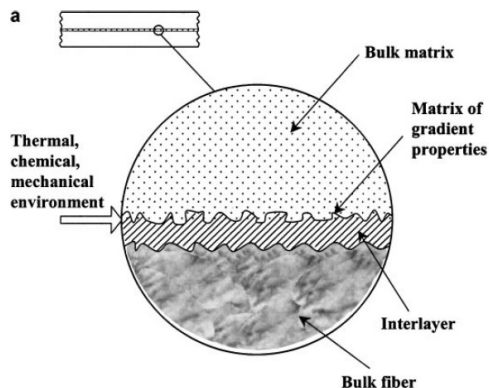
Interfacial Aspects of Electrodeposited Carbon Fiber-Reinforced Epoxy Composites Using Monomeric and Polymeric Coupling Agents



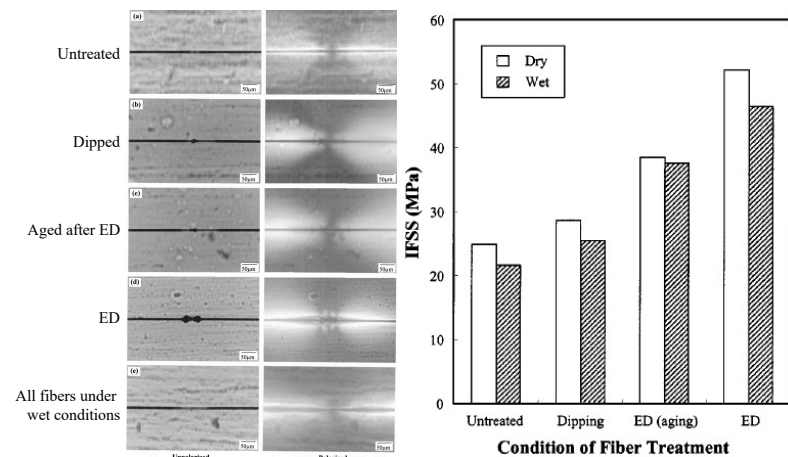
Schematic diagram of the ED system.



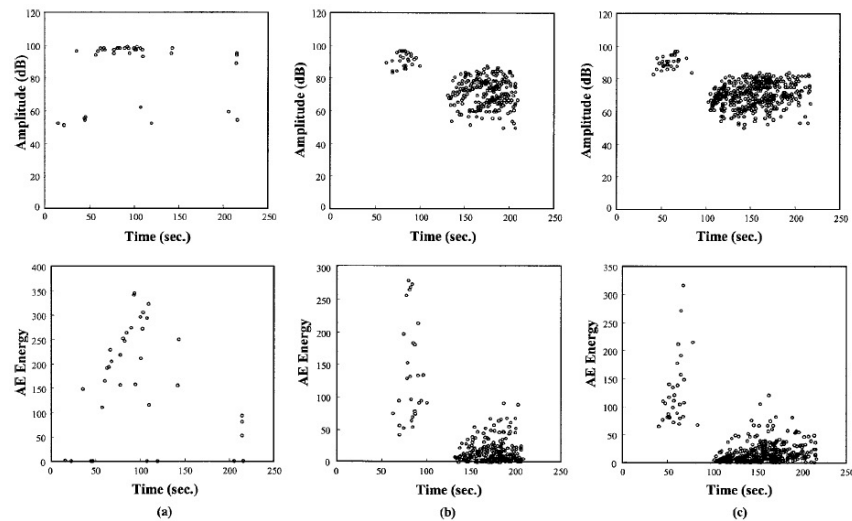
Schematic illustration of the AE system and SFC specimen.



Schematic illustrations showing (a) the longitudinal shape of the two-dimensional interphases between fiber and matrix, and (b) the cross-sectional region of the modulus and toughness of the components versus position.



Comparison of IFSS depending on various surface treatment methods under dry and wet conditions.

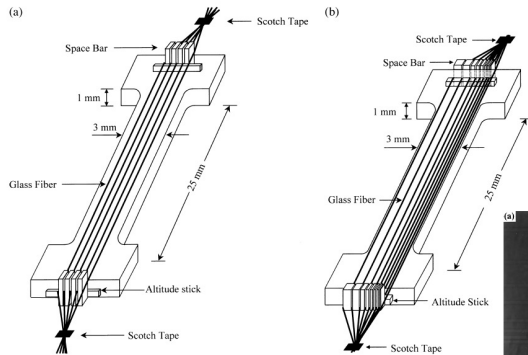


(top) AE amplitude and (bottom) AE energy as a function of measuring time for single-carbon fiber-embedded specimens: (a) untreated, (b) dipped, and (c) ED treated.

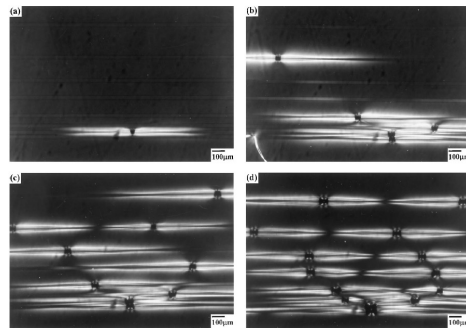
**Cited 32th**

**Composites Science and Technology 60, 439-450 (2000)**

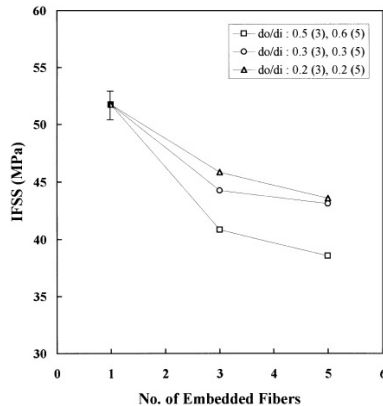
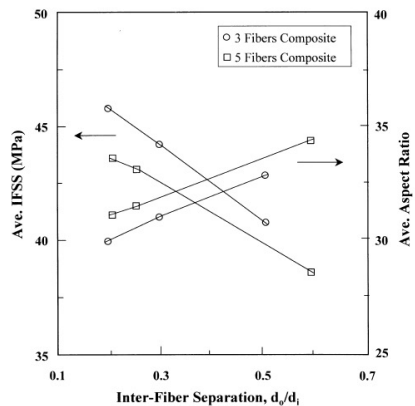
A new method of evaluating the interfacial properties of composites by means of the gradual multi-fiber fragmentation test



Schematic illustration showing the fiber arrangement and the inter-fiber separation in two-typed composites: (a) the regular multi-fiber composite; and (b) the gradual multi-fiber composite.

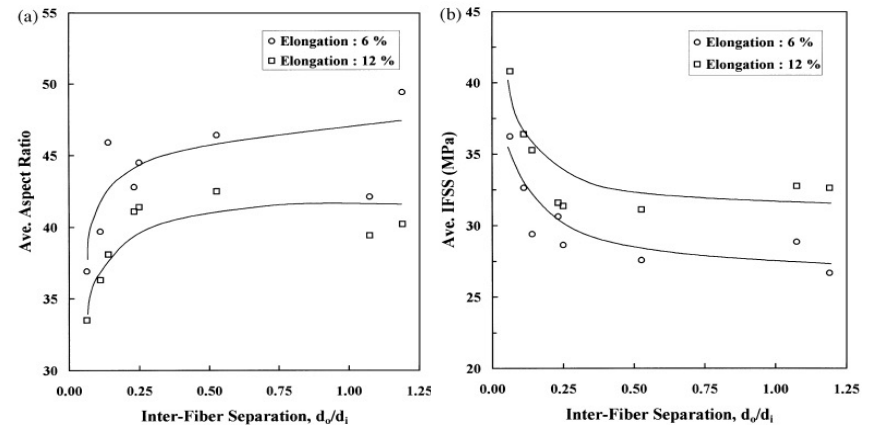


A series of photographs with increasing of the tensile strain: (a) 1% strain; (b) 4% strain; (c) 6% strain; (d) 10% strain.

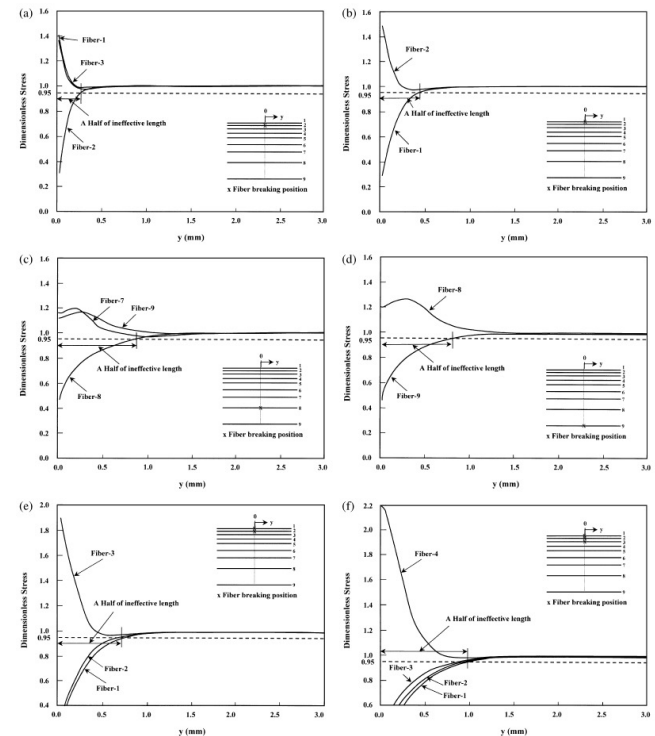


Effect of the inter-fiber separation on the average aspect ratio and IFSS in the regular three- and five-fiber composites.

IFSS as a function of the number of embedded fibers in the single-fiber and the regular multi-fiber composites.



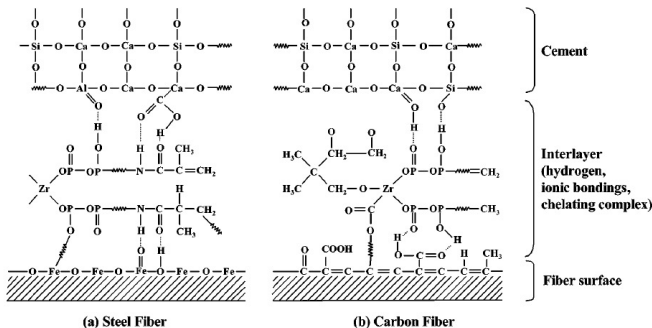
(a) The average aspect ratio and (b) IFSS as a function of the reciprocal of the inter-fiber separation at 6% and 12% elongation.



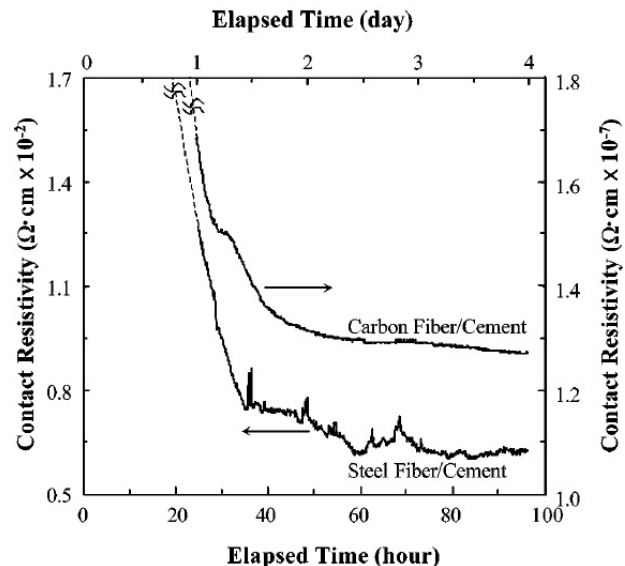
Fiber stress distributions around fiber breakage(s): (a) fiber-2 broken; (b) fiber-1 broken; (c) fiber-8 broken; (d) fiber-9 broken; (e) fiber-1 and -2 broken; (f) fiber-1, -2 and -3 broken.

Cited 11th

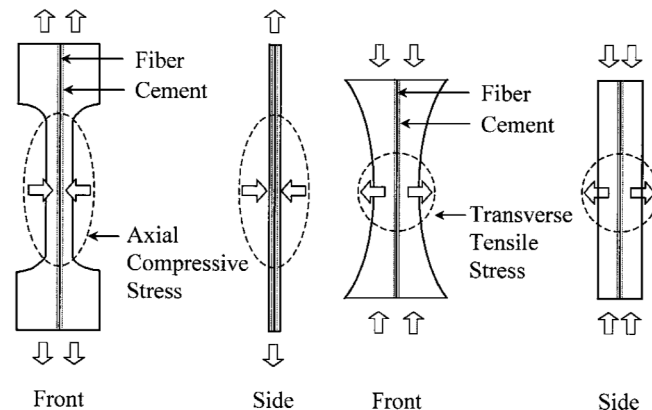
**Journal of Colloid and Interface Science 244, 410–422 (2001)**  
Interfacial and Microfailure Evaluation of Modified Single Fiber–  
Brittle Cement Matrix Composites Using an Electro Micromechanical  
Technique and Acoustic Emission



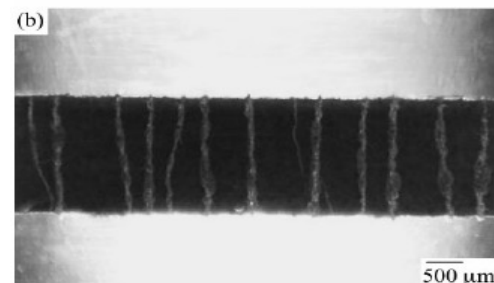
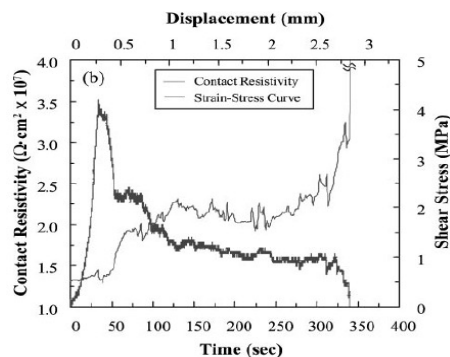
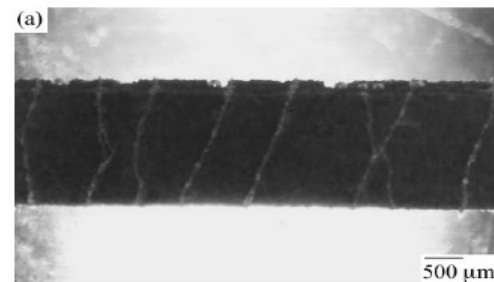
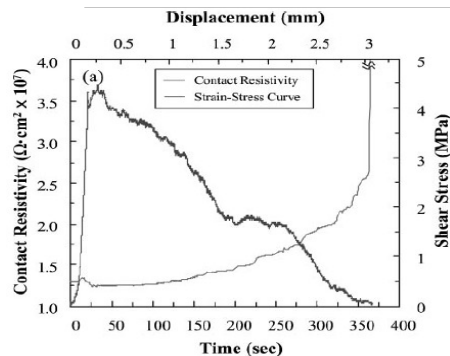
Possible schemes for chemical reaction among (a) steel and (b) carbon fibers, Zr-coupling agent, and cement matrix



The contact resistivity behavior for the untreated steel or carbon fiber/cement composites with elapsed time.



Schematic diagram for the stress transfer mechanisms depending on the applying load direction in DMC specimens



The contact resistivity and shear stress as a function of total measuring time and displacement

(a) no-fiber specimen and single glass fiber/cement composites under  
(b) tensile

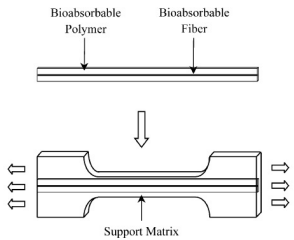




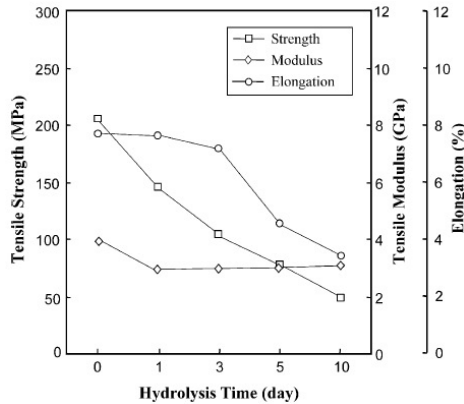
**Cited 49th**

**Composites Science and Technology 63, 403-419 (2003)**

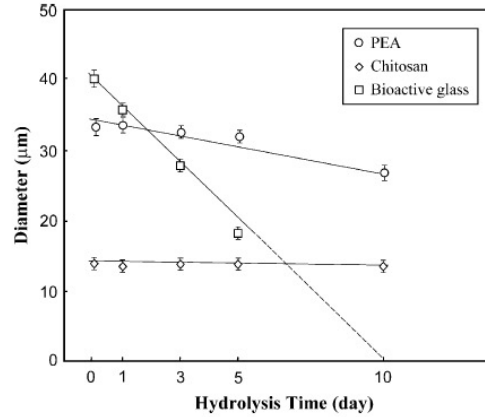
Interfacial properties and microfailure degradation mechanisms of bioabsorbable fibers/poly-L-lactide composites using micromechanical test and nondestructive acoustic emission



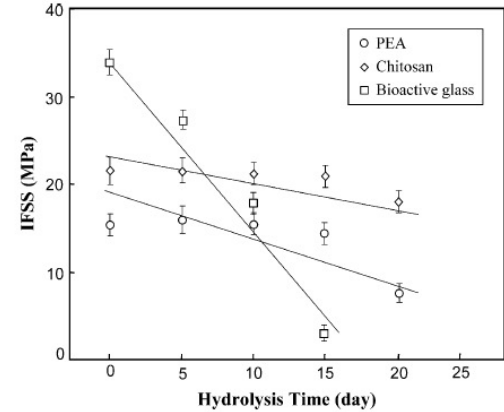
Scheme of DMC test.



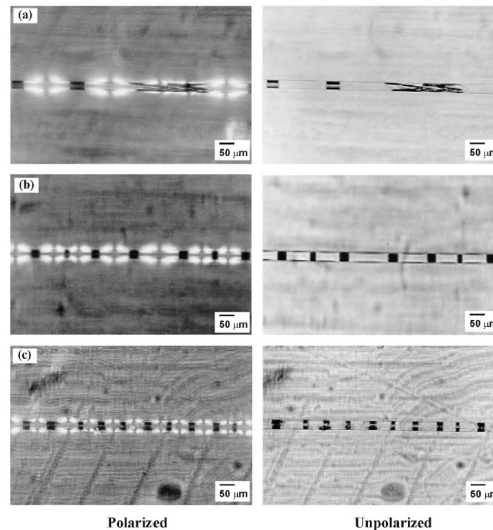
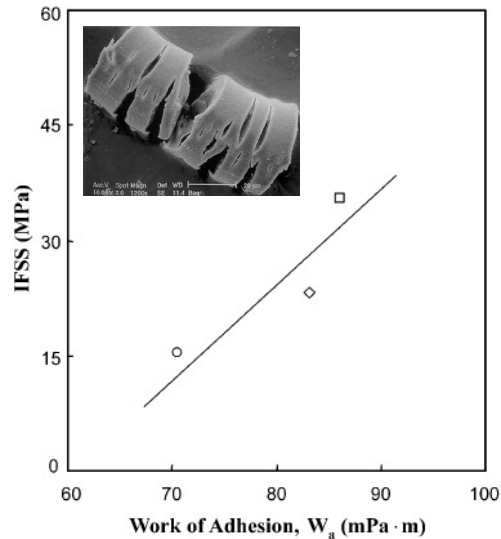
Mechanical properties for PEA fiber with hydrolysis time



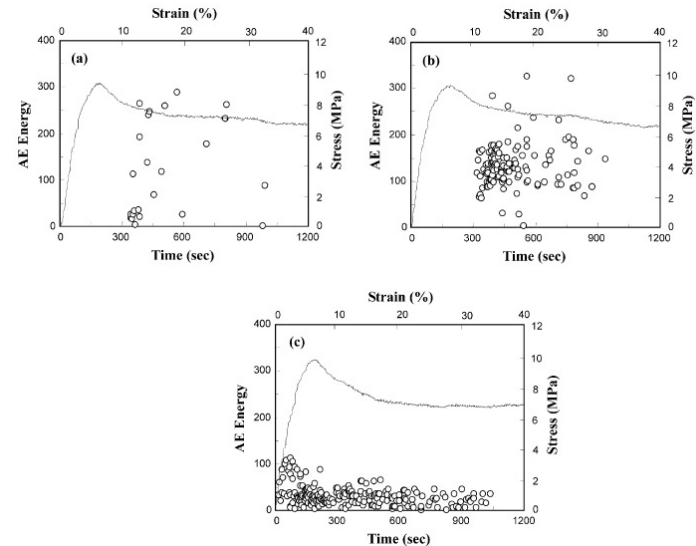
Change of diameter for bioabsorbable fibers with hydrolysis time



Change of IFSS of bioabsorbable fiber/PLLA composites with hydrolysis time



Microfailure modes of PEA fiber with hydrolysis time: in (a) the initial state, (b) after 5 days, and (c) after 10 days



AE energy of PEA fiber with hydrolysis time: (a) the initial state, (b) after 5 days, and (c) after 10 days



Cited 276th

Composites Science and Technology 66, 2686–2699 (2006)

Interfacial evaluation of modified Jute and Hemp fibers/polypropylene (PP)-maleic anhydride polypropylene copolymers (PP-MAPP) composites using micromechanical technique and nondestructive acoustic emission

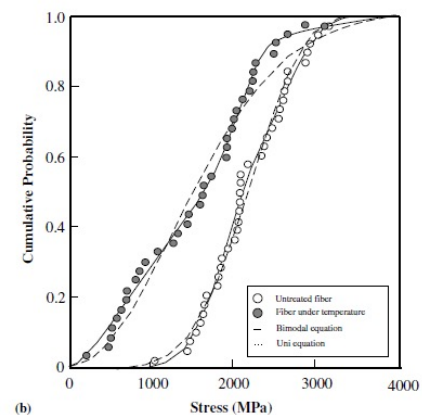
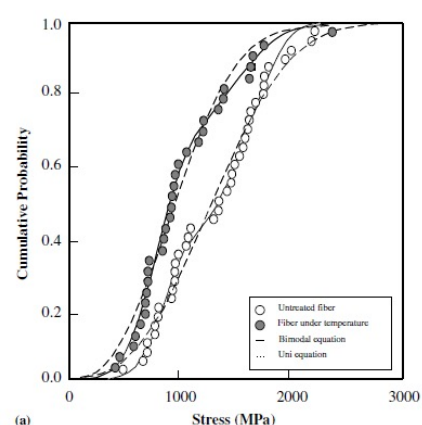
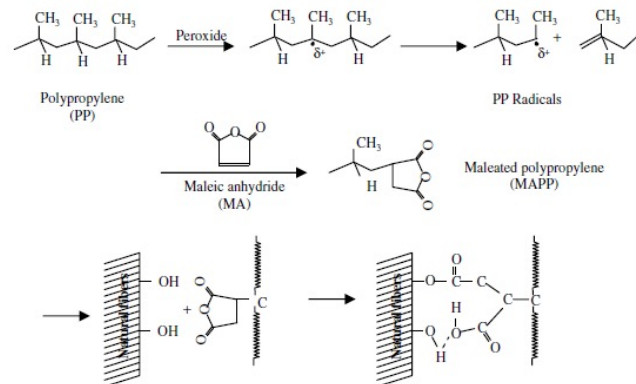


Fig. 3. Uni- and bimodal Weibull distributions of (a) Jute fiber and (b) Hemp fiber.

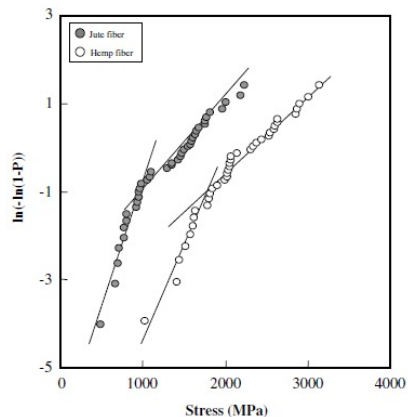


Fig. 4. Strength distribution of Jute and Hemp fibers at gauge length of 20 mm by two-parameter Weibull distribution equation.

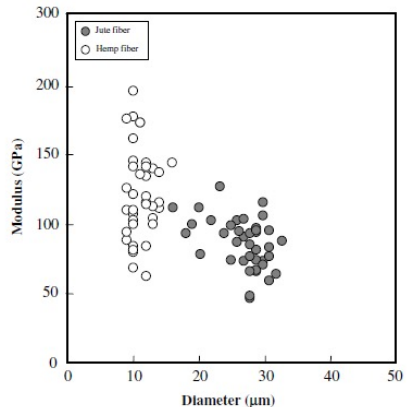


Fig. 5. The scattering of modulus with different diameters of Jute and Hemp fibers.

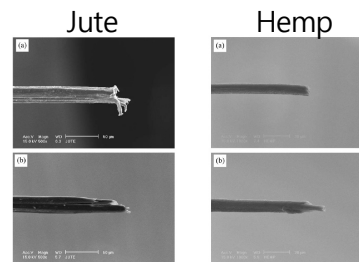
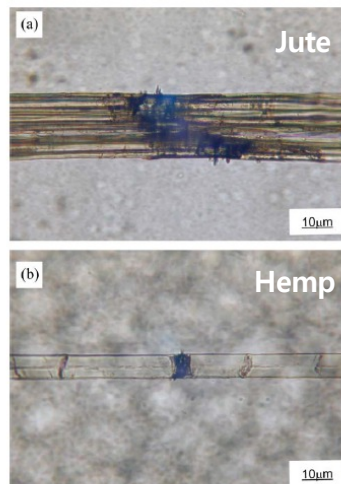


Fig. 16. Microfracture modes of neat single Jute fiber under tension for (a) high strength portion, and (b) low strength portion.

Fig. 17. Microfracture modes of neat single Hemp fiber under tension for (a) high strength portion, and (b) low strength portion.

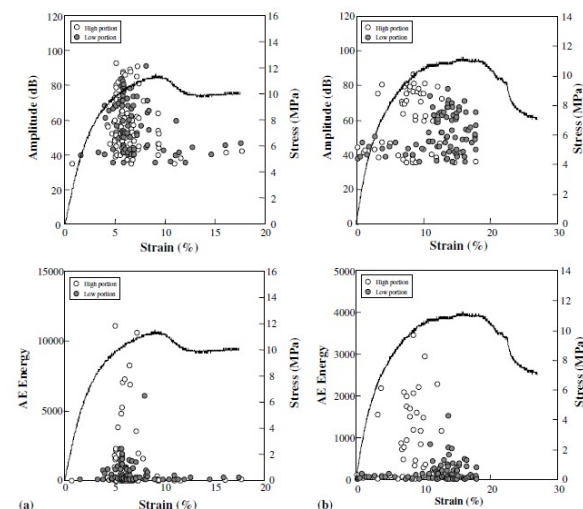


Fig. 18. AE amplitude and AE energy of single natural fibers/PP composites for (a) Jute fiber; and (b) Hemp fiber.

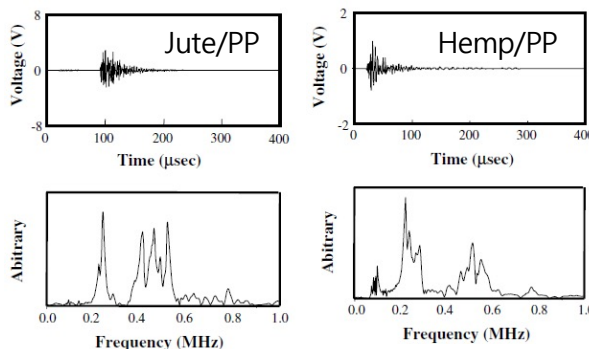


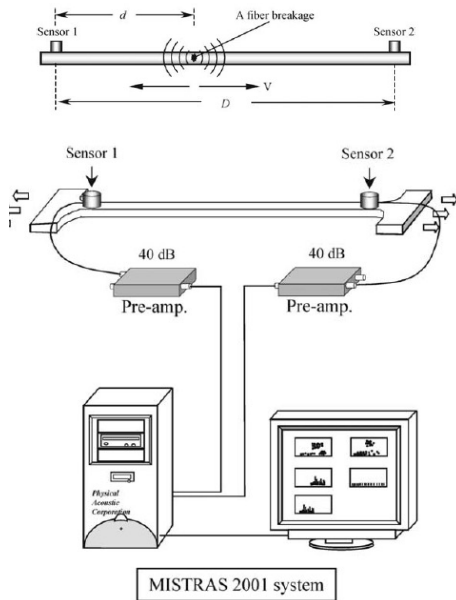
Fig. 16. Microfracture modes of neat single Jute fiber under tension for (a) high strength portion, and (b) low strength portion.

Fig. 17. Microfracture modes of neat single Hemp fiber under tension for (a) high strength portion, and (b) low strength portion.

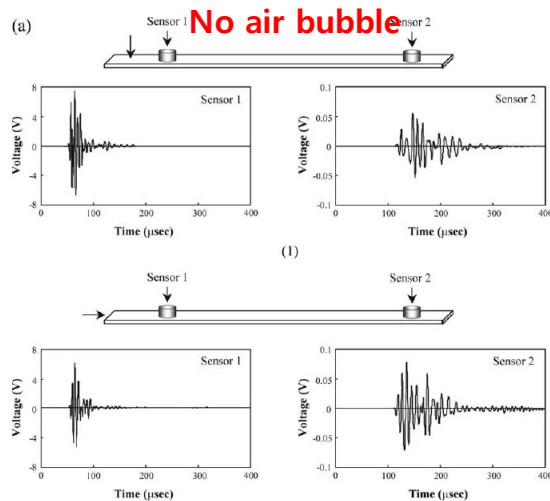
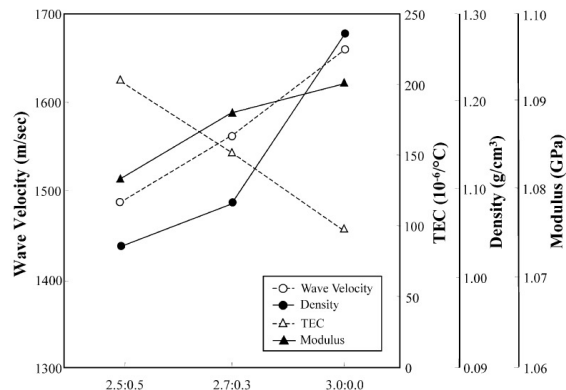
**Cited 49th**

**Composites Science and Technology 64, 983–999 (2004)**

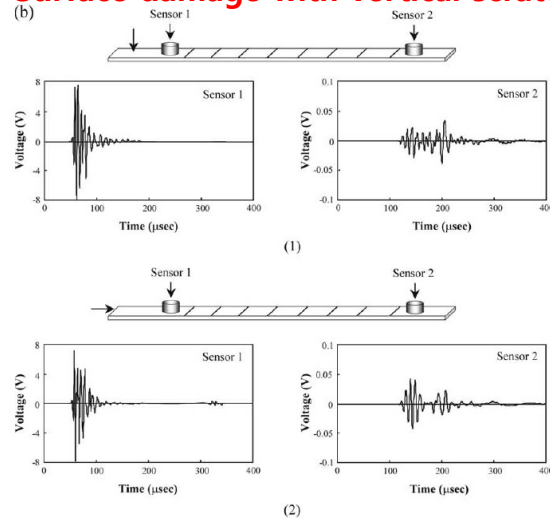
Interfacial properties and microfailure degradation mechanisms of bioabsorbable fibers/poly-l-lactide composites using micromechanical test and nondestructive acoustic emission



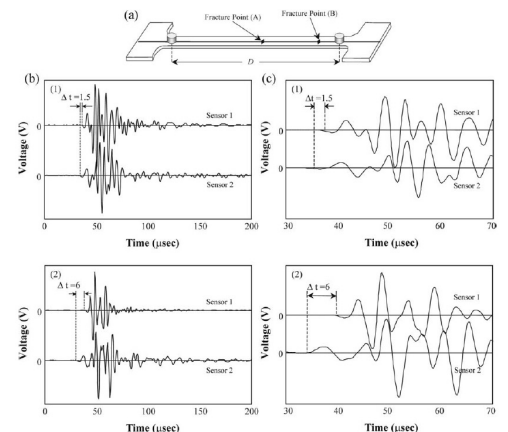
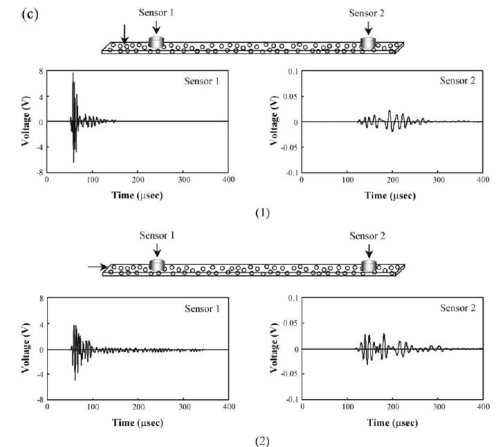
Source location test of carbon fiber/epoxy composite



Surface damage with vertical scratch



Internal damage with air bubble



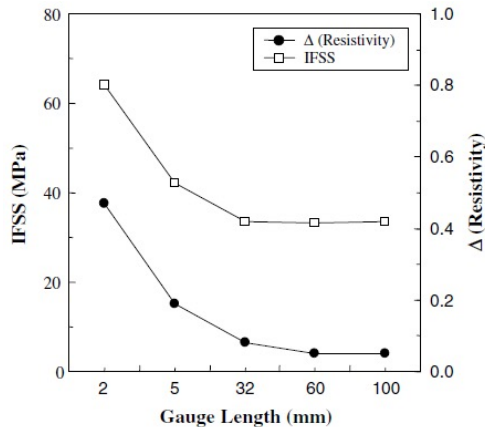
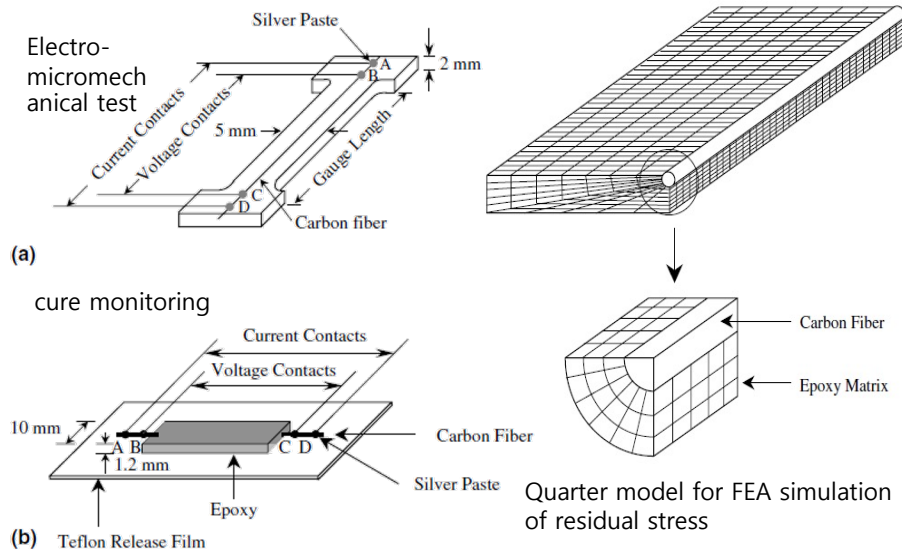
(a) SFC specimen, (b) waveforms of two fractured points, and (c) magnified waveform (D400:D2000=2.5:0.5).



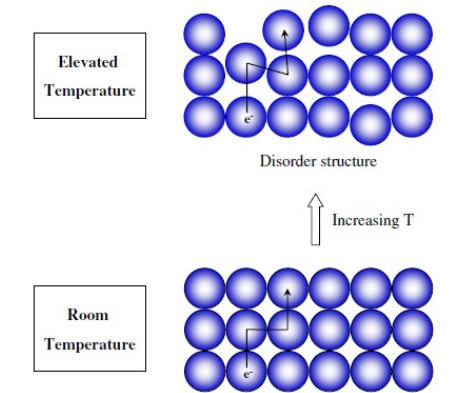
**Cited 59th**

**Composites Science and Technology 65, 571-580 (2005)**

Cure monitoring and residual stress sensing of single-carbon fiber reinforced epoxy composites using electrical resistivity measurement

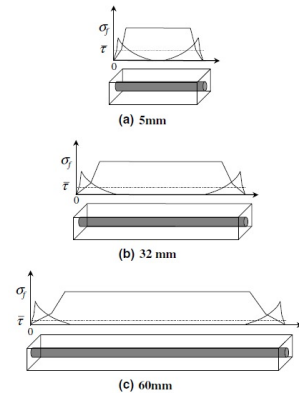


Difference in ER before and after curing and IFSS depending on the gauge length

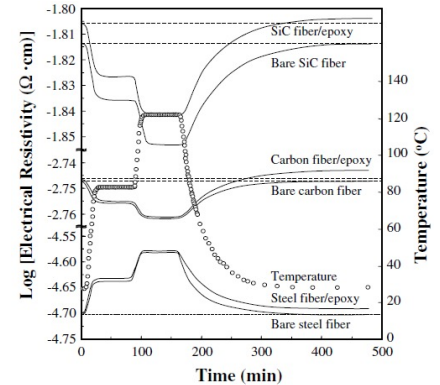


fine molecular structure in the steel fiber

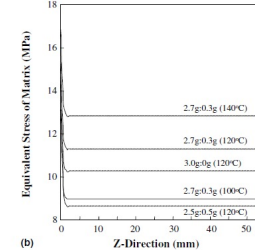
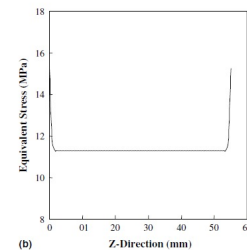
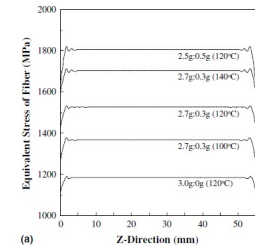
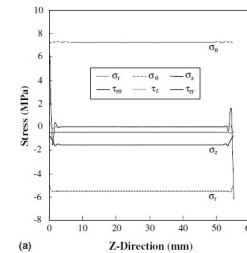
*"Residual stress between fiber and matrix"*



Fiber strength and average IFSS depending on the gauge length in SFC



Electrical resistivity as curing temperature

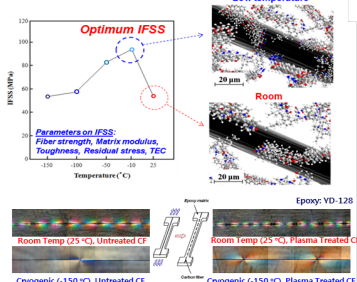
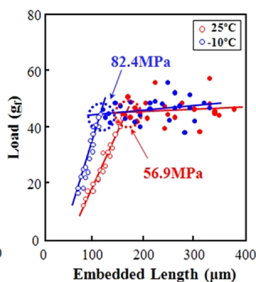
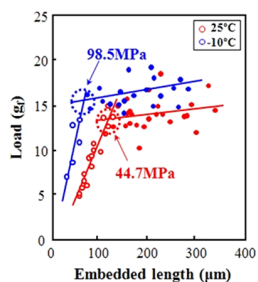
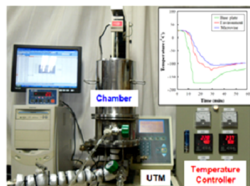


Equivalent residual stress by von Mises criterion depending on the curing conditions: (a) fiber; (b) matrix

**Cited 56th**

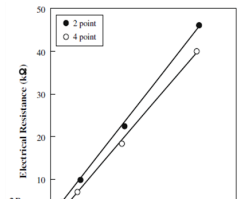
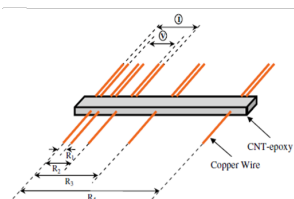
**Composites Part A 70, 1722–1731 (2009)**

Interfacial and hydrophobic evaluation of glass fiber/CNT–epoxy nanocomposites using electro-micromechanical technique and wettability test



Interfacial and micro-mechanical test at low temperature and cryogenic condition (-30°C ~ -150°C)

### ❖ Electric Micro-Mechanical test using ER

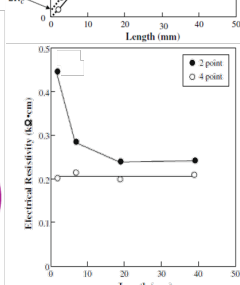
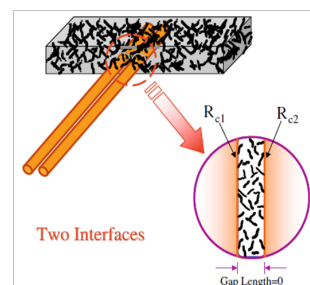


*Composites: Part A, 40(11), pp. 1722 (2009)*

Schematic diagram of specimen for electrical measurement:

(a) CNT–epoxy gradient specimen

(b) Two interfaces between two copper wires and CNT–epoxy



### ❖ Micro-mechanical test method

#### Dynamic Contact Angle Measurement

□ Wilhelmy plate technique

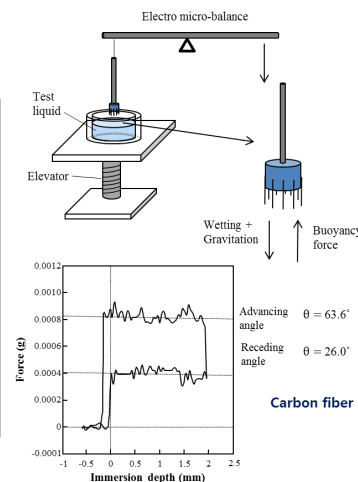
$$F = mg + P'_{LV} \cos \theta - F_b$$

□ Donor-acceptor surface free energy

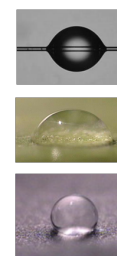
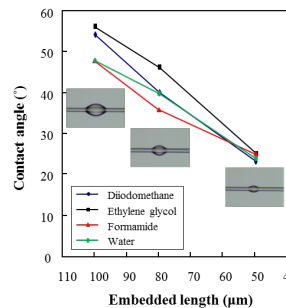
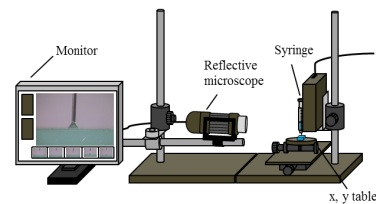
$$\frac{\gamma_1 (1 + \cos \theta) - 2(\gamma_1^{LV} \gamma_2^{LV})^{1/2}}{2\gamma_1^{LV}} = \sqrt{\gamma_s^+} \sqrt{\frac{\gamma_1^-}{\gamma_1^+}} + \sqrt{\gamma_s^-}$$

□ Work of adhesion

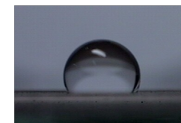
$$W_a = 2[(\gamma_m^{LV} \gamma_f^{LV})^{1/2} + (\gamma_f^+ \gamma_m^-)^{1/2} + (\gamma_f^- \gamma_m^+)^{1/2}]$$



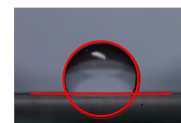
### Static contact angle



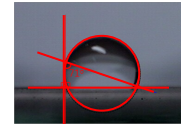
Step 1



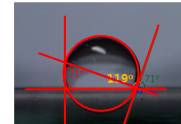
Step 2



Step 3



Step 4

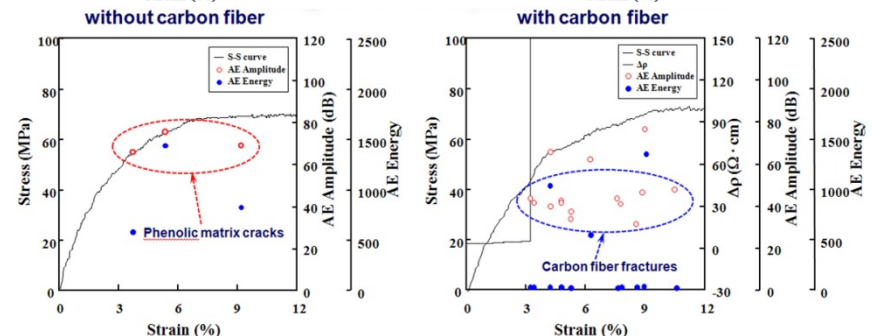
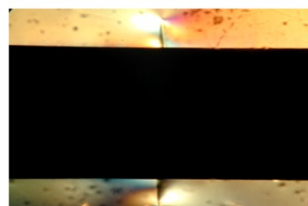
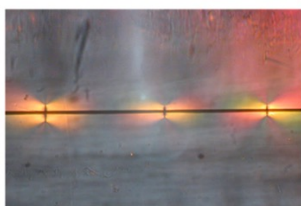
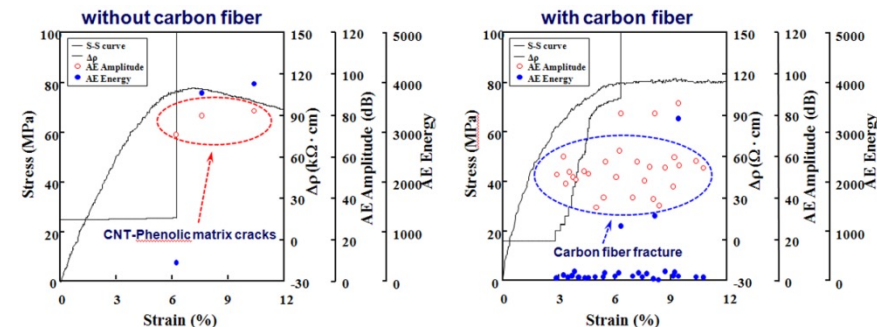
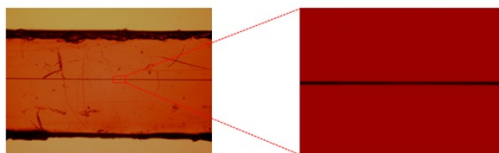
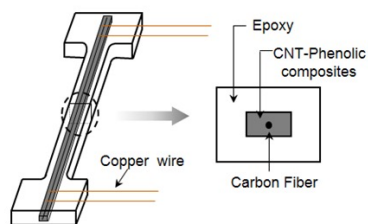
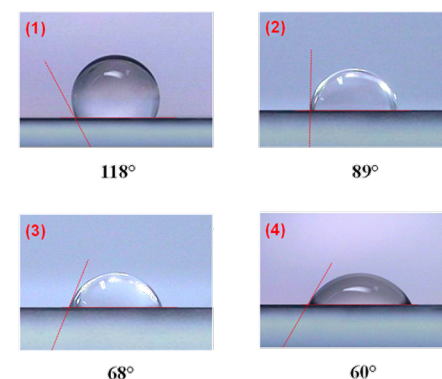
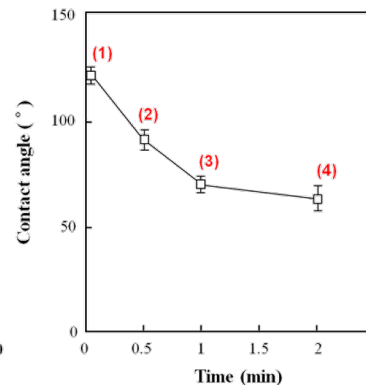
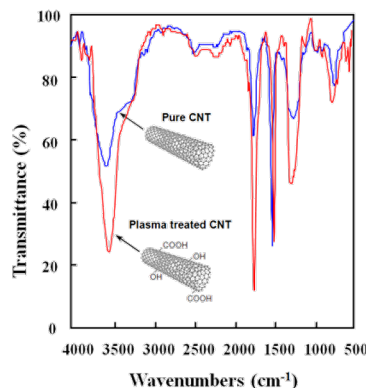
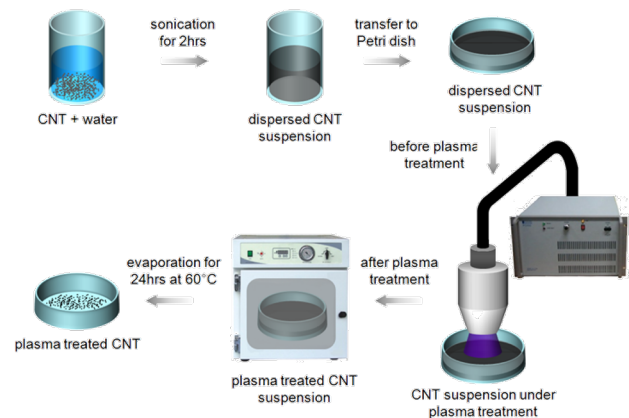




**Cited 19th**

**Composites: Part A 52, 151–158 (2013)**

Evaluation of interfacial properties of atmospheric pressure plasma-treated CNT-phenolic composites by dual matrix fragmentation and acoustic emission tests



Carbon fiber cracks inside phenolic matrix

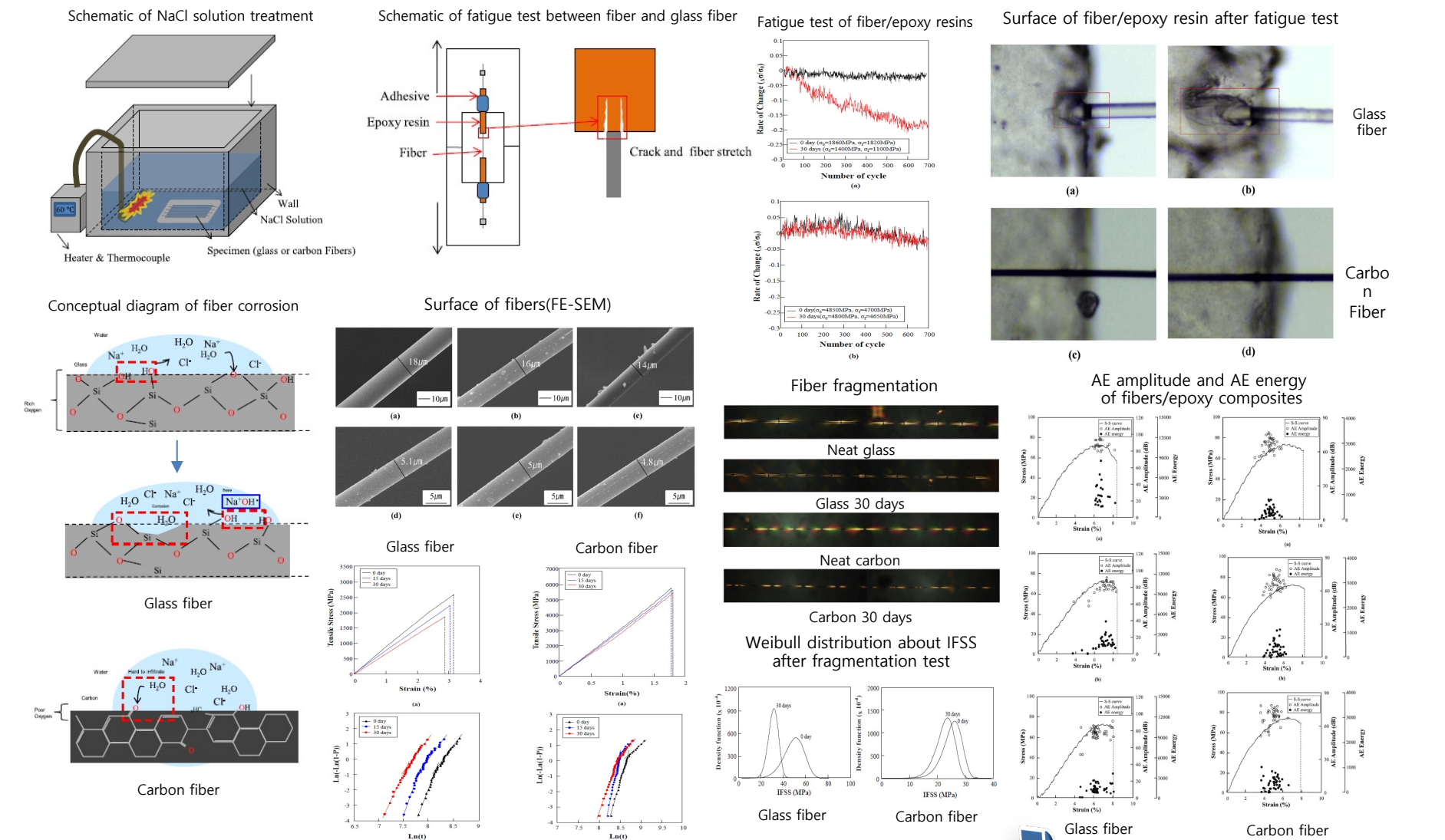
Carbon fiber and phenolic matrix cracks inside epoxy matrix

Carbon fiber and CNT-phenolic matrix cracks inside epoxy matrix

Cited 21th

# Composites Science and Technology 122, 59-66 (2016)

The change in mechanical and interfacial properties of GF and CF reinforced epoxy composites after aging in NaCl solution

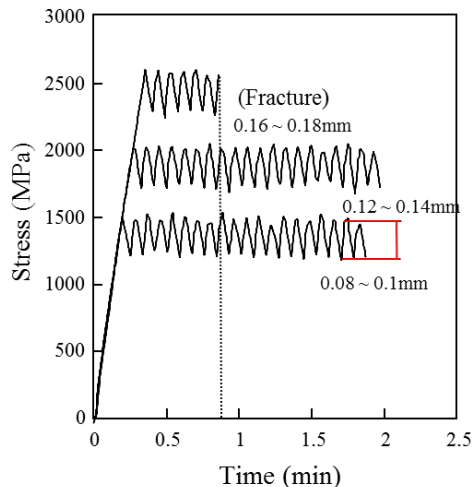




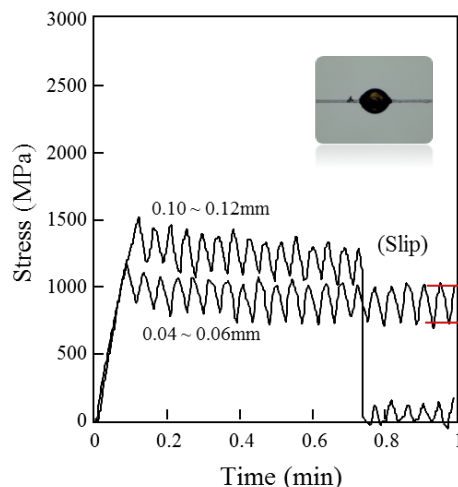
*The Journal of Adhesion* 97(5), 438-455 (2021)

Advanced interfacial properties of glass fiber/dopamine-epoxy composites using a microdroplet pull-out test and acoustic emission

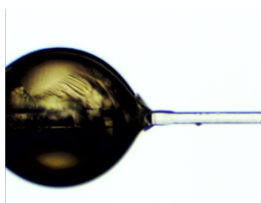
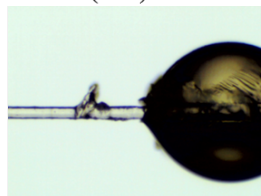
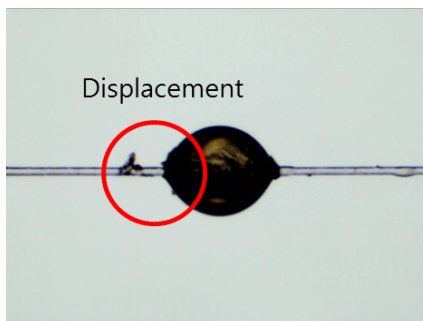
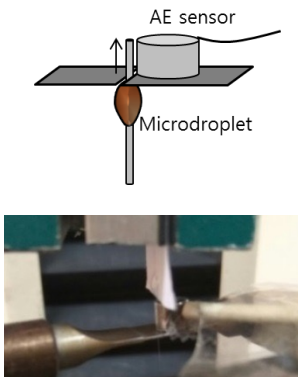
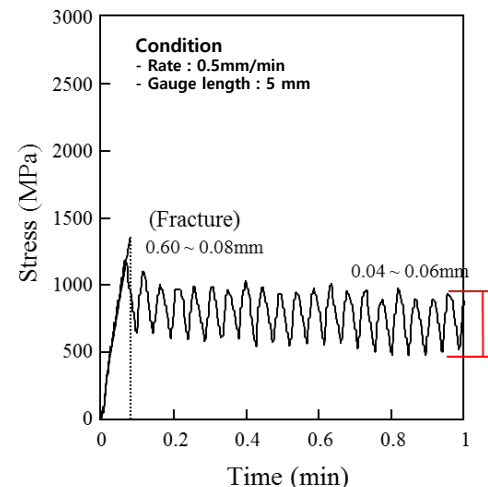
Fiber fracture



Interface slip

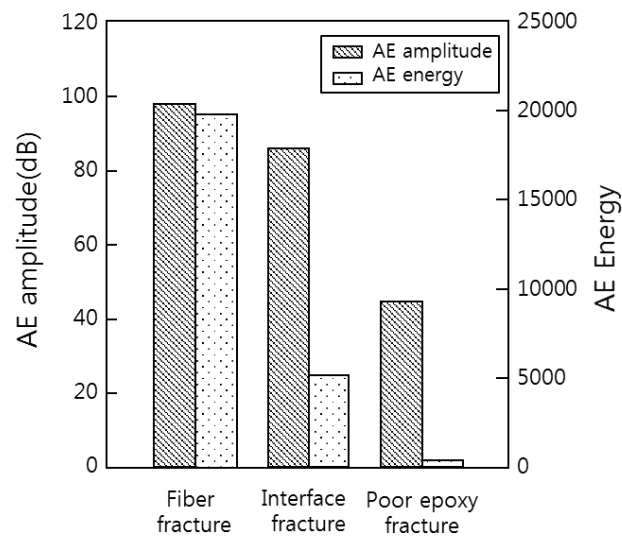


Epoxy fracture



Condition

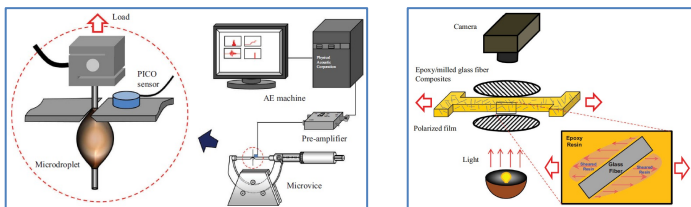
- Rate : 0.5mm/min
- Gauge length : 5mm
- Glass fiber : SE-1500
- Epoxy resin : YD-128



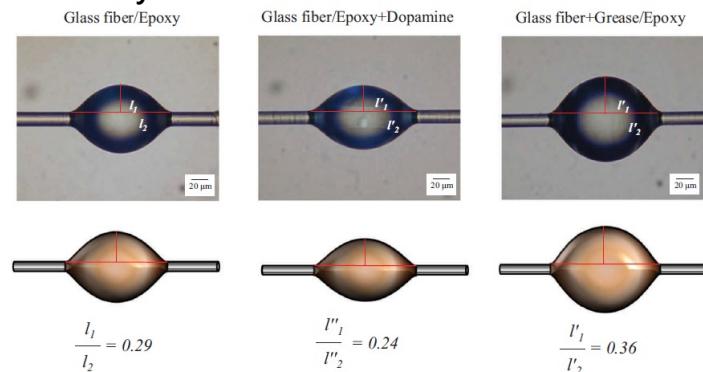
*The Journal of Adhesion* 97(5), 438-455 (2021)

Advanced interfacial properties of glass fiber/dopamine-epoxy composites using a microdroplet pull-out test and acoustic emission

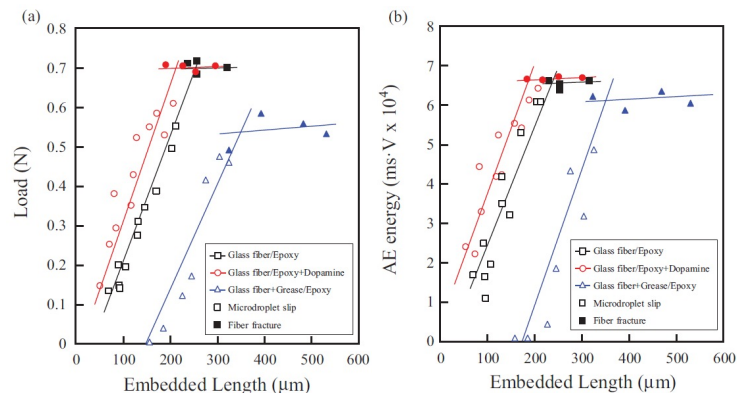
### Scheme of micromechanical test



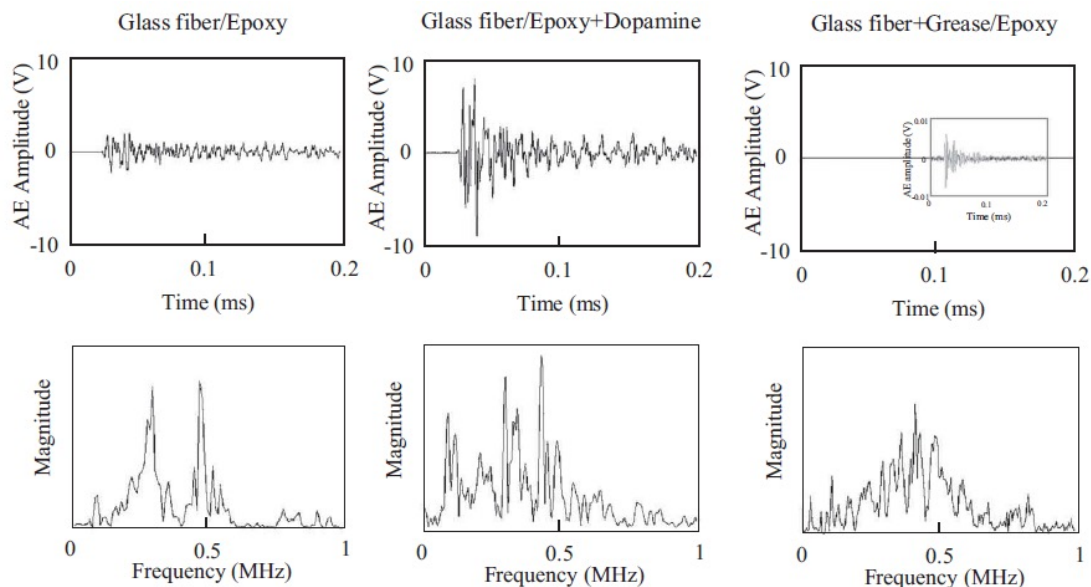
### Wettability test



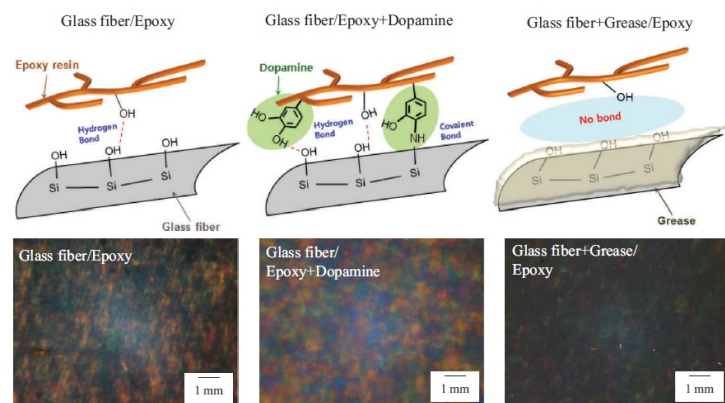
### Microdroplet pull-out test



### AE amplitude and FFT during microdroplet pull-out test



### Short fiber fragmentation test



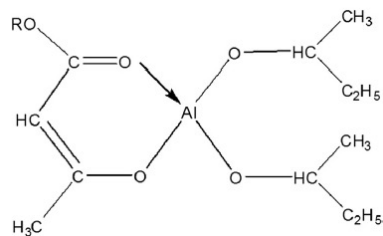
## Part 2

# Interfacial adhesion via wettability test *versus* ER

**Cited 93th**

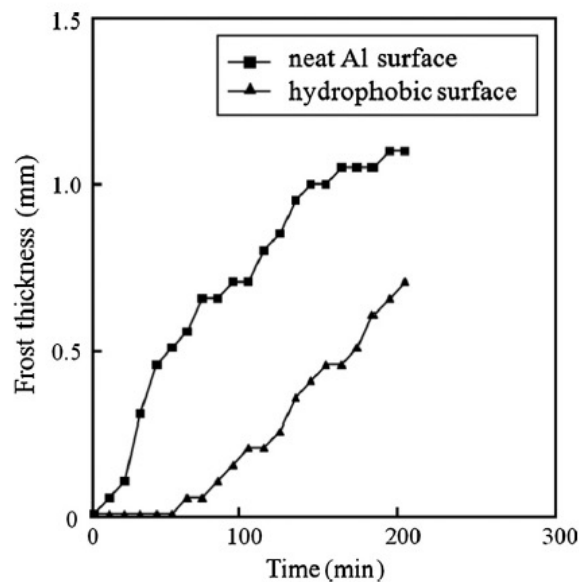
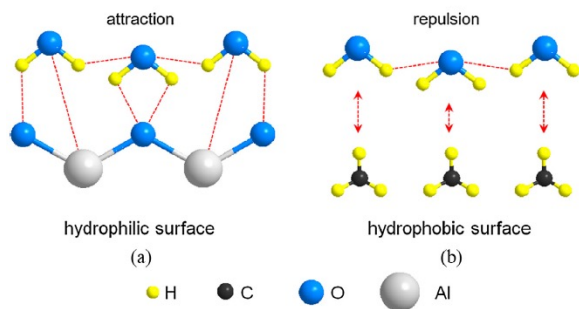
**Experimental Thermal and Fluid Science 60, 132–137 (2015)**

**Frost formation and anti-icing performance of a hydrophobic coating on aluminum**



Temperature (°C)	Neat Al surface	Hydrophobic surface
25		
-10		

Time (sec)	Neat Al surface	Hydrophobic surface
10		
30		
60		



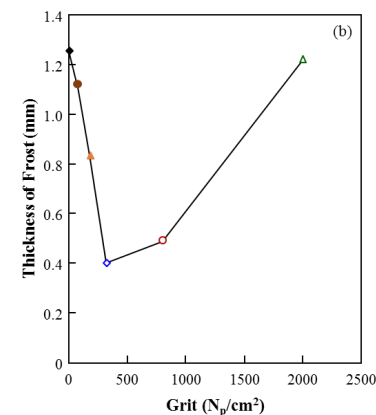
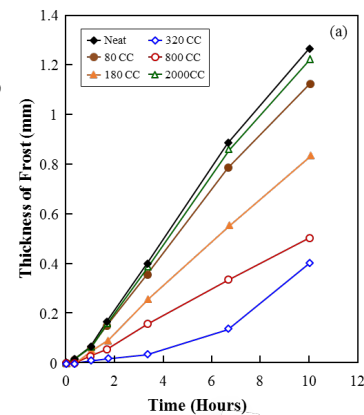
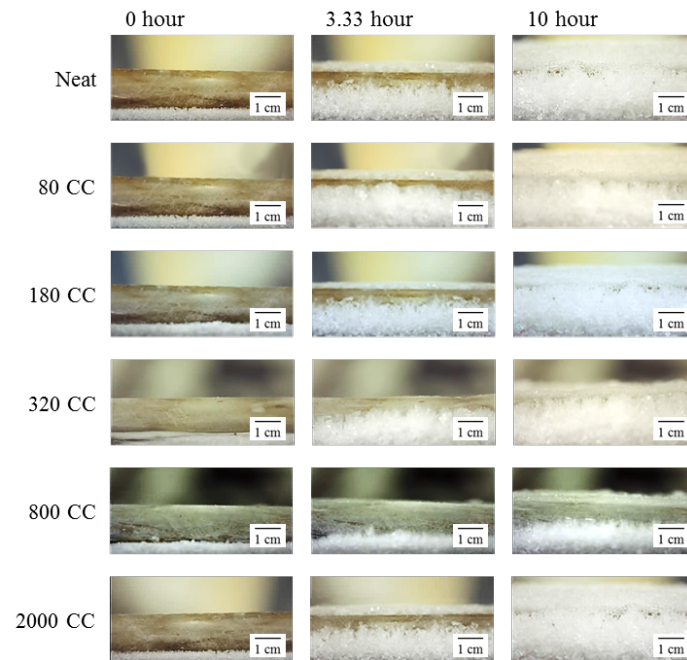
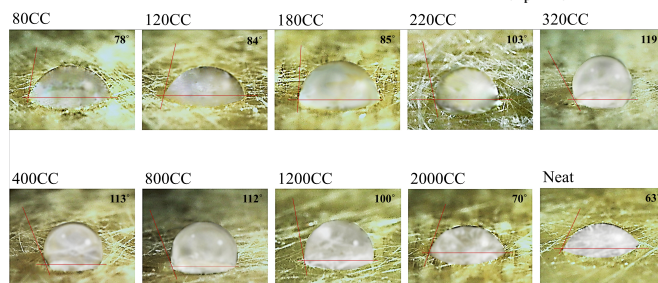
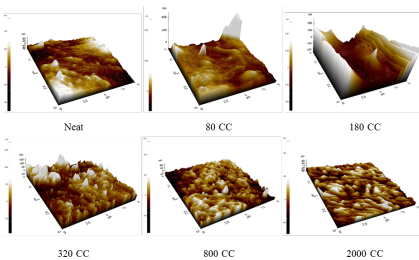
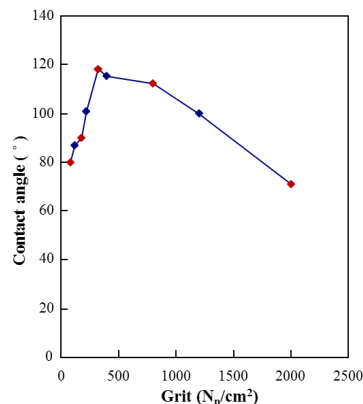
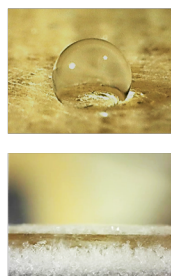
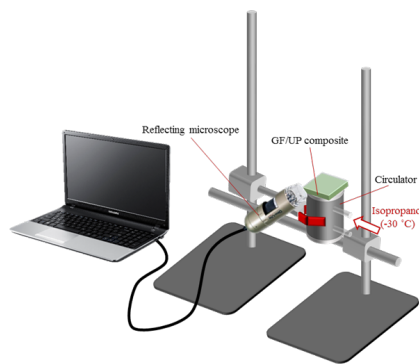
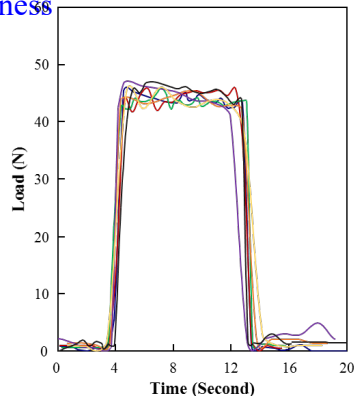
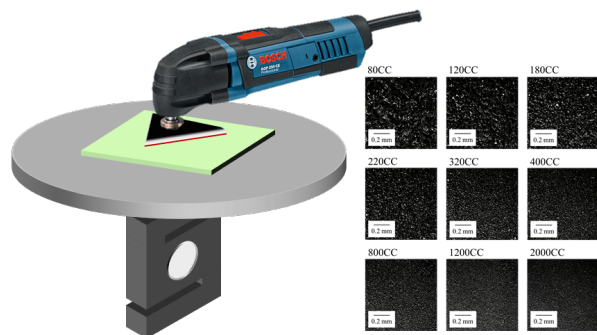
Time (min)	Neat Al surface	Hydrophobic surface
10		
20		
40		



**Cited 23th**

**Composites Part B** 170, 11-18 (2019)

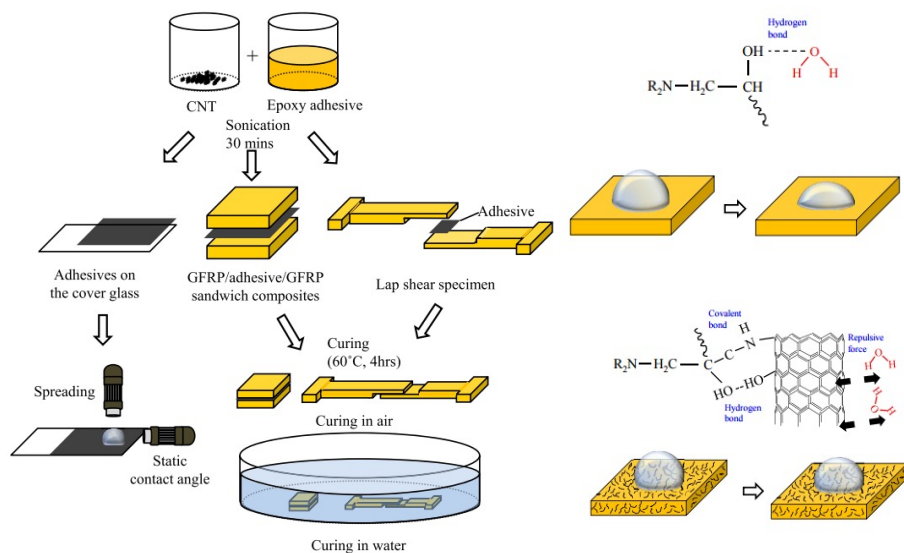
Comparison of interfacial adhesion of hybrid materials of aluminum/carbon fiber reinforced epoxy composites with different surface roughness



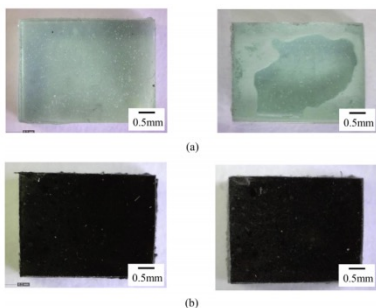
Cited 30th

*Composites science and technology* 142, 98–106 (2017)

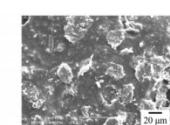
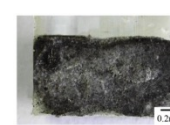
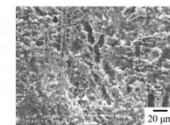
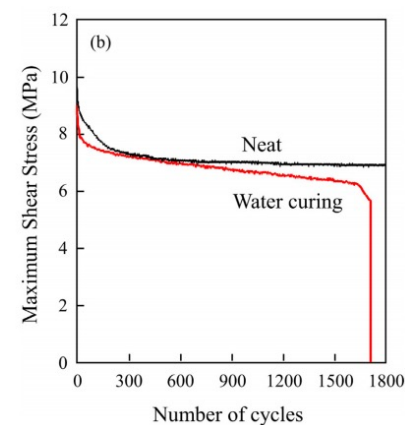
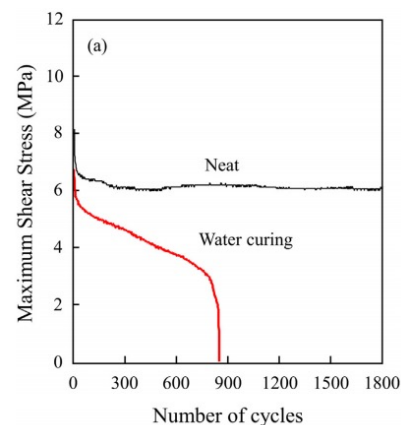
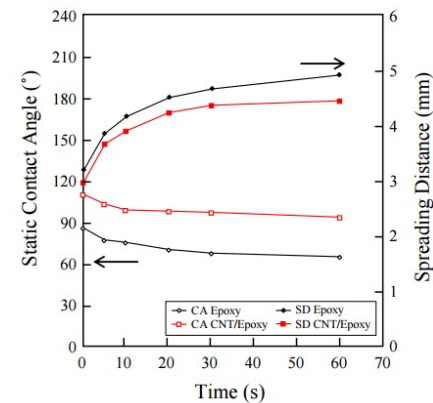
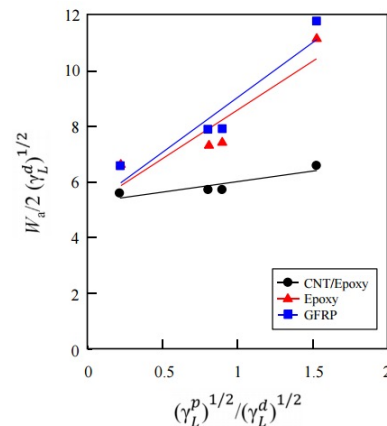
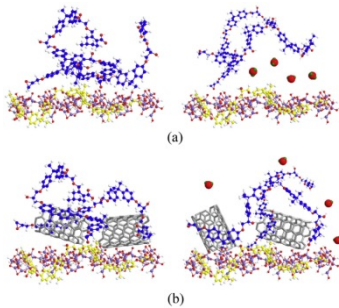
Interfacial properties and water resistance of epoxy and CNT-epoxy adhesives on GFRP composites



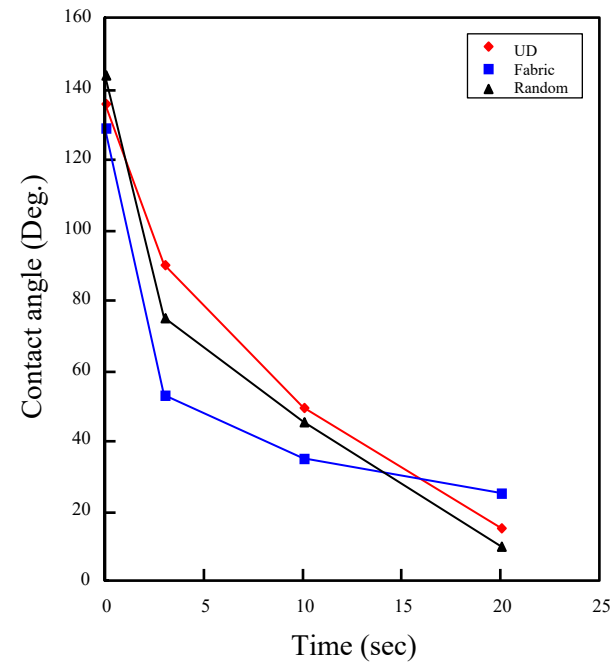
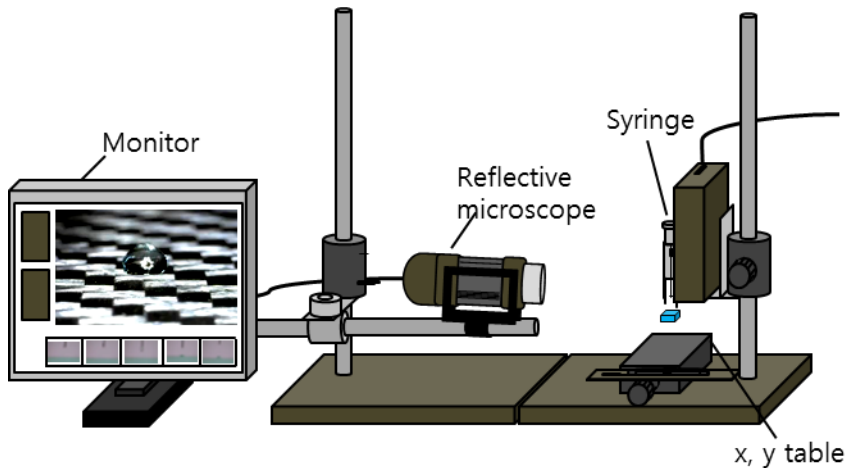
Schematic of preparation process of GFRP/adhesives specimens



Change of epoxy adhesion after water curing



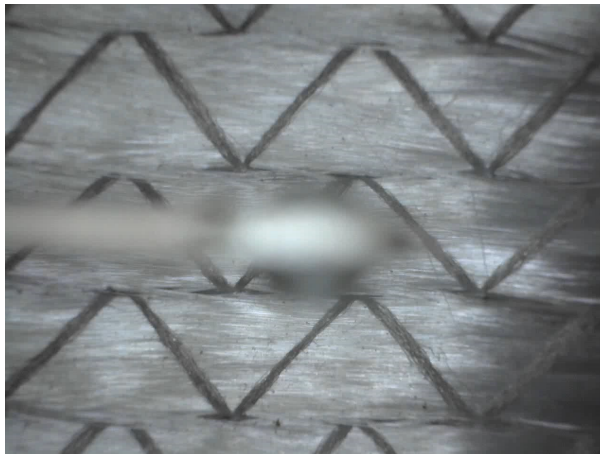
# Application of contact angle method for RTM



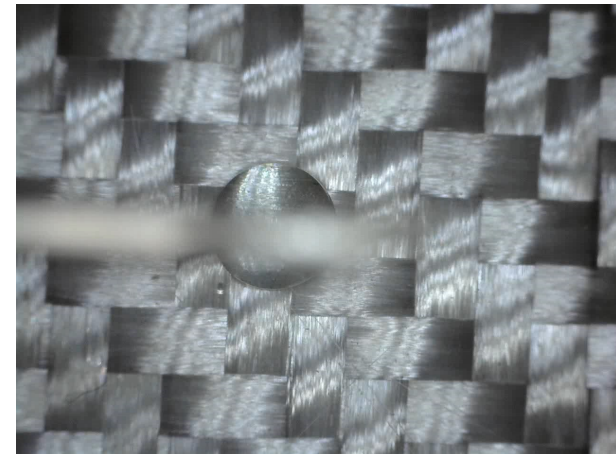
Random



UD

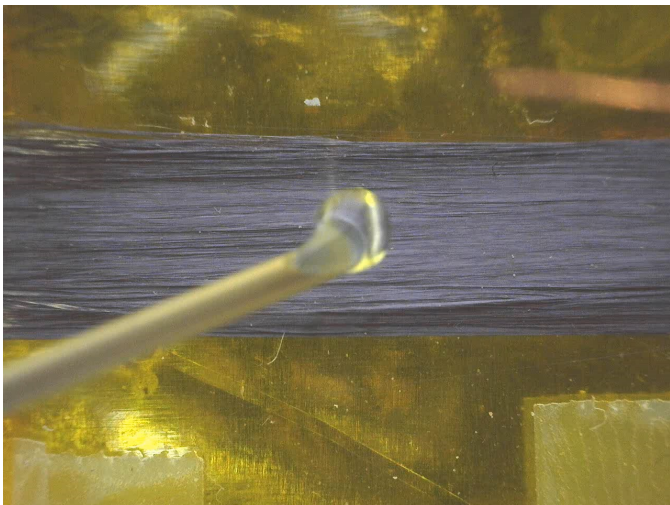


Fabric (Woven)

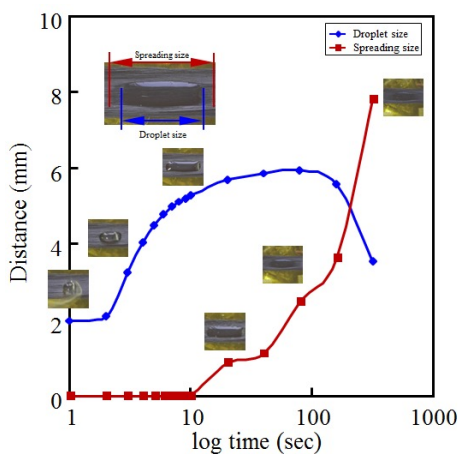
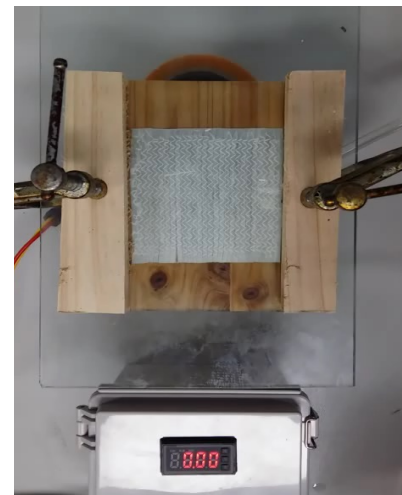




## Spreading condition of epoxy on the CF tow using ER method

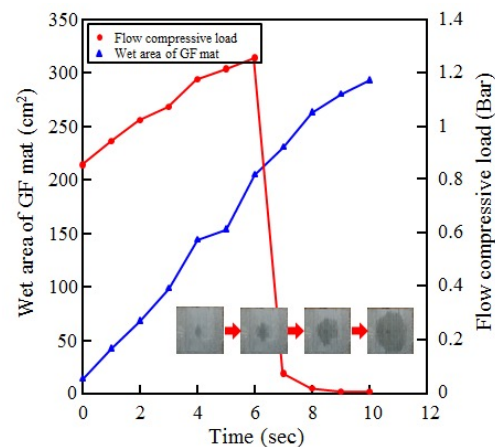


## Spreading condition of epoxy on the GF UD mat using video



### Condition

- Tow : Carbon fiber
- (T-700)
- Droplet : Epoxy (Bisphenol A type)
- Distance of prove : 30 mm



### Condition

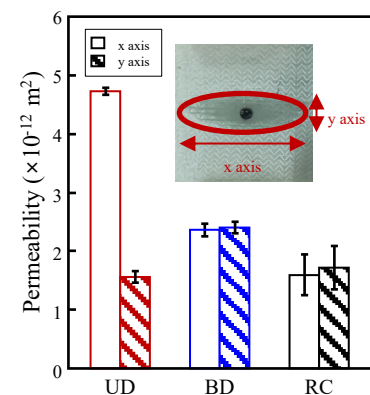
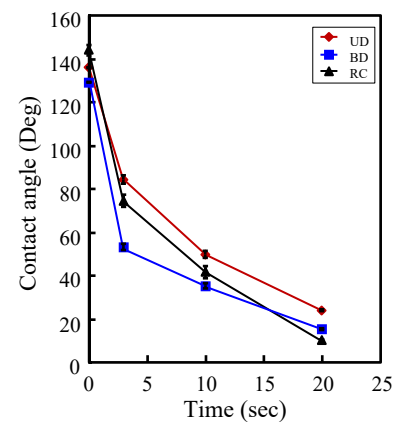
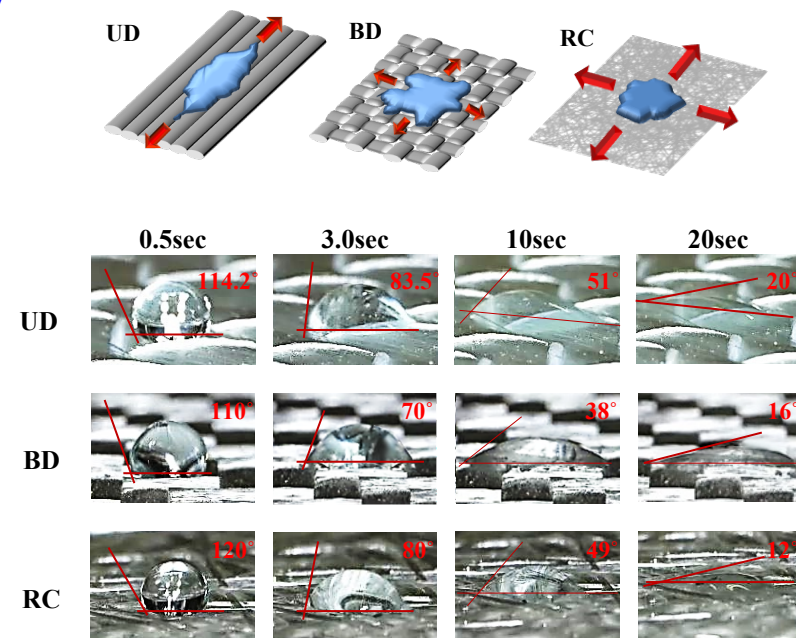
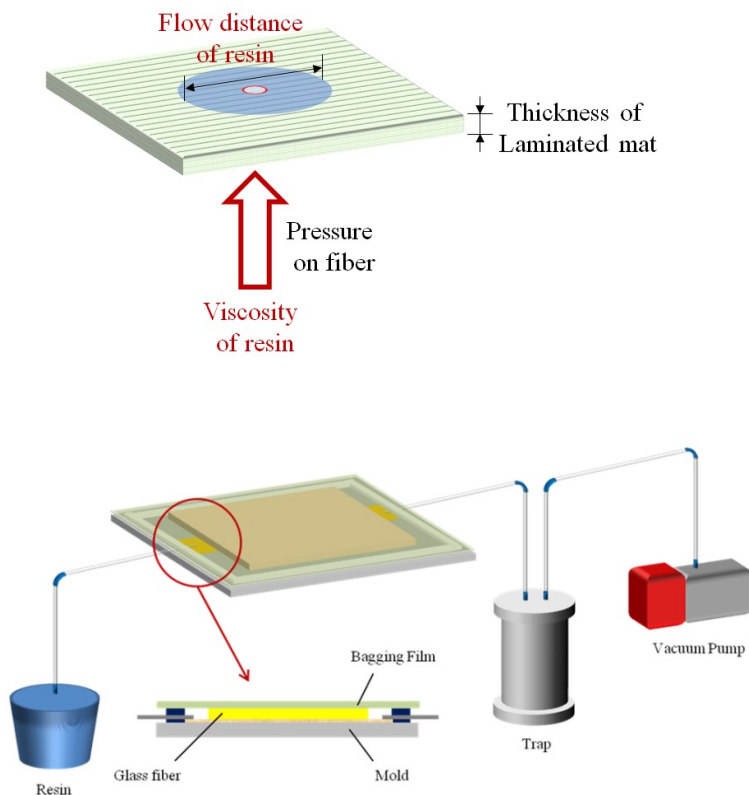
- Droplet : Epoxy (Bisphenol A type)
- Tow : Glass fiber (SE-1500)
- Area: 200 X 200 X 0.1 mm



**Cited 17th**

**Composites: Part B** 148, 61-67 (2018)

Interfacial Properties and Permeability of Three Patterned Glass Fiber/Epoxy Composites by VARTM

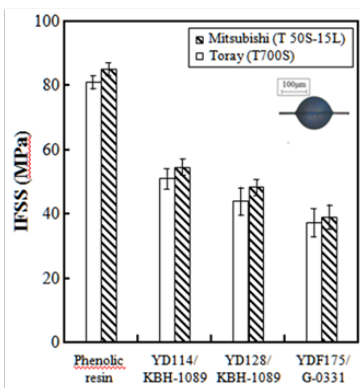


**Cited 11th**

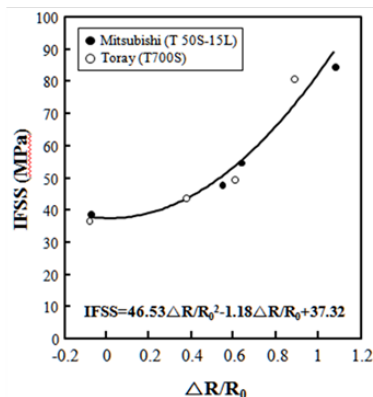
**Journal of Adhesion Science and Technology** 28, 1677–1686 (2014)

New method for interfacial evaluation of carbon fiber/thermosetting composites by wetting and electrical resistance measurements

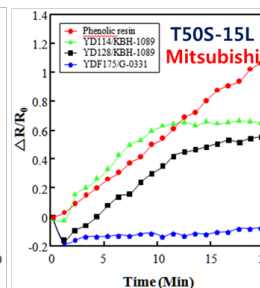
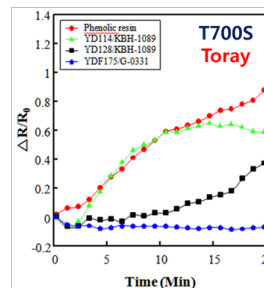
## IFSS VS ER wetting signal



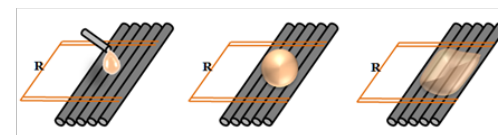
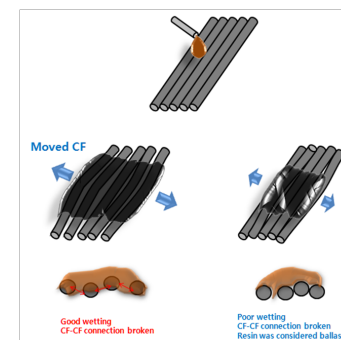
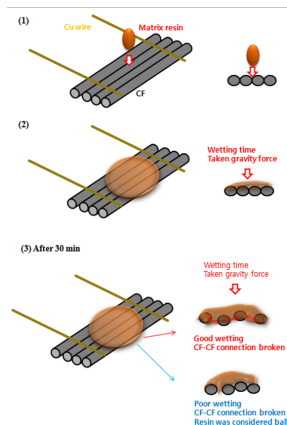
IFSS results of different carbon fibers and polymer resins



The relationship of IFSS and electric resistance change

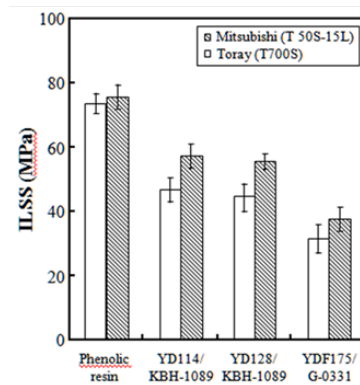


Test method and theory

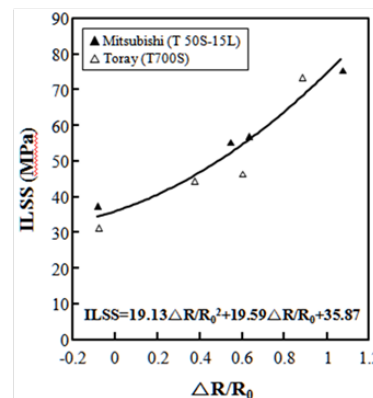


**Toray CF have better wettability than Mitsubishi CF.**

## ILSS VS ER wetting signal



ILSS results of different carbon fibers and various polymer resins



The relationship of ILSS and ER change ratio

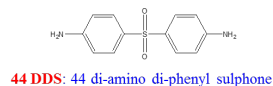
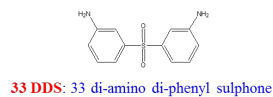
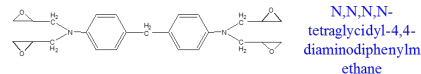
## Cited 6th

## Polymer Testing 53, 293-298 (2016) Defense

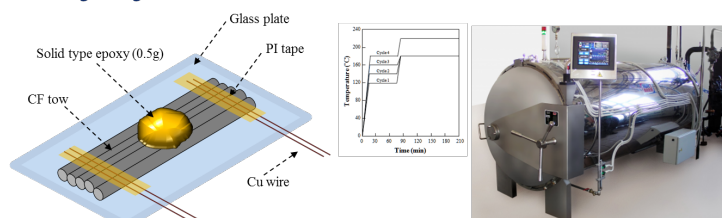
Interfacial and wetting properties of carbon fiber reinforced epoxy composites with different hardeners by electrical resistance measurement

### Experimental

#### - Materials

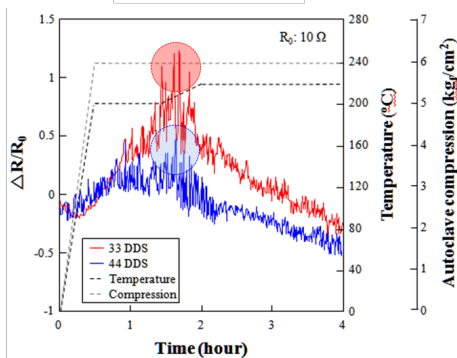
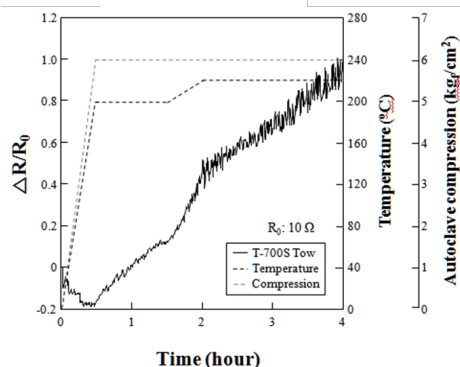
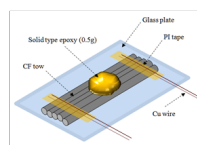
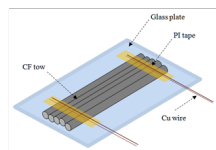


#### - Wetting using ER method in autoclave

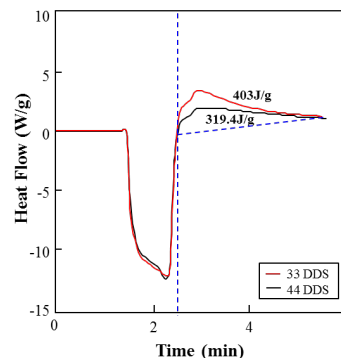


- DSC: Heat of reaction evaluation for obtaining the optimum curing condition
- Tensile test: Tensile strength for different epoxies with hardeners
- IFSS with different epoxies and hardeners

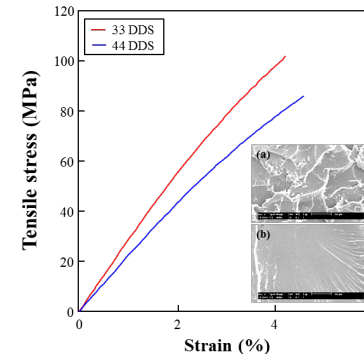
### Interfacial and wetting property of TGDDM/DDS resins in CF tow with 2 different hardeners in an autoclave



### Optimum curing cycle of TGDDM/33-, 44-DDS using heat of reaction and their tensile strength and fractured surfaces

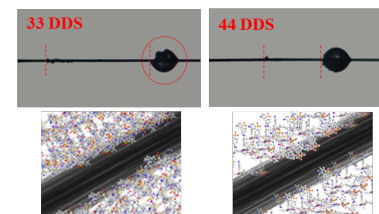
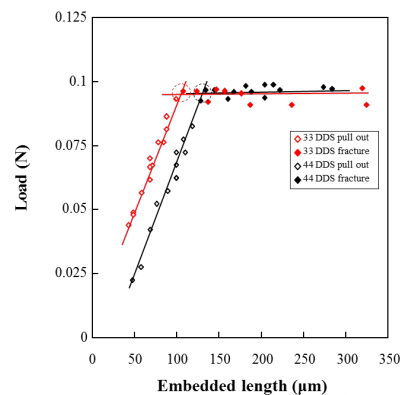


DSC thermograph for two epoxies by 100°C/min



Tensile stress of epoxies and fractured surface: (a) 33-DDS; and (b) 44-DDS

### IFSS and wetting property of TGDDM/DDS in CF tow with two different hardeners



33 DDS CEL: 103 μm,  
33 DDS IFSS: 42.5 MPa  
44 DDS CEL: 130 μm  
44 DDS IFSS: 33.5 MPa  
Fiber fracture load: 0.958 N

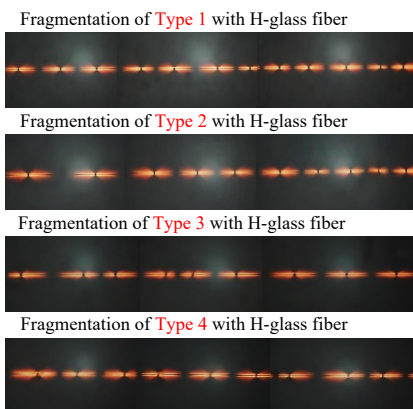
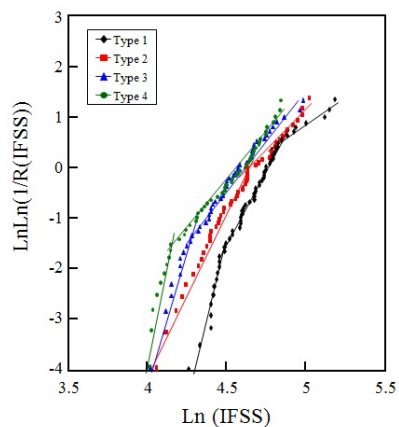
# Construction, Processing

**Cited 11th**

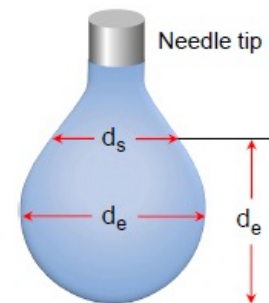
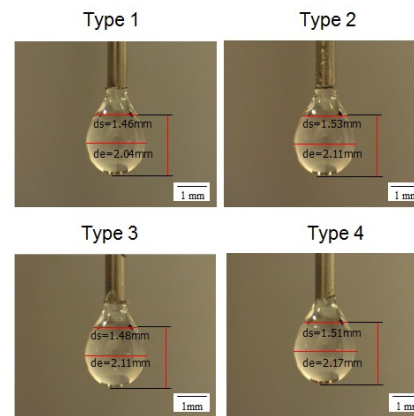
**Colloids and Surfaces A: Physicochemical and Engineering Aspects 544, 68-77 (2018)**

Interfacial and wetting properties between glass fiber and epoxy resins with different pot life

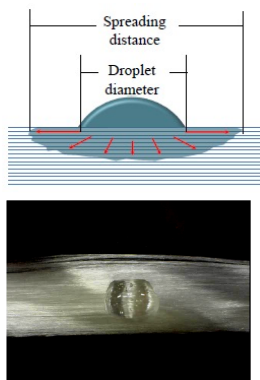
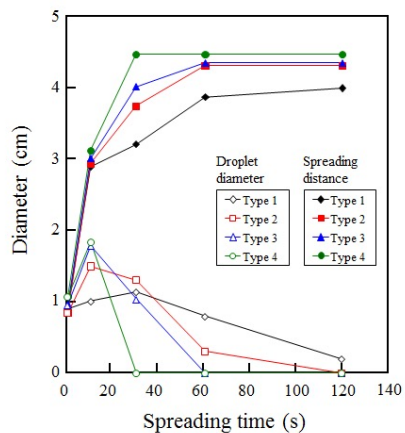
## Fragmentation Test



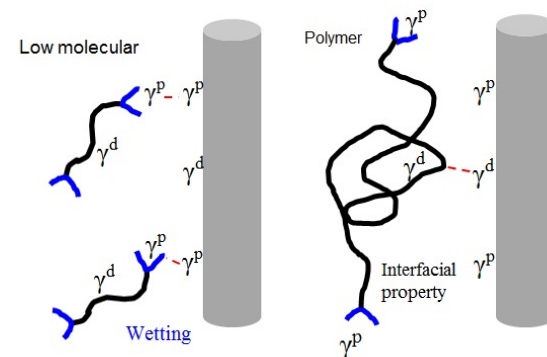
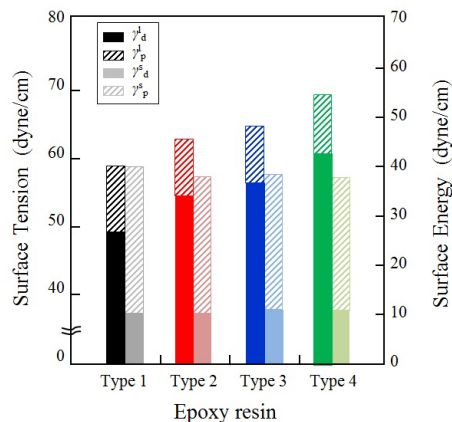
## Pendent Test



## Wetting Test



## The relationship between wetting and interfacial property





## Part 3

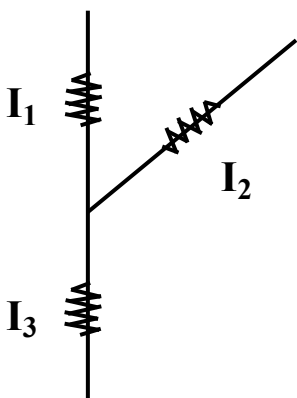
# **Damage sensing** of Nanocomposites by Electrical Resistance (ER)

## Basic principle for measuring electrical resistance (ER)

- using Kirchhoff's law ER can be measured for damage detection due to ER change due to electro-circuit disconnection and fracture
- **Prediction of internal micro-damage prediction**

### *Kirchhoff's Law*

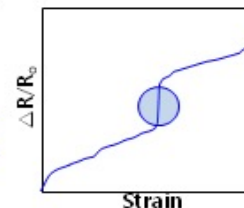
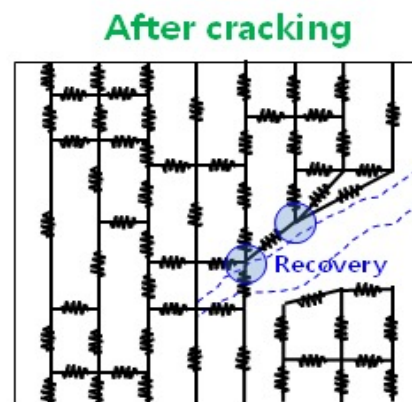
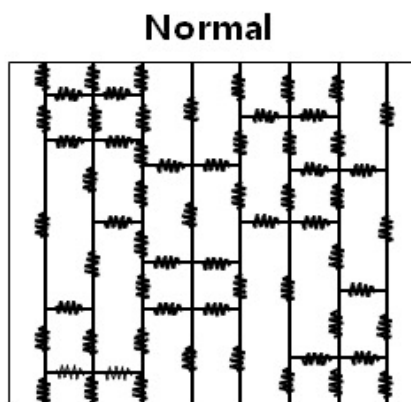
: theory explaining why electrical resistance increases from damage



$$I_3 = I_1 + I_2$$

$$(R = L / A \rho)$$

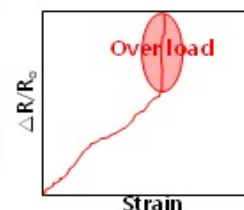
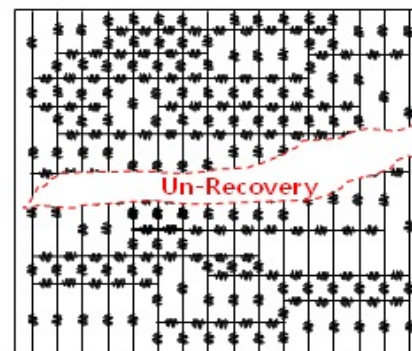
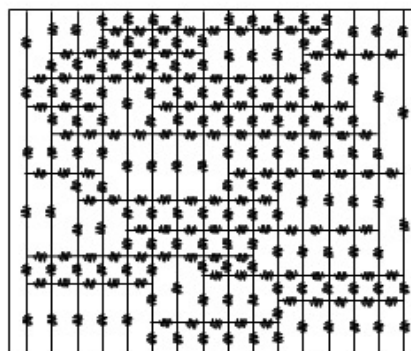
Micro composites



ER of CF

☞ Contacted ER

Nano composites



ER of CNT

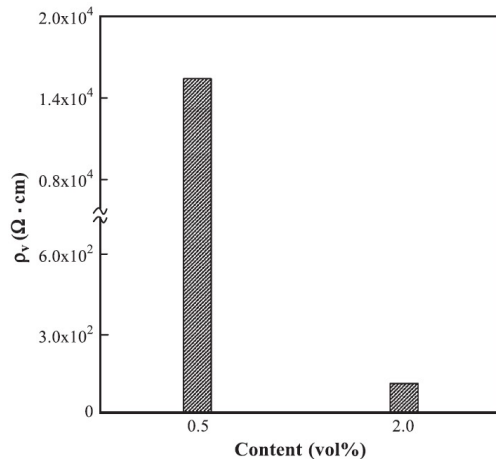
\* Contacted ER

**Cited 134th**

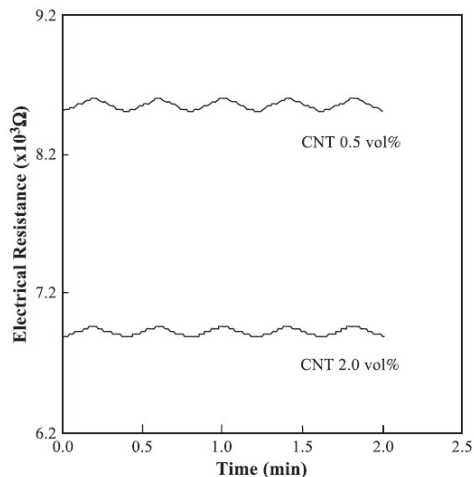
**Materials Science and Engineering C, 23, 971–975(2003)**

Nondestructive damage sensitivity and reinforcing effect of carbon nanotube/epoxy composites using electro-micromechanical technique

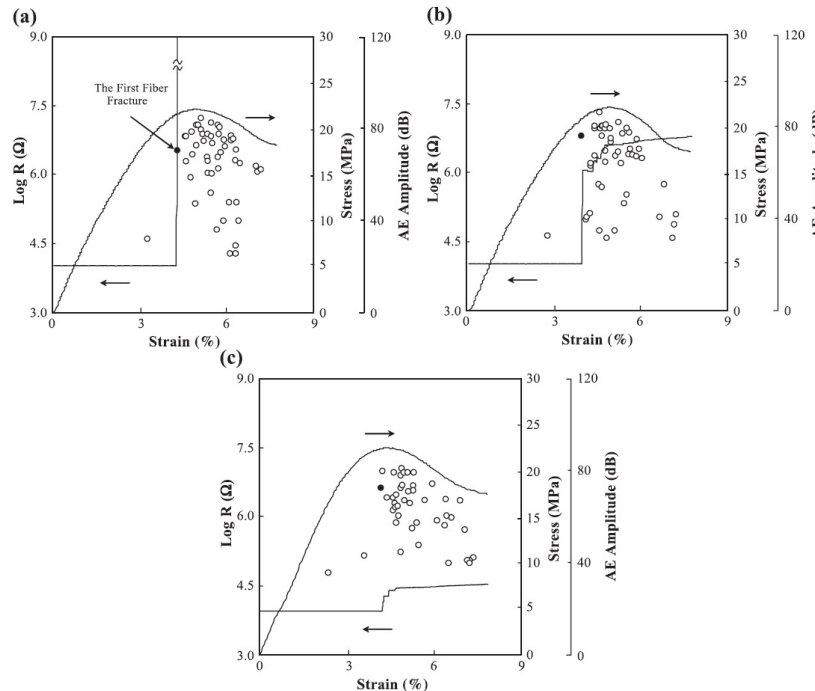
**First Paper (2003): “ER sensing using CNT”**



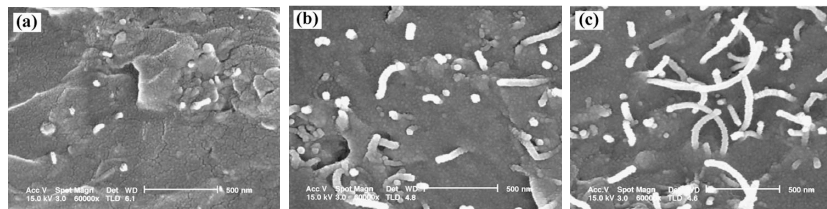
Electrical volume resistivity for CNT/epoxy composites with CNT volume fraction.



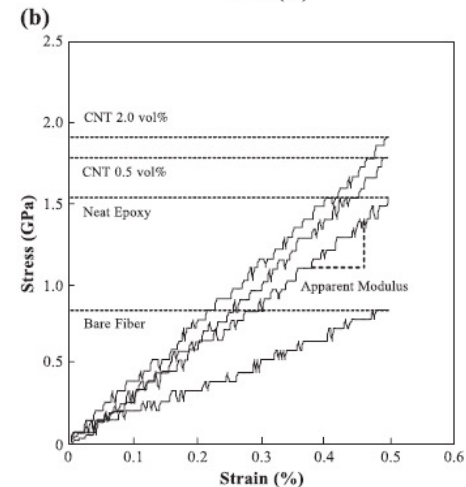
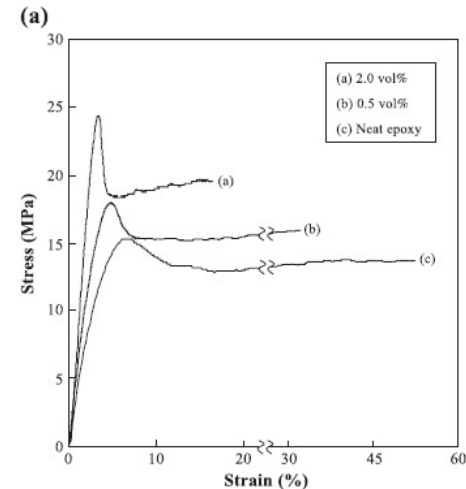
The change in electrical resistance for fiber tension with CNT content under electro-pullout test.



Damage sensitivity of fiber fracture for (a) 0.1 vol% CNT, (b) 0.5 vol% CNT and (c) 2.0 vol% CNT under DMC test.



FE-SEM photographs for fracture surface of (a) 0.1 vol% CNT, (b) 0.5 vol% CNT and (c) 2.0 vol% CNT composites.

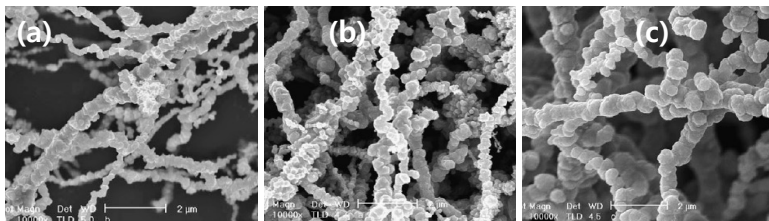
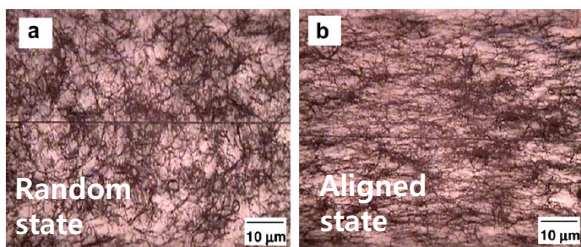
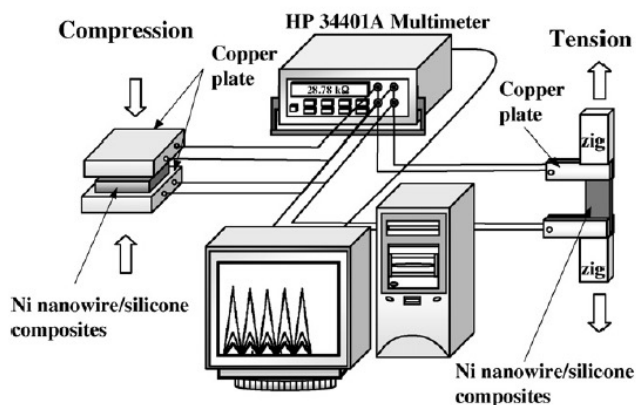


Stress–strain curve of CNT composites by (a) tensile test and (b) apparent modulus measurement.

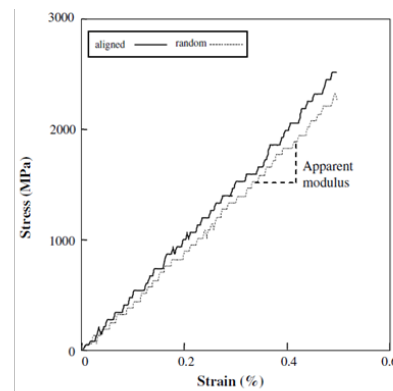
Cited 37th

Composites Science and Technology 67, 2121-2134 (2007)

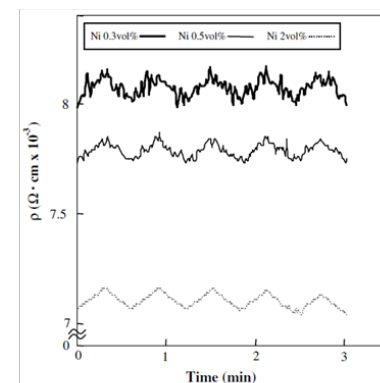
Self-sensing and interfacial evaluation of Ni nanowire/polymer composites using electro-micromechanical technique



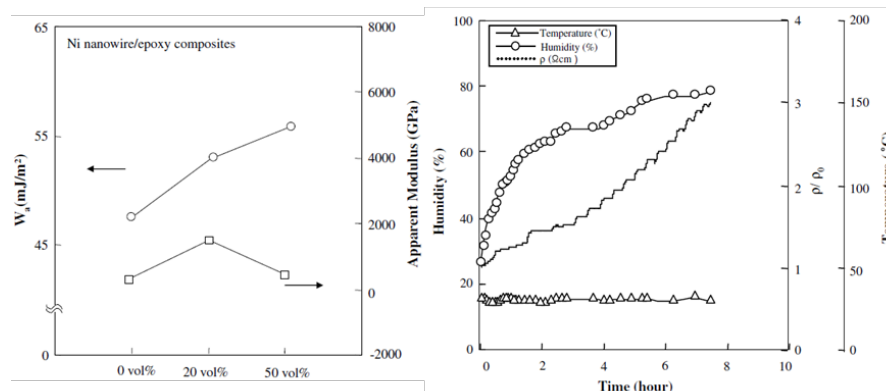
(a) 100–300 nm; (b) 300–800 nm and (c) 1–3 μm



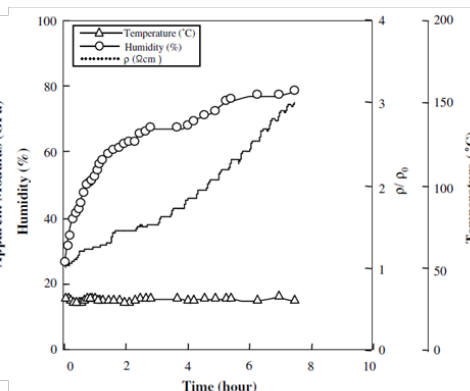
Strain-stress curve of Ni nanowire/epoxy composites with random and aligned states under magnetic field



The change in electrical contact resistivity of Ni nanowire/epoxy composites with different Ni contents



The relationship of apparent modulus and work of adhesion between carbon fiber and Ni nanowire/epoxy composites with different contents



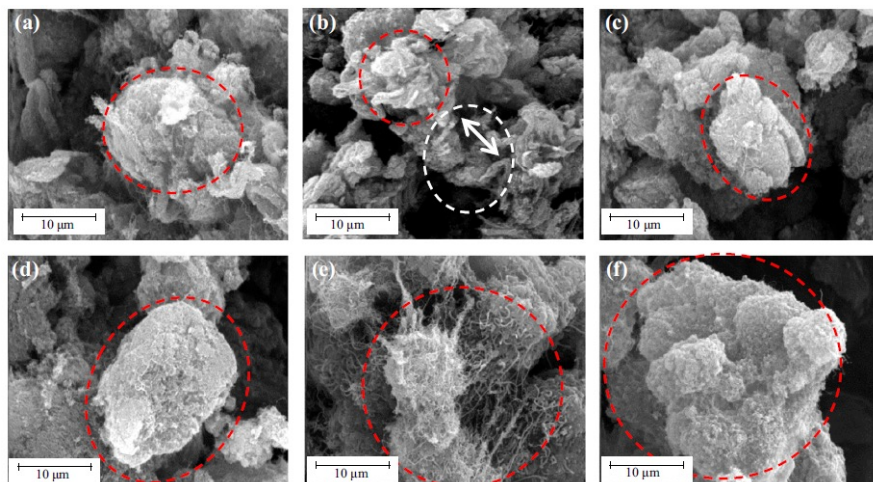
The change in the electrical resistivity with increasing humidity at constant temperature



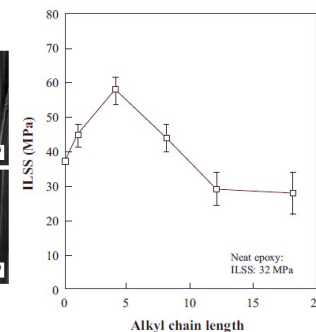
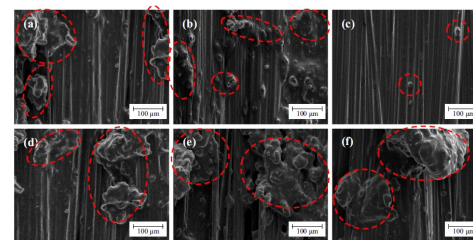
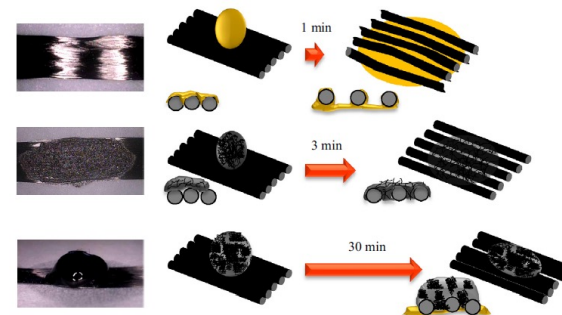
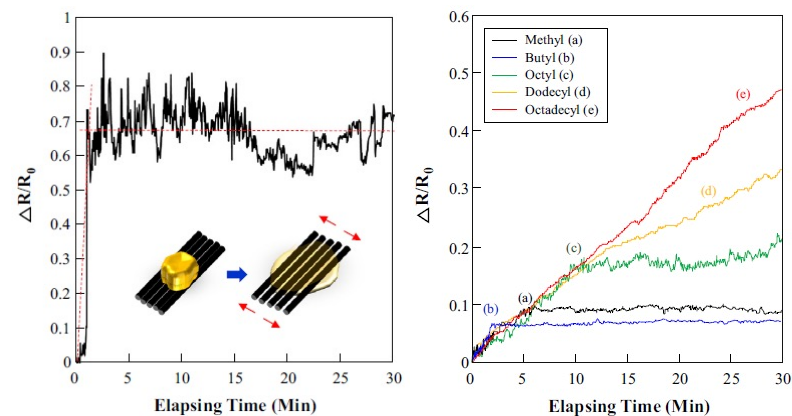
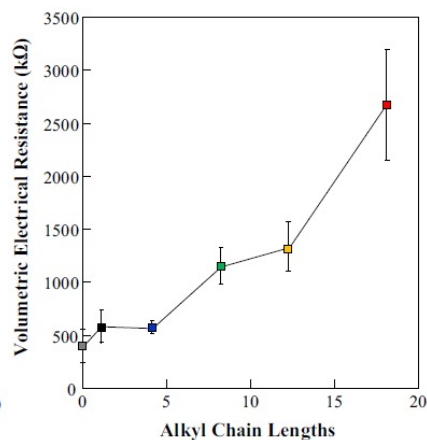
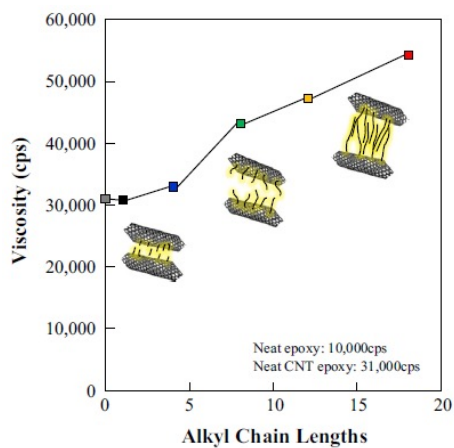
**Cited 15th**

**Composites: Part A 82, 190–197 (2016)**

Interfacial and mechanical properties of epoxy composites containing carbon nanotubes grafted with alkyl chains of different length



(a) neat CNT; (b) methyl; (c) butyl; (d) octyl; (e) dodecyl; (f) octadecyl



# Interfacial Properties and **Damage Sensing** on CFRP Composites by **VARTM** using **2D or 3D ER Mapping**

# • Background

## Application

- Increasing in conductive materials, e.g, CNT, CFRP in nonconductive GF/PP composites
- New NDE for detecting durability evaluation of inter- and external parts
- Importance of dispersion of nano- and micro-particles such as carbon nanotube (CNT)



<Plastic module>



<Audio Case>

Conductive  
nanocomposites  
(high modulus, light  
Weight)



<CF Composites examples>



<New materials for car>

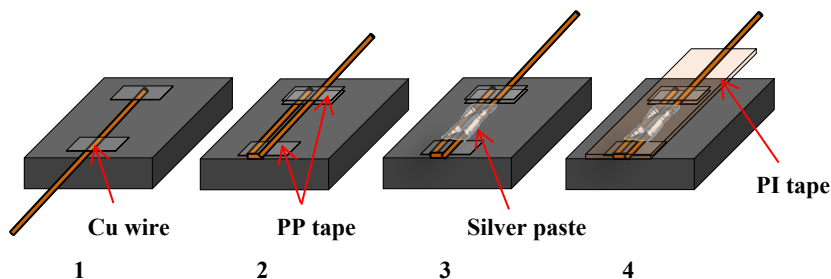


Damage evaluation methods  
for new materials parts  
(rapid, accurate)

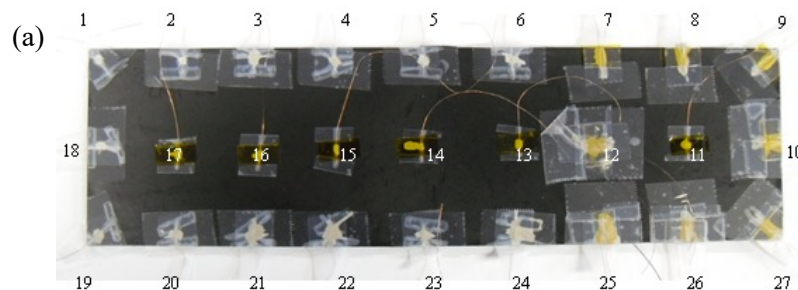
# • Results and Discussions

*Park et al, Composites: Part A, pp. 417 (2016).*

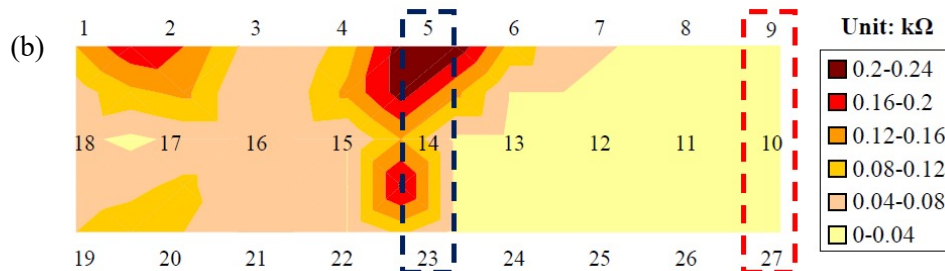
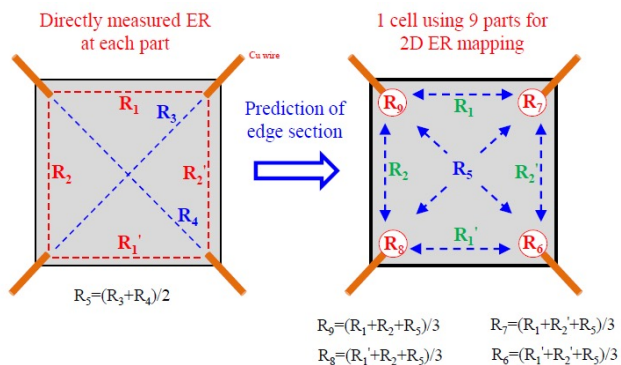
Steps of manufacture of contact **ER probe** on CF/polypropylene (PP)-polyamide (PA)



Specimen and dispersion results of **CF/PP-PA using 2D mapping ER method**: (a) specimen for dispersion; and (b) dispersion results of CF/PP-PA using 2D mapping



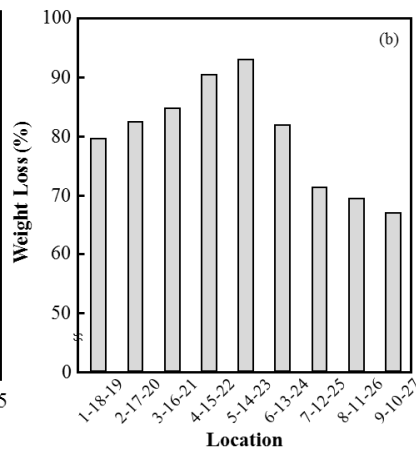
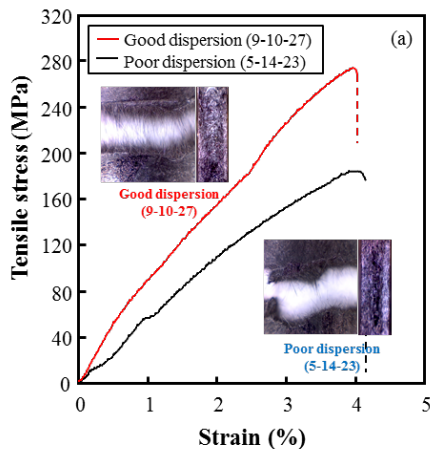
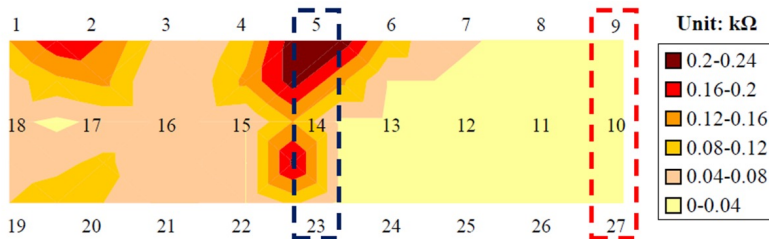
Arrangement of **2D ER mapping using 1 cell ER**



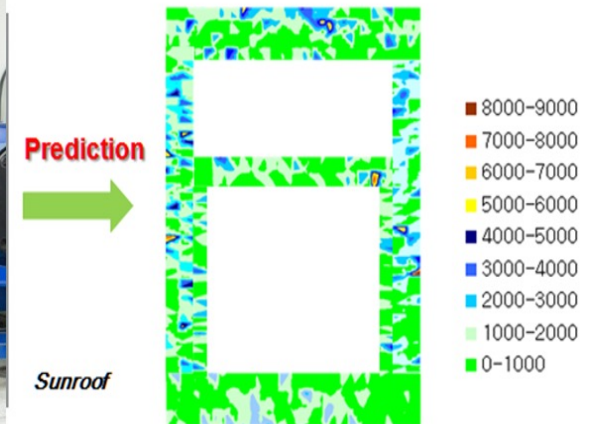
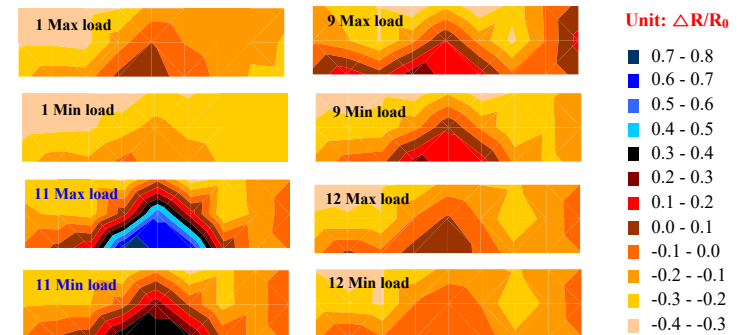


# • Results and Discussions

**Tensile results and weight loss of CF/PP-PA composites with different CF/PP-PA parts:** (a) tensile results; and (b) weight loss results

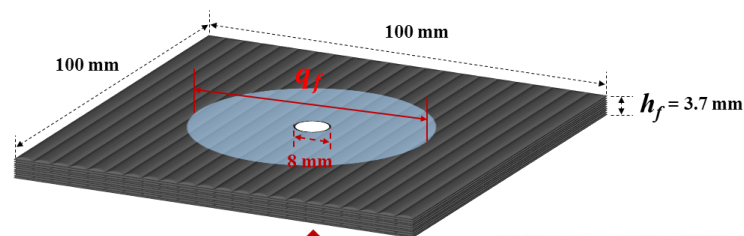
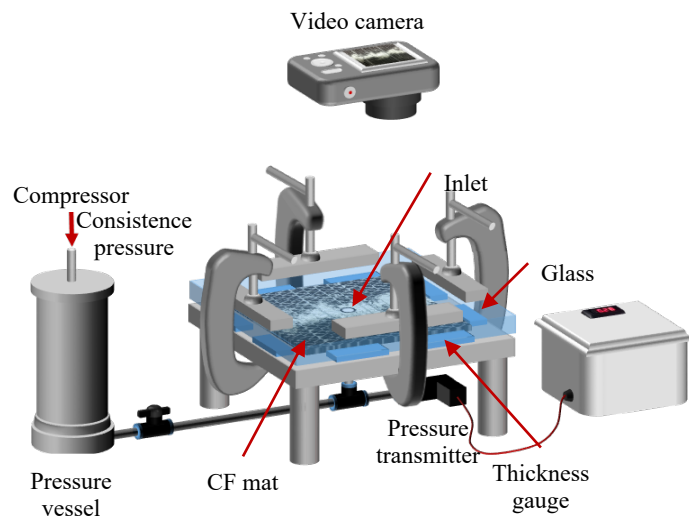


**Cyclic bending test of CF/PP-PA composites using 2D ER mapping**



# • Experimental

## Schematic of permeability measurement

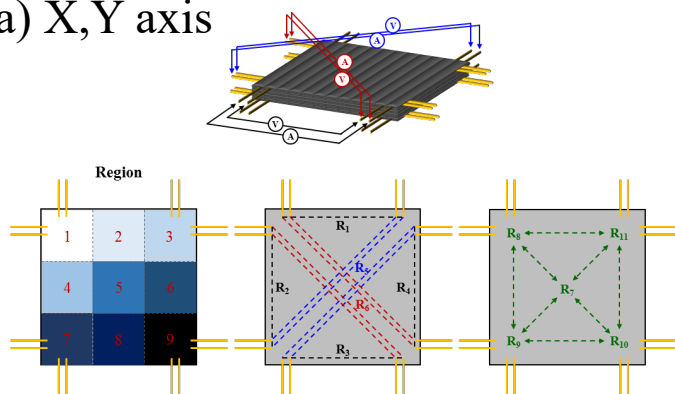


$$K_f = -q_f \frac{\mu \cdot h_f}{P_f}$$

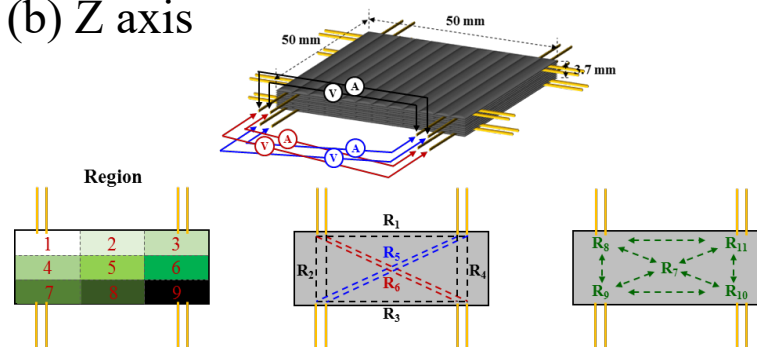
Where  $K_f$  : fiber permeability  
 $q_f$  : flow rate in fiber  
 $\mu$  : viscosity of resin  
 $P_f$  : pressure on fiber  
 $h_f$  : fiber thickness

## Arrangement of 3D ER mapping on a 1 cell ER: (a) X,Y axis; (b) Z axis

(a) X,Y axis



(b) Z axis



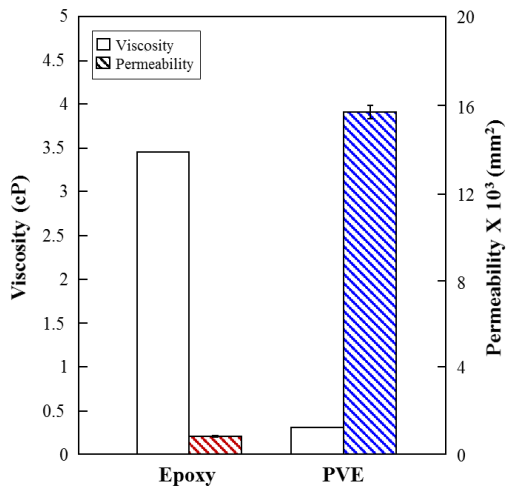
# • Results and discussion

**Cited 4th**

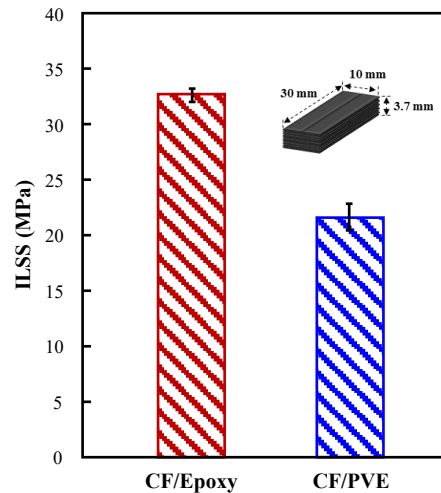
**Composites Part B 115, pp. 178-186 (2018)**

New evaluation of interfacial properties and damage sensing in CFRC by VARTM using 3D ER mapping

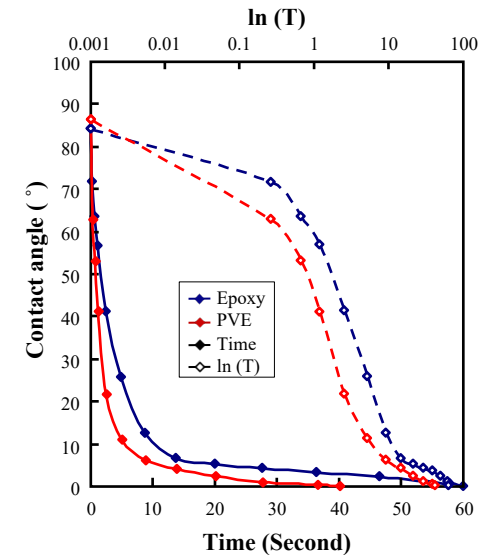
## Viscosity and permeability of epoxy and PVE



## ILSS test of CF/epoxy and CF/PVE composites



## Static contact angle change about resin and CF mat in-situ



Epoxy



PVE

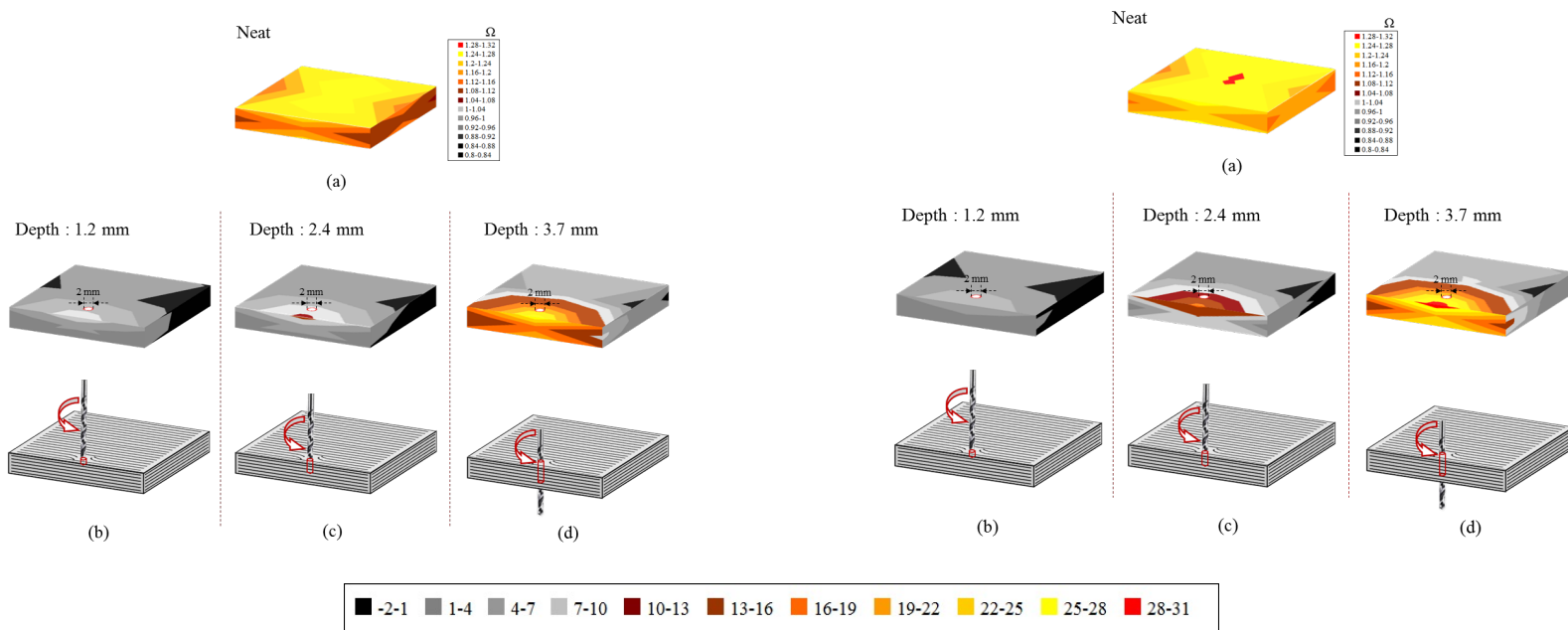


# • Results and discussion

*Cited 4th*

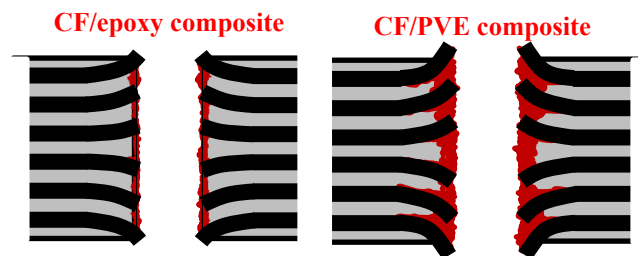
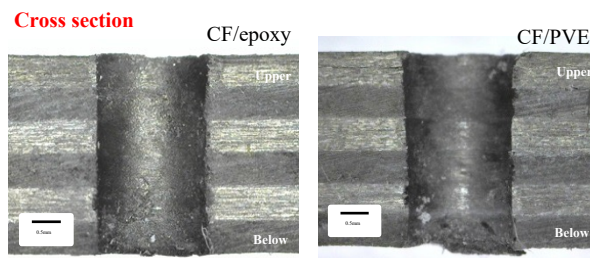
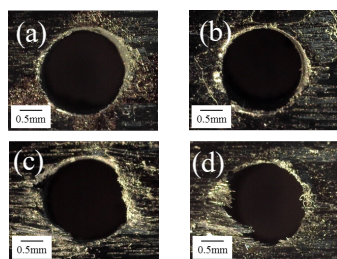
*Composites Part B 115, pp. 178-186 (2018)*

New evaluation of interfacial properties and damage sensing in CFRC by VARTM using 3D ER mapping



3D ER mapping as depth of hole: (a) Neat CF/epoxy composite;  
(b) 1.2 mm; (c) 2.4 mm; and (d) 3.7 mm

3D ER mapping as depth of hole: (a) Neat CF/PVE composite;  
(b) 1.2 mm; (c) 2.4 mm; and (d) 3.7 mm

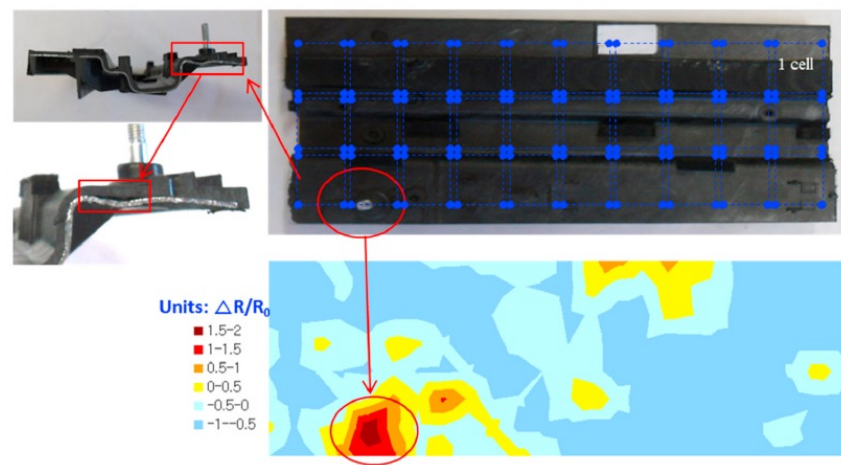
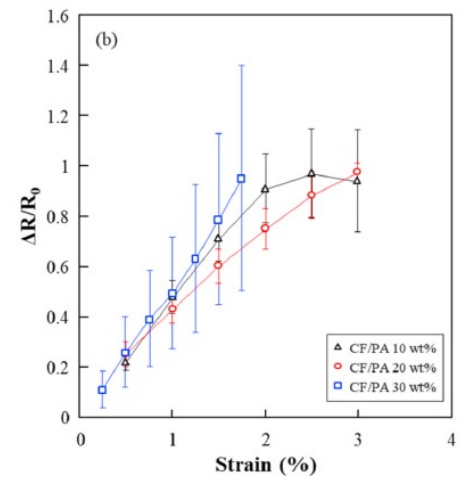
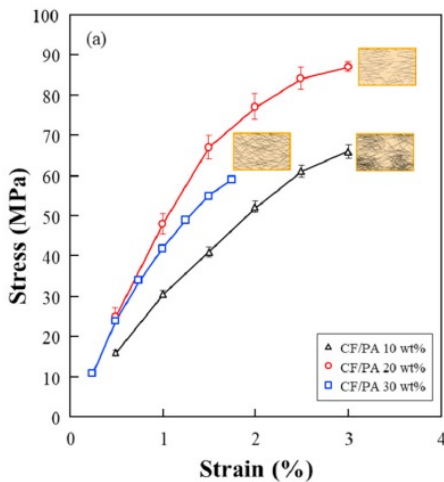
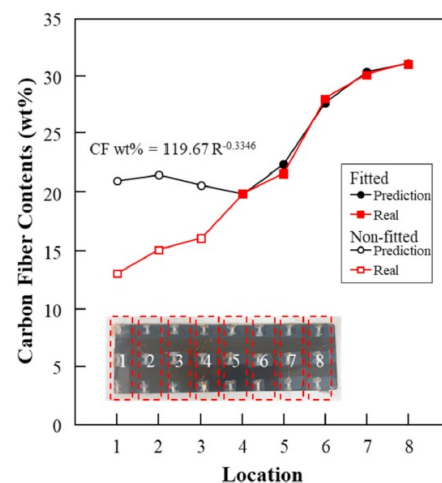
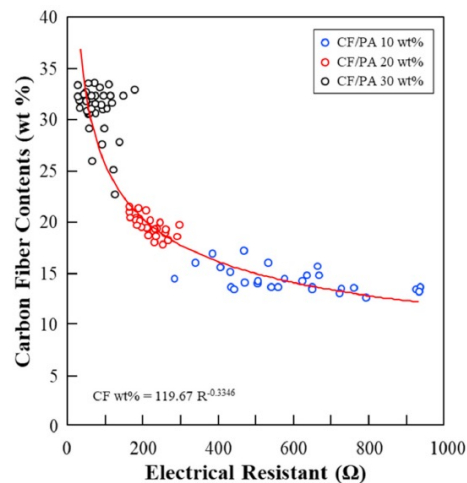
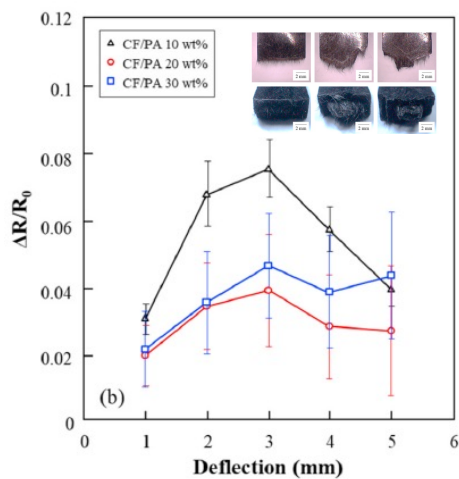
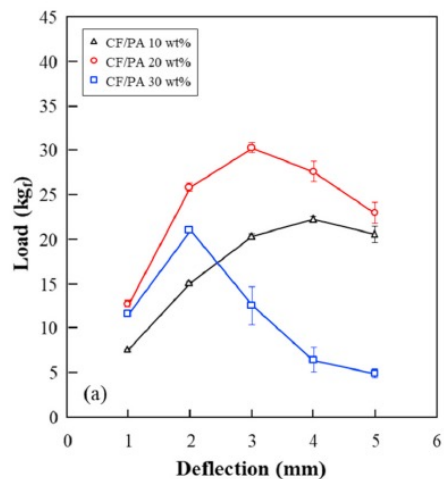


Observation after drilling hole : (a) upper hole of CF/epoxy; (b) below hole of CF/epoxy; (c) upper hole of CF/PVE; and (d) below hole of CF/PVE



**Cited 7st*****Composites Science and Technology 201, 108480 (2021)***

2D electrical resistance (ER) mapping to Detect damage for carbon fiber reinforced polyamide composites under tensile and flexure loading



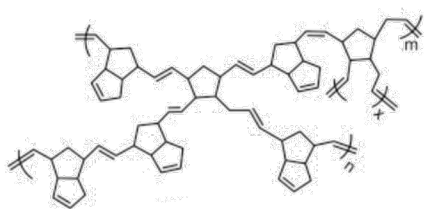
## Part 4

**Applications:** Transportation, Aerospace, Fire Retardant, Recycling, Construction, Marine etc

# Transportation

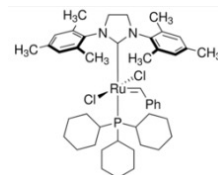
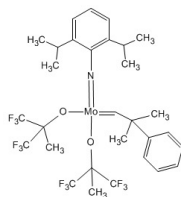
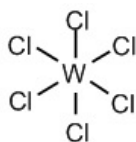
## *p*-DCPD introduction: *Defense, transportation etc*

*p*-DCPD



1, 2, 3 generation Catalysts

Tungsten(**W**)    Molibdenium(**Mo**)    Ruthenium(**Ru**)



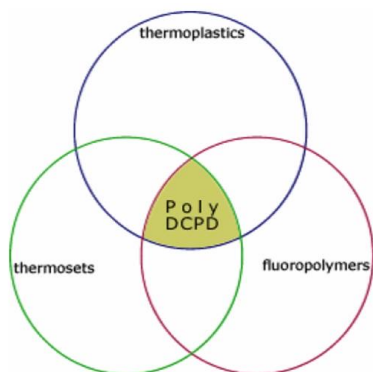
Objectives:  
Improving neat *p*-DCPD properties

- Impact strength ↑
- Low temperature Impact strength ↑
- Water-resisting properties ↑
- Machinability ↑

Application



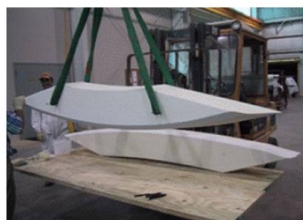
P-DCPD Form



Pipe



High toughness



Ocean boat



Wood coating



Adding  
GF, CF

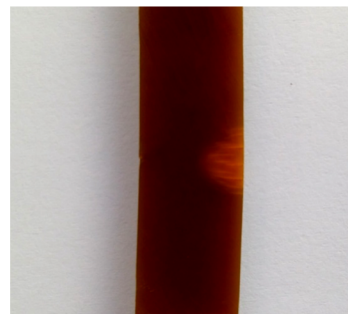
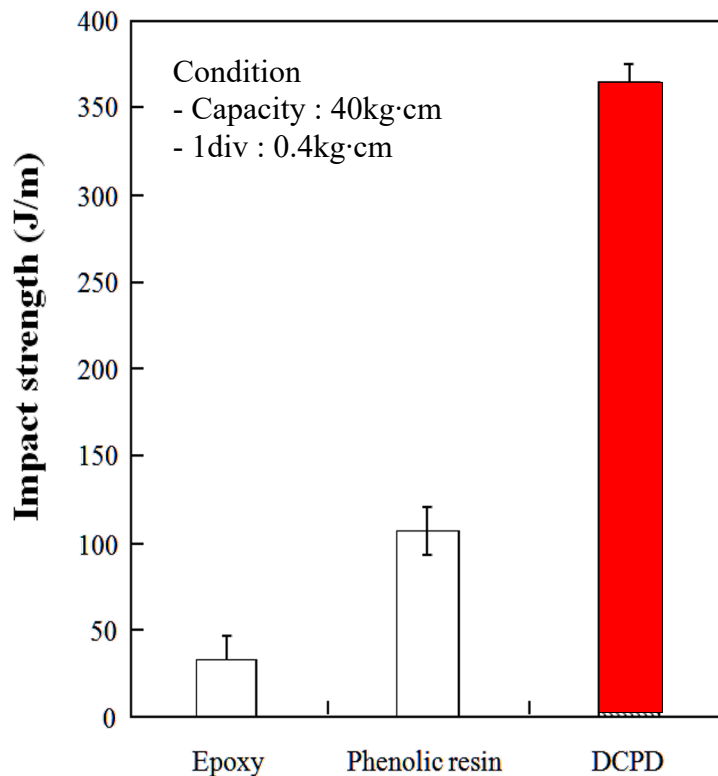
Targets

- Improved higher **mechanical** and **interfacial** properties
- Civil & Military applications

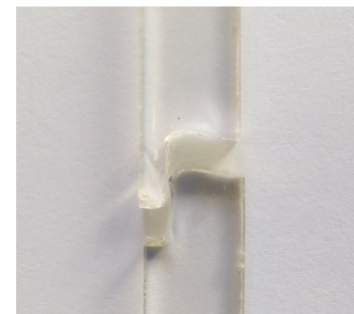
## Transportation

# DCPD advantage: Impact property

Comparison of Izod test



P-DCPD



Epoxy



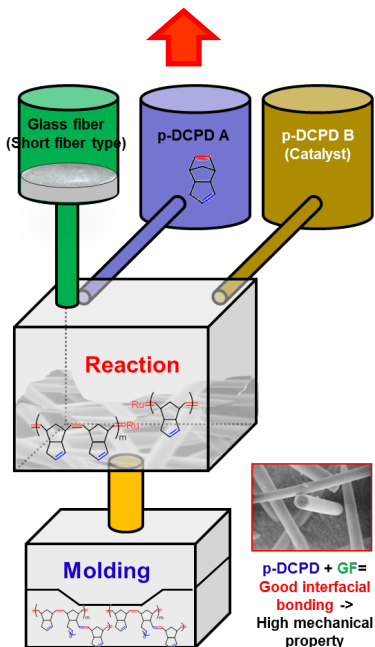
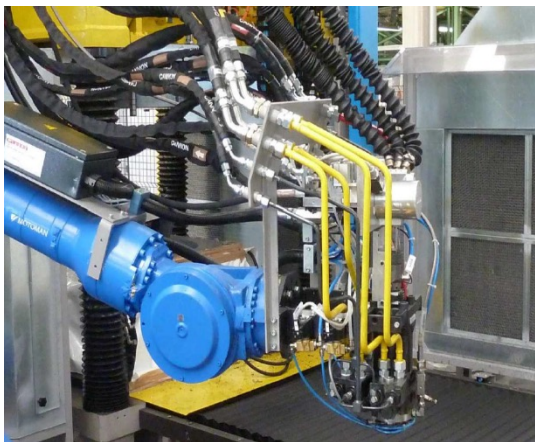
- Izod impact strength is much better than thermosetting polymer  
(Volvo Truck bump)



# Transportation

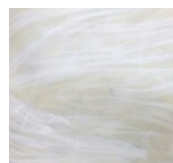
## Lately quality of LGF/p-DCPD

R-RIM (Wet Injection molding)



## Lately quality of LGF/p-DCPD

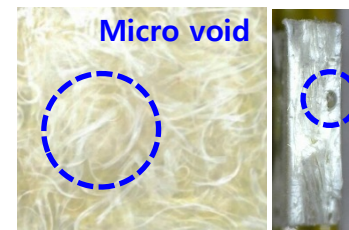
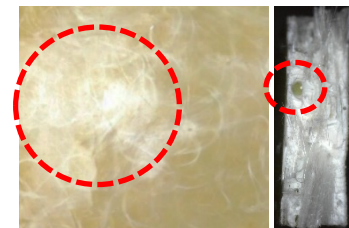
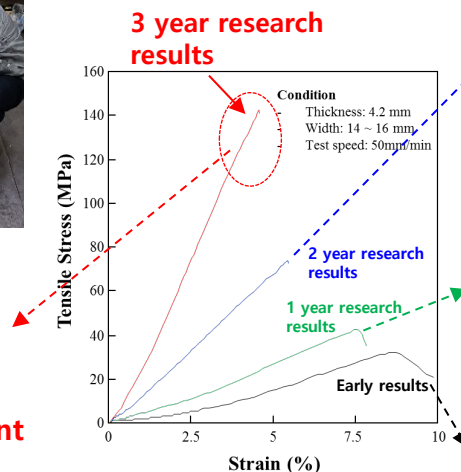
Target



Fiber arrangement



Interface fractured



Pull out

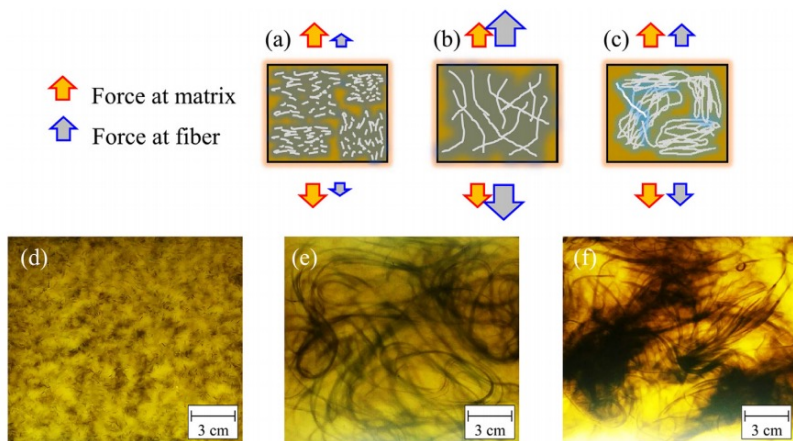
**Tensile strength: 118 MPa**  
**Flexural strength: 118 MPa**  
**Impact strength: 1420 MPa (25°C)**  
**1400 MPa (-40°C)**

# Transportation

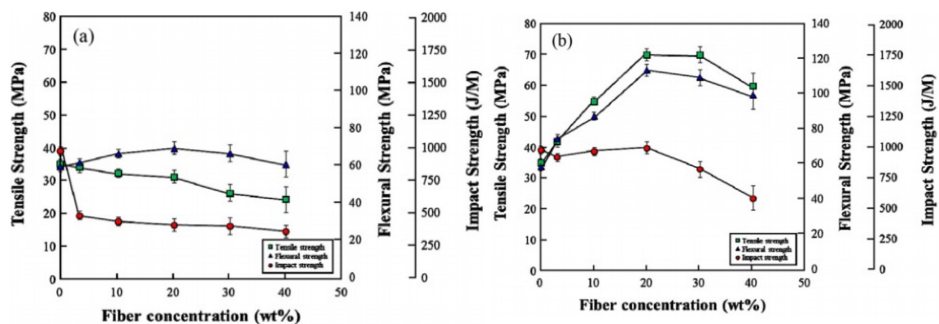
Cited 14st

Composites Part B 123, 74-80 (2017)

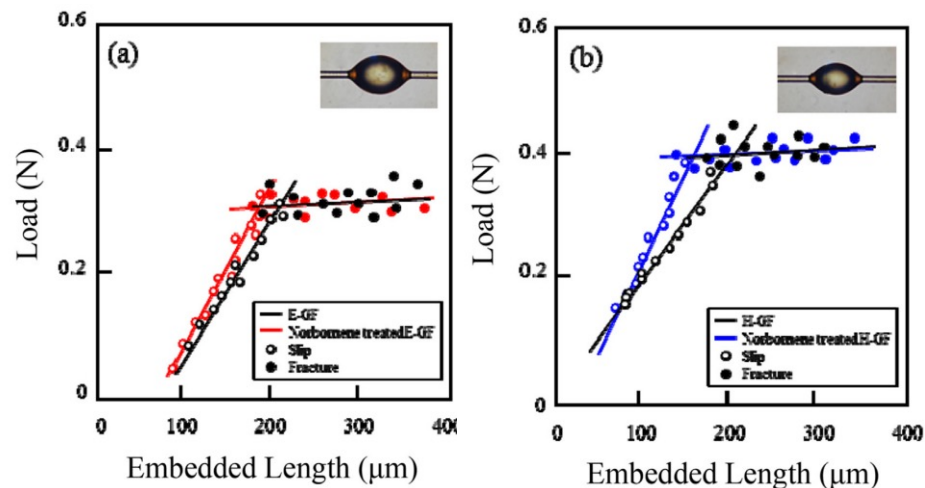
Reinforcing effects of glass fiber/p-DCPD with fiber concentrations, types, lengths and surface treatment



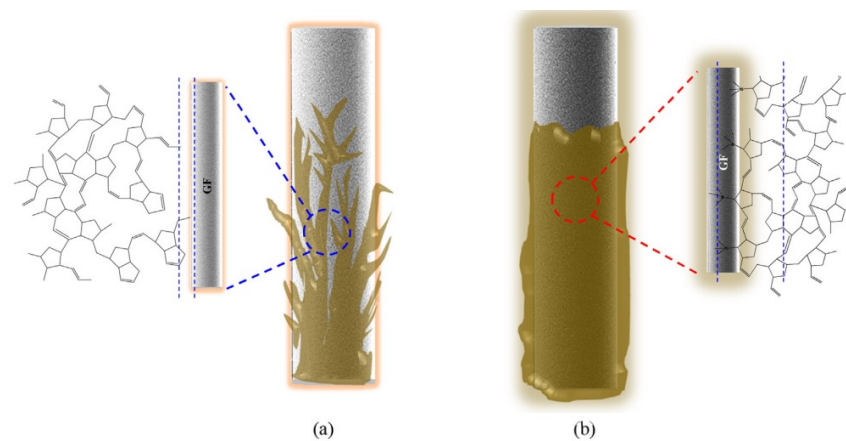
Modeling and photos of GF/p-DCPD illustrating the GF length effect:  
(a), (d) 3 mm GF/p-DCPD; (b), (e) 100 mm GF/p-DCPD; and (c), (f) 500 mm GF/p-DCPD



Mechanical property of LGF/p-DCPD composites with different fiber concentration:  
(a) 0.3 mm E-GF/p-DCPD; (b) 50 mm E-GF/p-DCPD



Microdroplet test load versus embedded lengths of GF/p-DCPD with different surface treatments; (a) E-GF, and (b) H-GF.



Schematic model of GF/p-DCPD fiber surfaces with different treatments: (a) neat H-GF/p-DCPD; and (b) norbornene treated H-GF/p-DCPD.

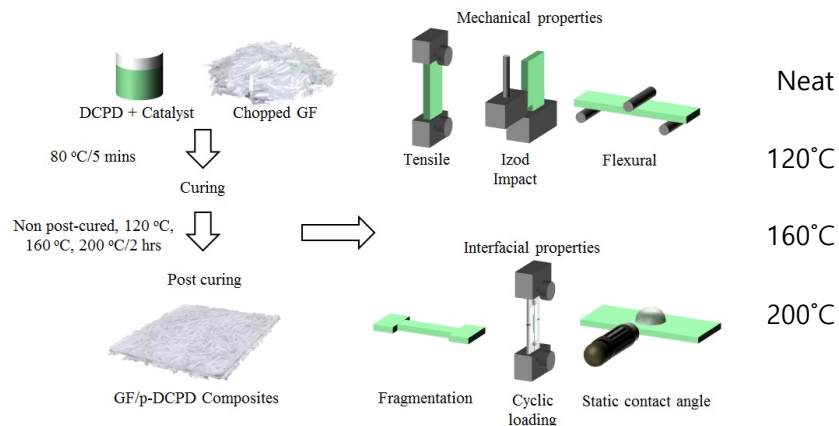
# Transportation

*Cited 2nd*

*Fibers and Polymers 19, 1989-1996 (2018)*

Mechanical and Interfacial Properties of Glass Fiber (GF)/Poly-Dicyclopentadiene (p-DCPD) Composites for Different Post Curing Conditions at Ambient and Low Temperatures

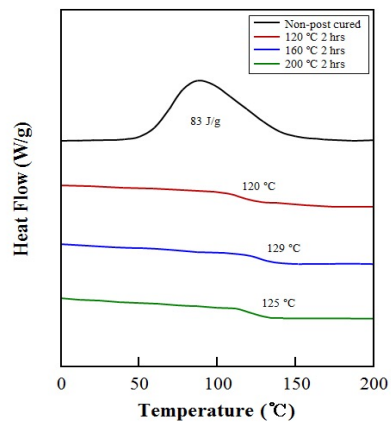
## Process to manufacture GF/p-DCPD composites



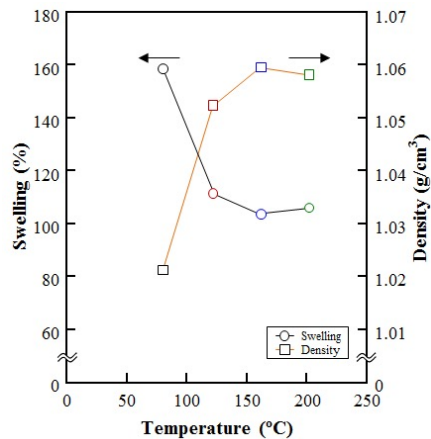
## Polarized photos of composites as different thermal treatment



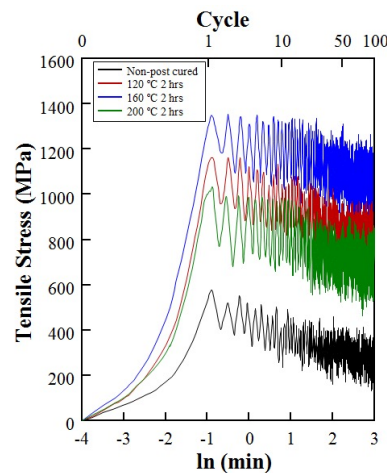
## DSC data



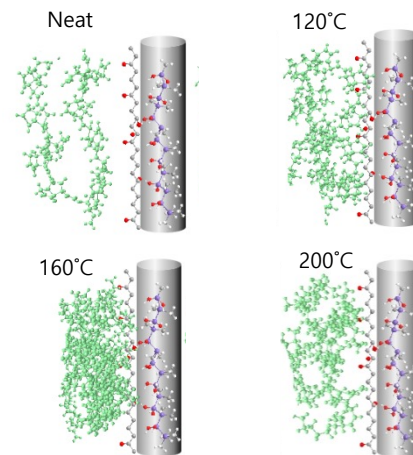
## Swelling and Density



## Cyclic Loading Test



## Interfacial bonding





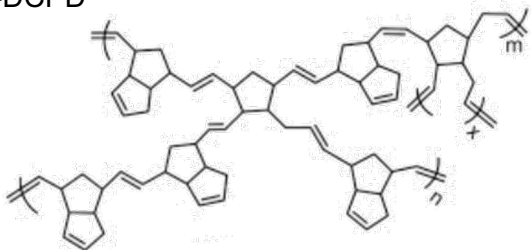
# Transportation

Cited 5th

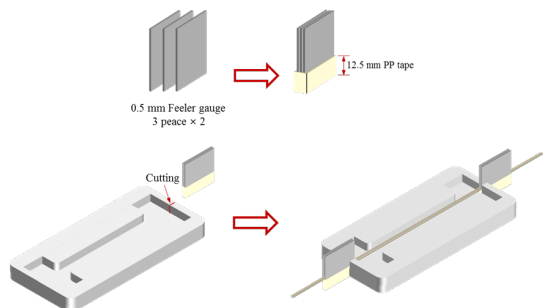
Composites Part B 153, 420-428 (2018)

Evaluation of Interfacial and Mechanical Properties of Glass Fiber (GF) and p-DCPD Composites with Surface Treatment of Glass Fiber

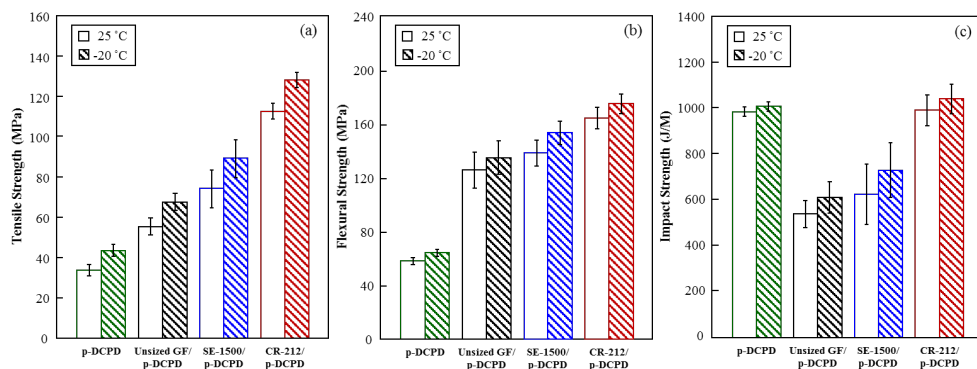
p-DCPD



Process to manufacture Fragmentation specimen



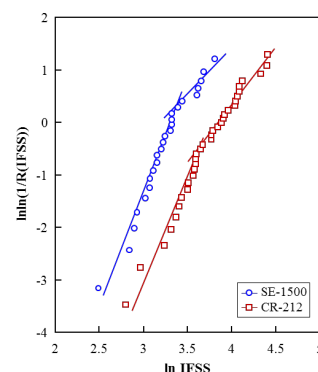
Mechanical property



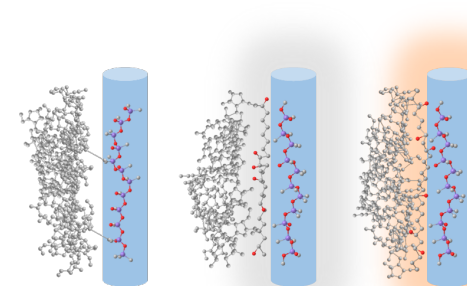
Polarized photos



Weibull distribution for IFSS



Schematics of interface between p-DCPD and GF



Surface energy of materials

	$\gamma_s$	$\gamma_s^{LW}$	$\gamma_s^{AB}$	$\gamma_s^+$	$\gamma_s^-$	$\gamma^d$	$\gamma^p$	$W_a$
DCPD	24.9	19.6	5.2	17.8	0.4	10.1	8.6	-
Unsize	32.6	25.8	6.9	36.6	0.3	12.0	29.3	57.3
SE-1500	34.2	25.5	8.7	22.1	0.8	15.5	21.0	58.4
CR-212	38.1	35.4	2.7	4.2	0.4	32.4	4.6	60.8

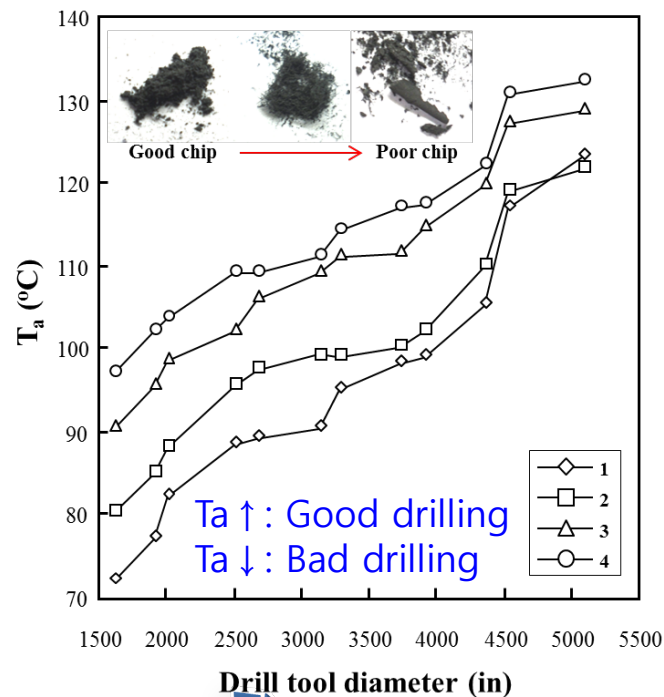
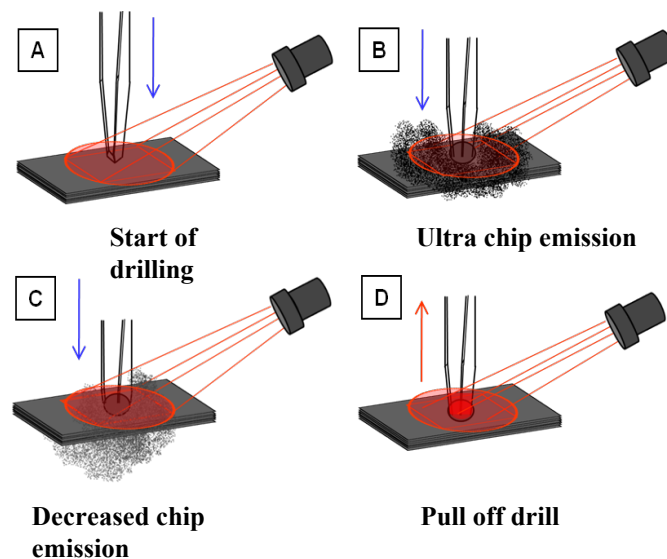
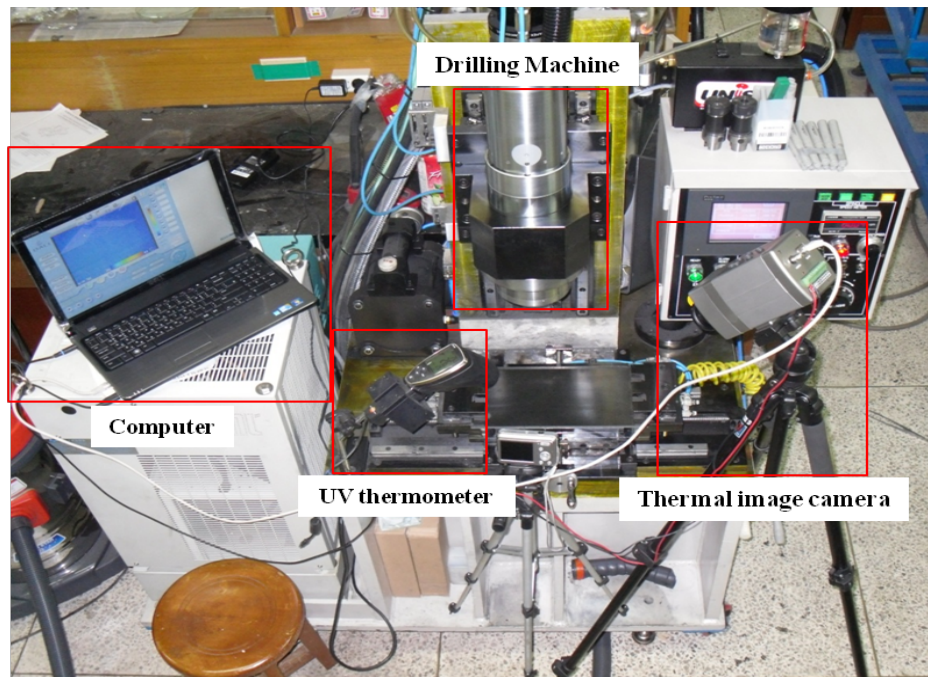


# Aerospace

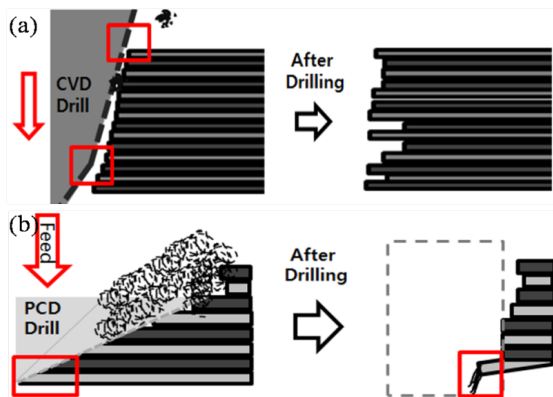
Cited 6th

*Journal of Composite Materials* 47 (2013) 2005–2012

A new strategy of carbon fiber reinforced plastic drilling evaluation using thermal measurement



Modeling of drilling result of a) CVD Drill; (b) PCD Drill

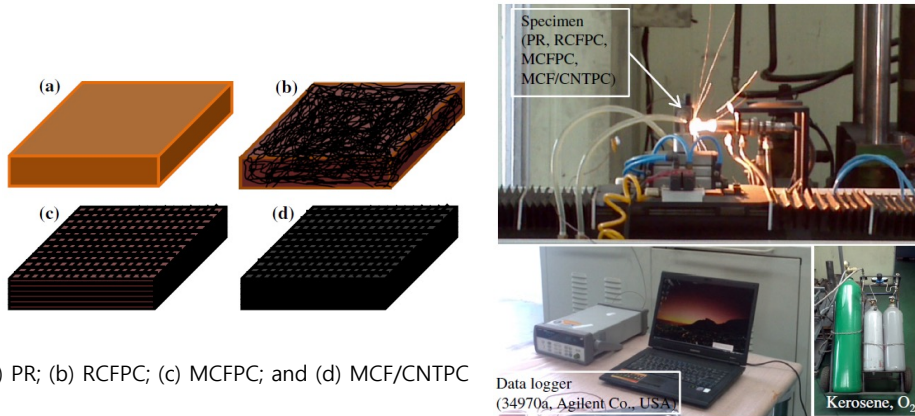


# Fire Retardant

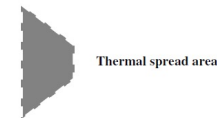
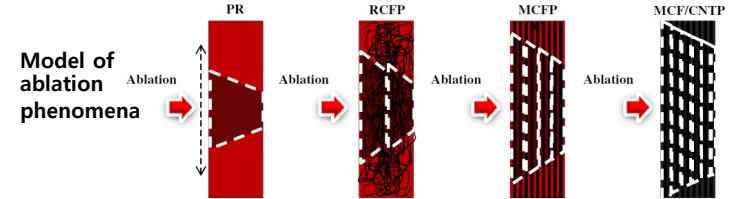
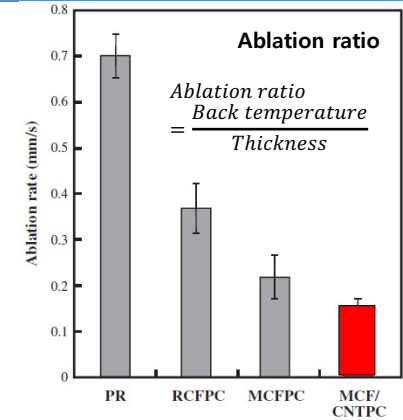
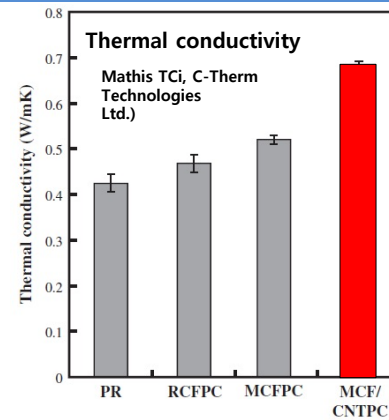
*Cited 76th*

*Composites: Part B* 67, 22–29 (2014)

Effects of carbon nanotubes and carbon fiber reinforcements on thermal conductivity and ablation properties of carbon/phenolic composites

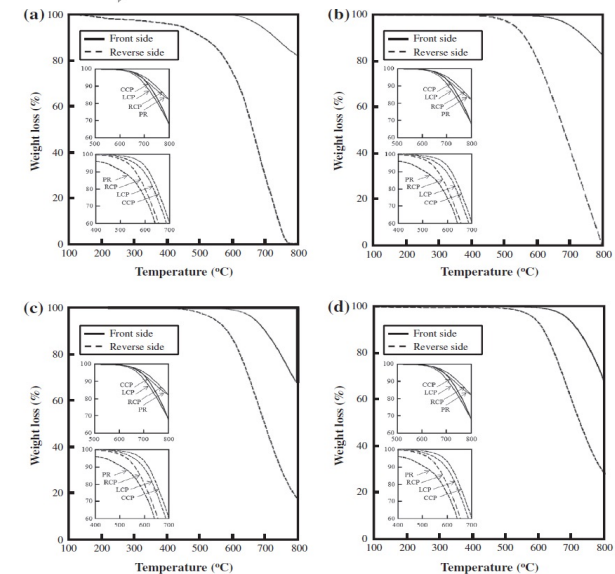
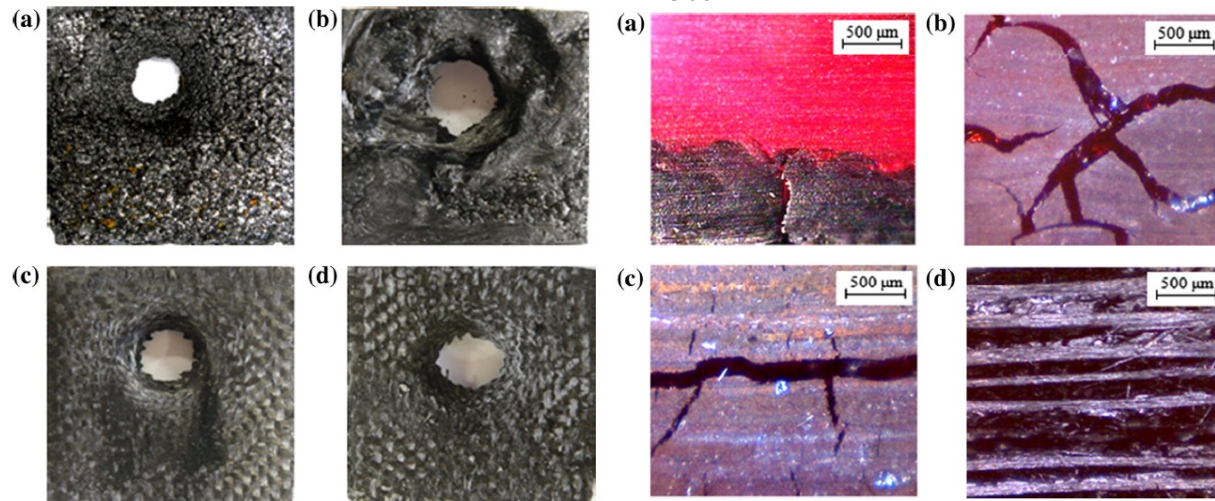


(a) PR; (b) RCFPC; (c) MCFPC; and (d) MCF/CNTPC



Front

Side



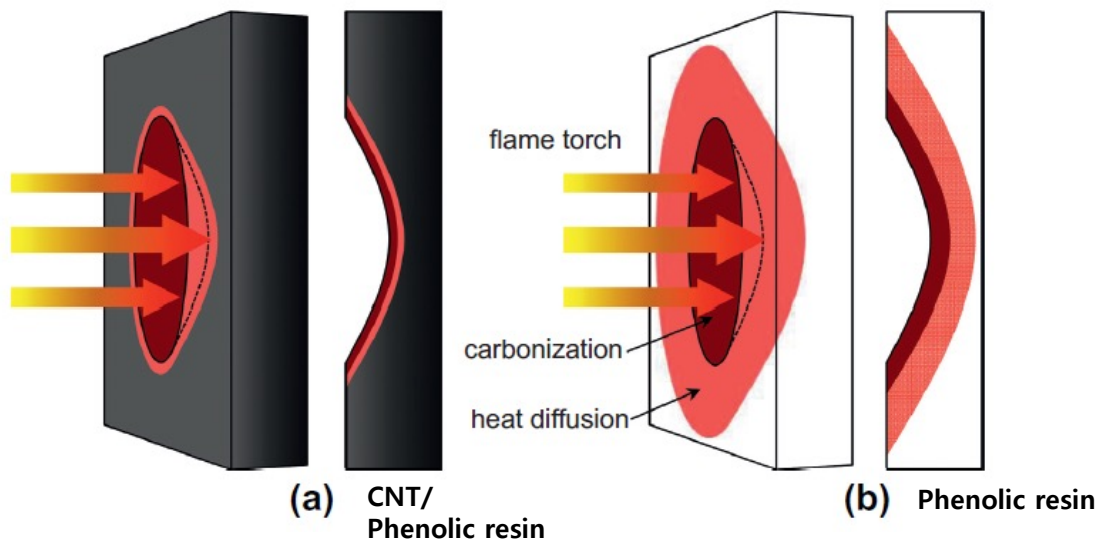
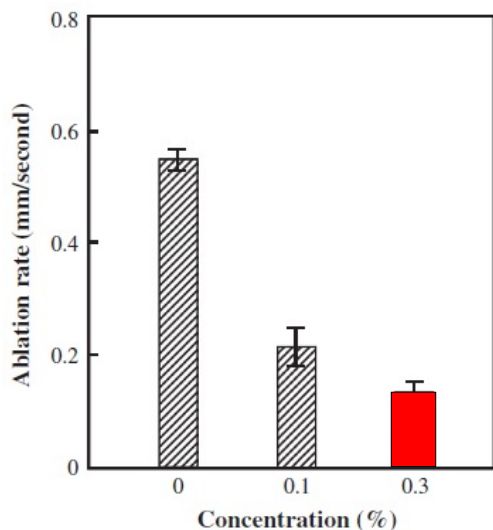
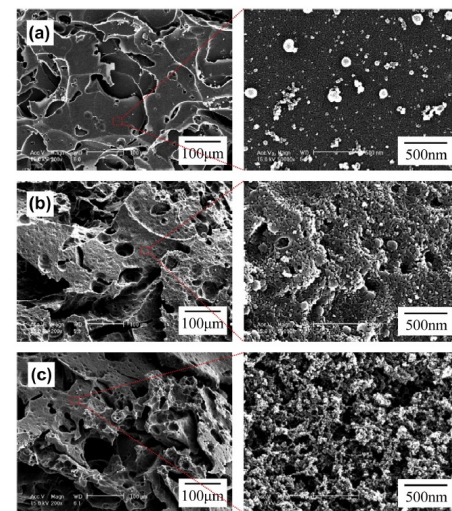
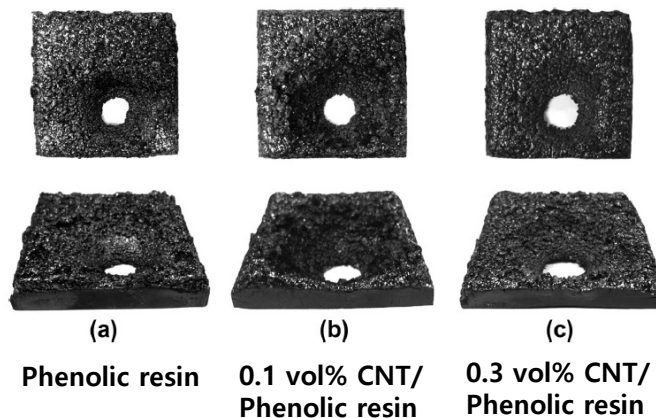
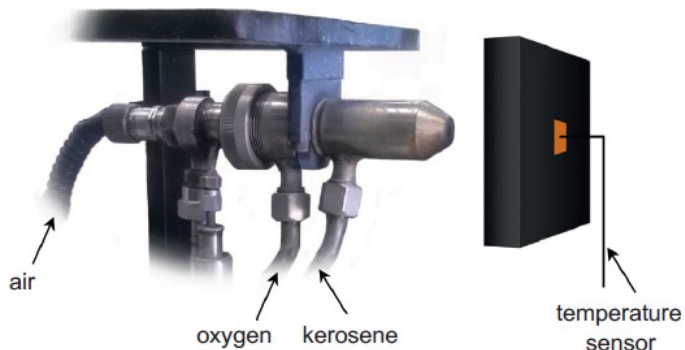


# Fire Retardant

*Cited 59th*

*Composites: Part B 60, 597–602 (2014)*

Ablative and mechanical evaluation of CNT/phenolic composites  
by thermal and microstructural analyses

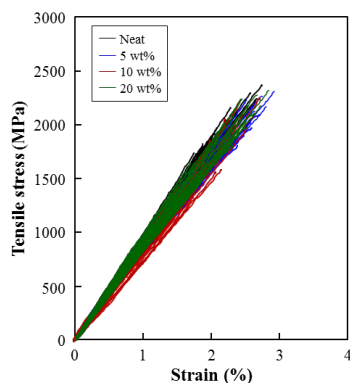
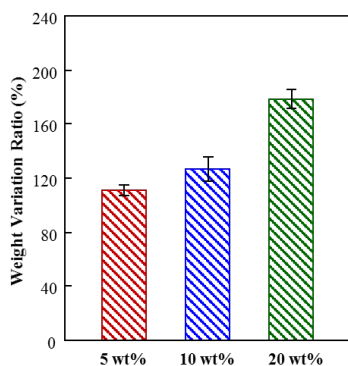
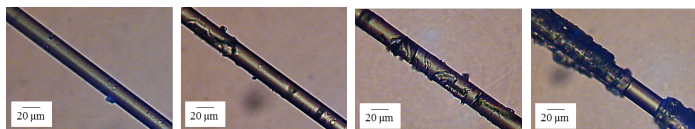
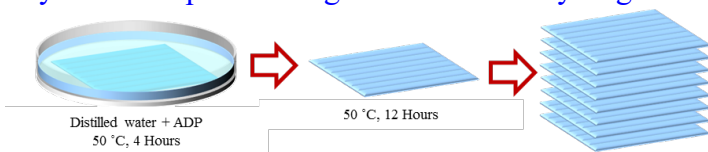


# Fire Retardant

*Cited 20th*

**Composites: Part B** 167, 221-230 (2017)

Interfacial Properties and Fire Retardance of Glass fiber/Unsaturated Polyester Composite using Ammonium Dihydrogen Phosphate

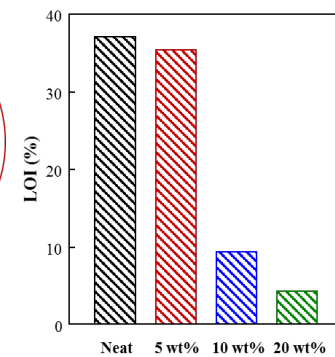
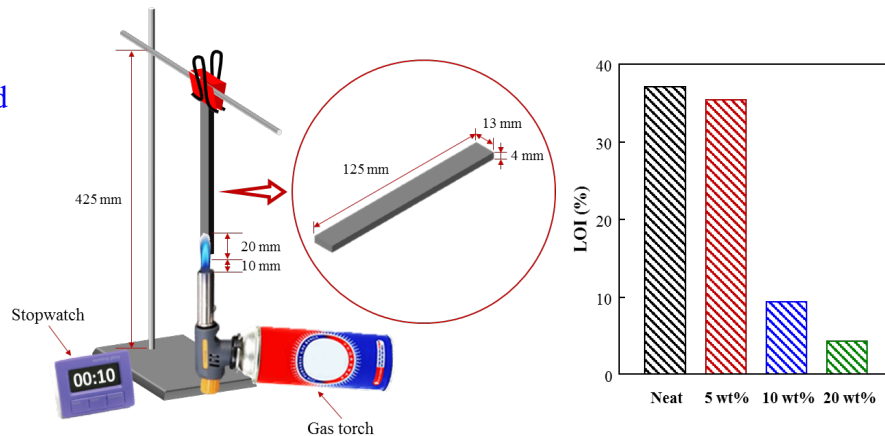


Type	Diameter (µm)	Strength (MPa)	Modulus (GPa)	Elongation (%)	$\alpha^2$	$\beta^3$	$\alpha_1$	$\beta_1$	$\alpha_2$	$\beta_2$
Neat	17.1 (0.15) <sup>1</sup>	1823.9 (231.4)	81.6 (1.68)	2.24 (0.31)	1926	8.7	1758	17.8	1902	6.2
5 wt%	17.2 (0.18)	1824.8 (251.5)	80.2 (1.69)	2.28 (0.32)	1935	8.0	1775	14.2	1914	5.9
10 wt%	17.2 (0.13)	1821.9 (253.5)	80.9 (1.70)	2.26 (0.37)	1932	7.9	1779	13.7	1908	5.8
20 wt%	17.1 (0.16)	1827.9 (243.1)	79.1 (1.76)	2.31 (0.42)	1934	8.3	1769	15.9	1906	5.8

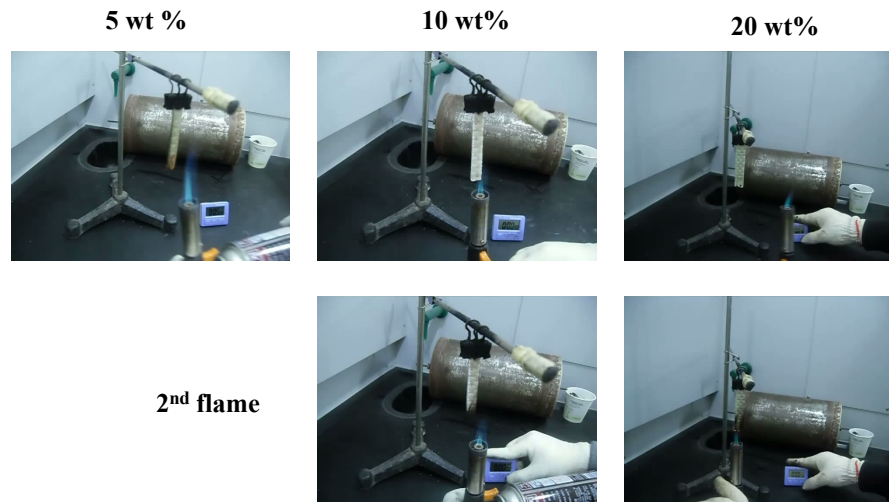
<sup>1)</sup> Standard deviation (SD)

<sup>2)</sup> Scale parameter for fiber strength

<sup>3)</sup> shape parameter for fiber strength



1<sup>st</sup> flame



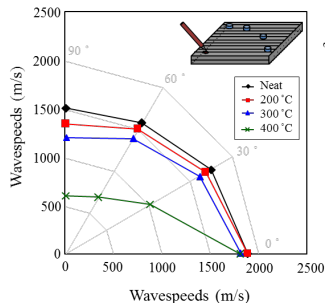
Type	T <sub>1</sub> (second)	T <sub>2</sub> (second)	UL-94 V	L.O.I. <sup>1)</sup> (g)
Neat	All burning	-	-	1.74
5 wt%	All burning	-	-	1.68
10 wt%	37	0	V-2	0.45
20 wt%	8	18	V-1	0.21



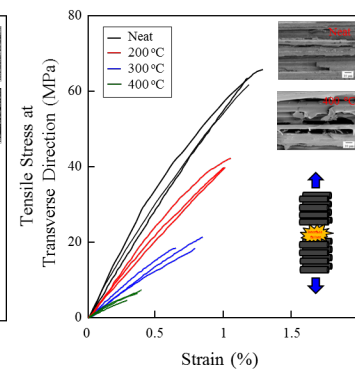
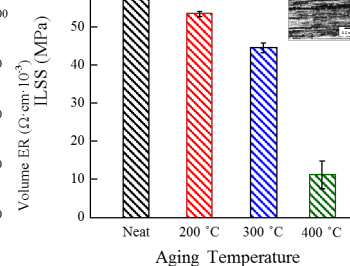
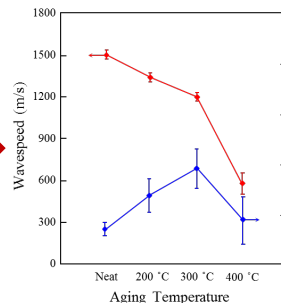
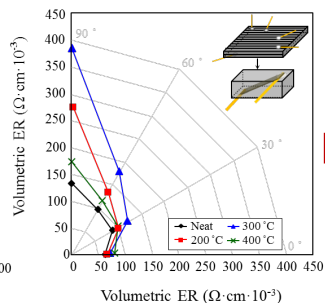
Cited 9th

*Composite Structures 196, 21-29 (2018)*Evaluation of Thermally-Aged Carbon Fiber/Epoxy Composites using  
Acoustic Emission, Electrical Resistance and Thermogram

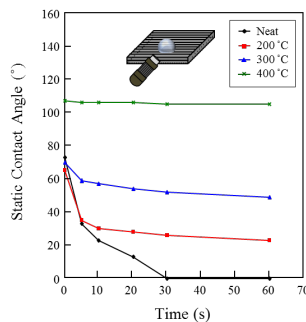
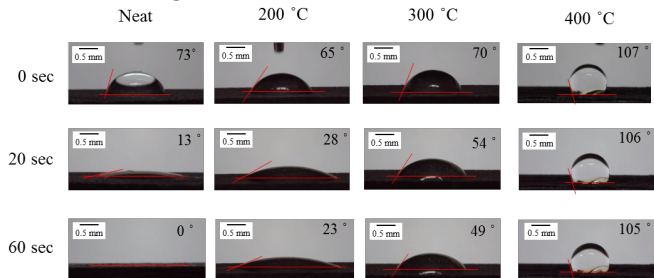
## AE evaluation



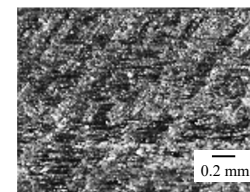
## Electrical Evaluation



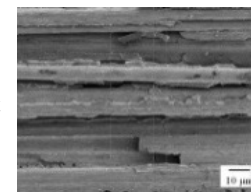
## Contact Angle



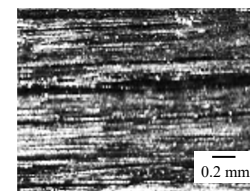
Neat



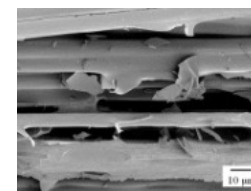
Neat



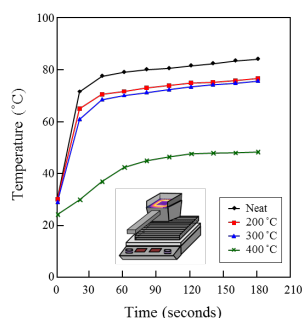
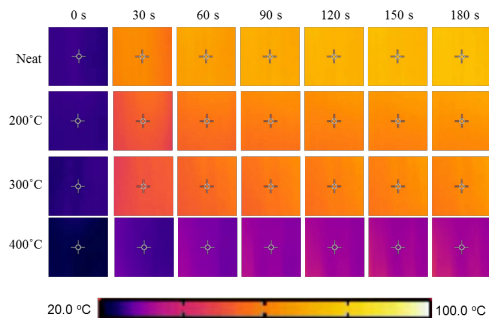
400 °C



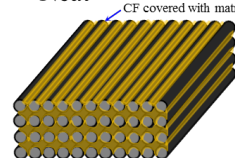
400 °C



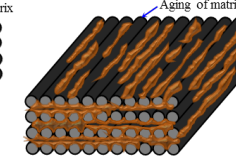
## Thermal evaluation



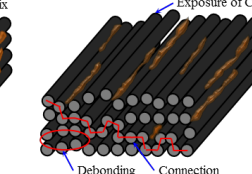
Neat



300 °C



400 °C



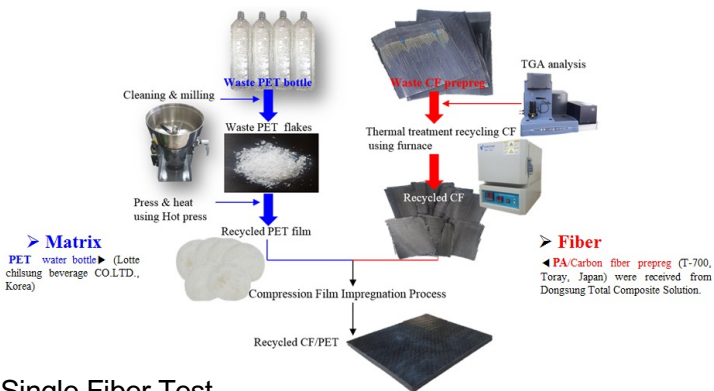
# Recycling

*Cited 9st*

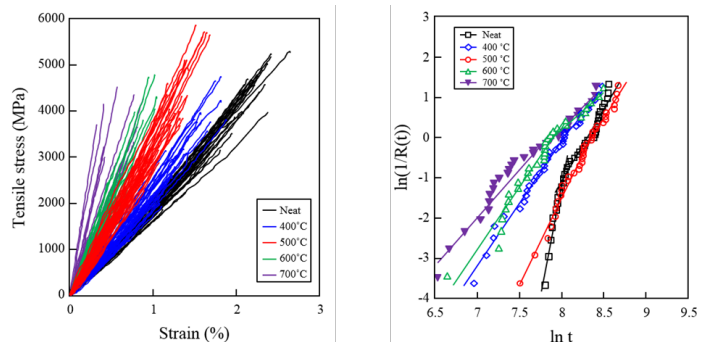
*Fibers and Polymers* 19, 1767-1775 (2018)

# Investigation of Interfacial and Mechanical Properties of Various Thermally-Recycled Carbon Fibers/Recycled PET Composites

## Materials from waste CF, PET



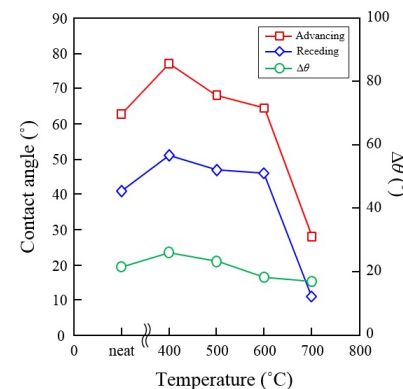
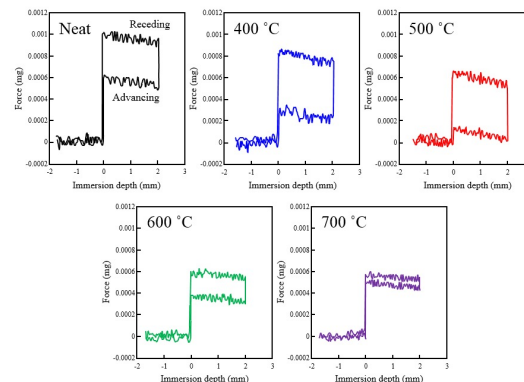
## Single Fiber Test



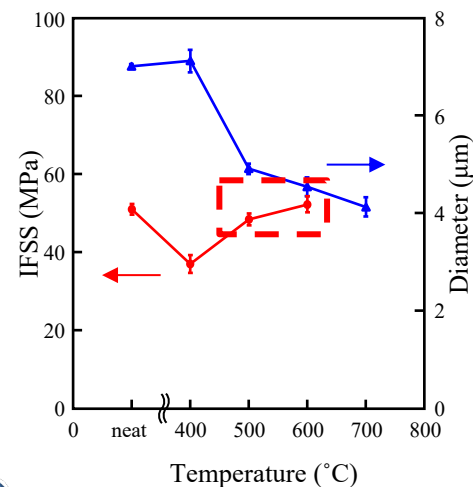
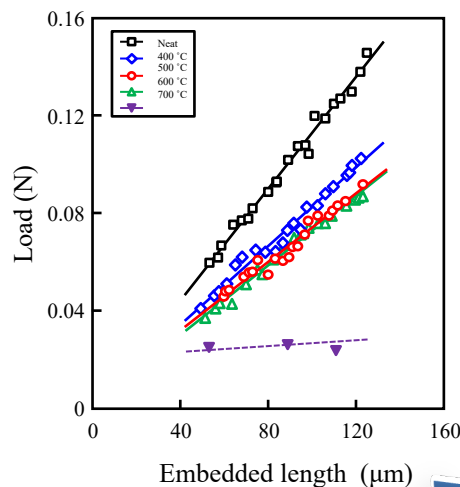
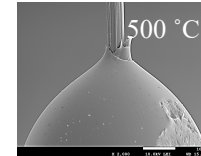
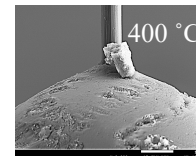
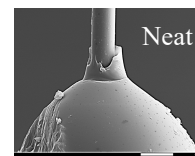
Recycled Temperature (°C)	Diameter (mm)	Strength (MPa)	Modulus (GPa)	Elongation (%)	COV(%)	$\alpha^3$	$\beta^4$	$a_1$	$B_1$	$a_2$	$\beta_2$
neat	7.02 (0.09)	4231 (964) <sup>91</sup>	225 (26.4)	1.9 (0.41)	0.22	4138	4.7	3343	10.9	4083	3.6
400	7.13 (0.46)	2781 (981)	238 (91.9)	1.2 (0.33)	0.6	3121	3.0	3046	3.1	3035	2.5
500	4.92 (0.21)	3726 (1042)	300 (54.2)	1.3 (0.28)	0.26	4328	4.0	4211	4.3	4237	3.3
600	4.55 (0.38)	2561 (1104)	305(105)	0.95(0.33)	0.39	2890	2.7	2738	3.1	2539	1.6
700	4.14(0.40)	2349(1128)	382(157)	0.62(0.20)	0.48	2668	2.1	2394	2.5	2858	2.36

<sup>1)</sup> Standard deviation (SD)<sup>2)</sup> Coefficient of variation (COV) of fiber tensile strength<sup>2)</sup> Scale parameter for fiber strength<sup>4)</sup> Shape parameter for fiber strength

## Dynamic Contact Angle



## Microdroplet Pull-out Test



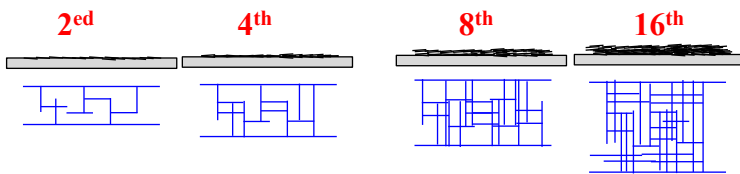
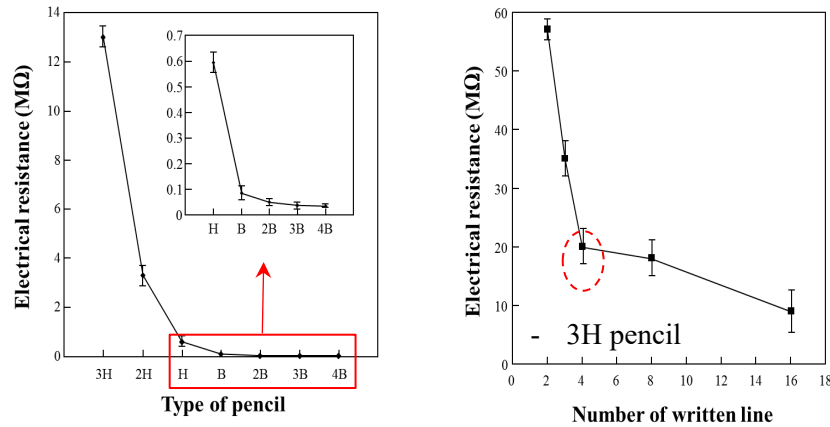
## Part 5

### Recent & Current Works

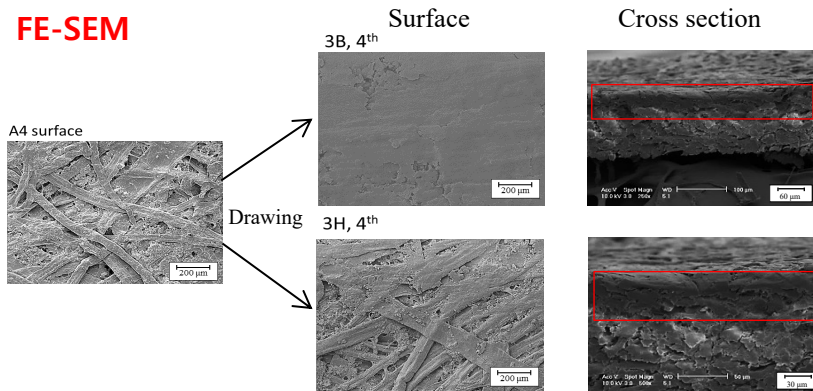
# Current works

## Pencil Drawn Paper Sensor (PDPS)

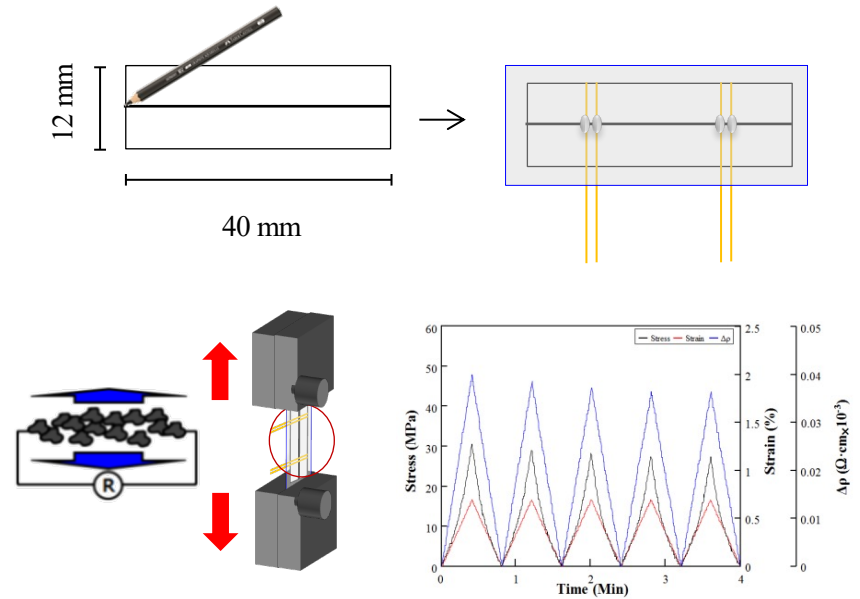
### Pencil drawing



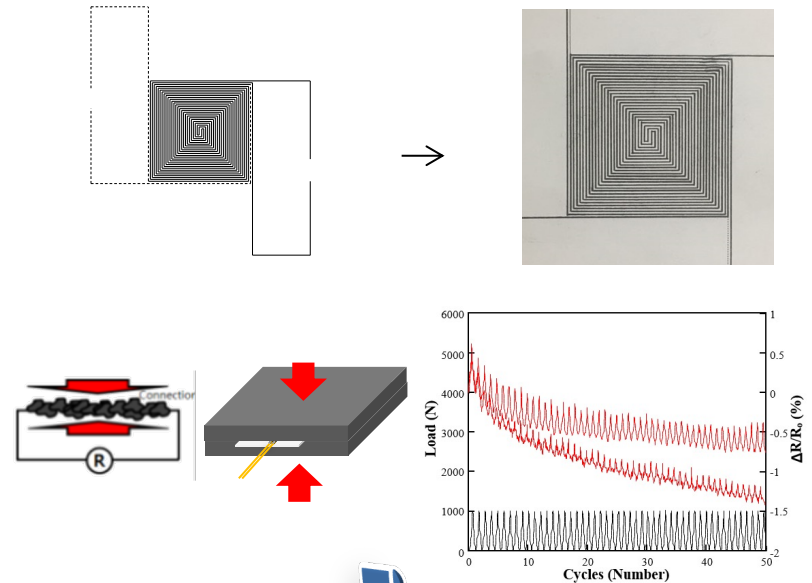
### FE-SEM



### Tensile sensor



### Compressive sensor





*Fibers and Polymers* 21, 1560-1565 (2020)

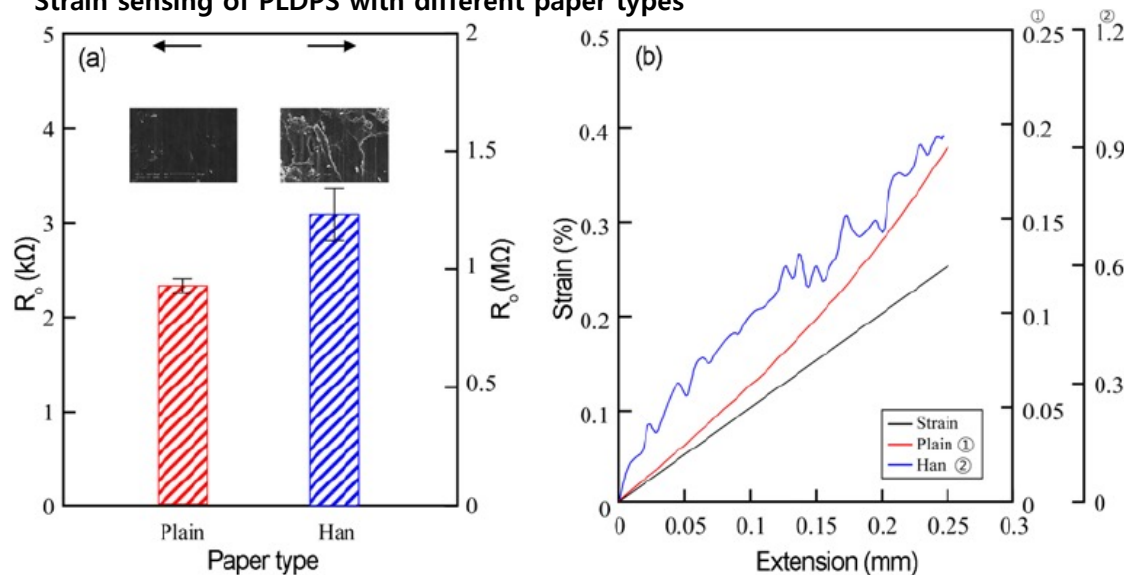
Innovation of Pencil Lead Drawn Paper Sensors (PLDPS) Using Electrical Resistance (ER) Measurement:

I. Optimal Conditions of Interfacial, Mechanical, and Sensing Properties

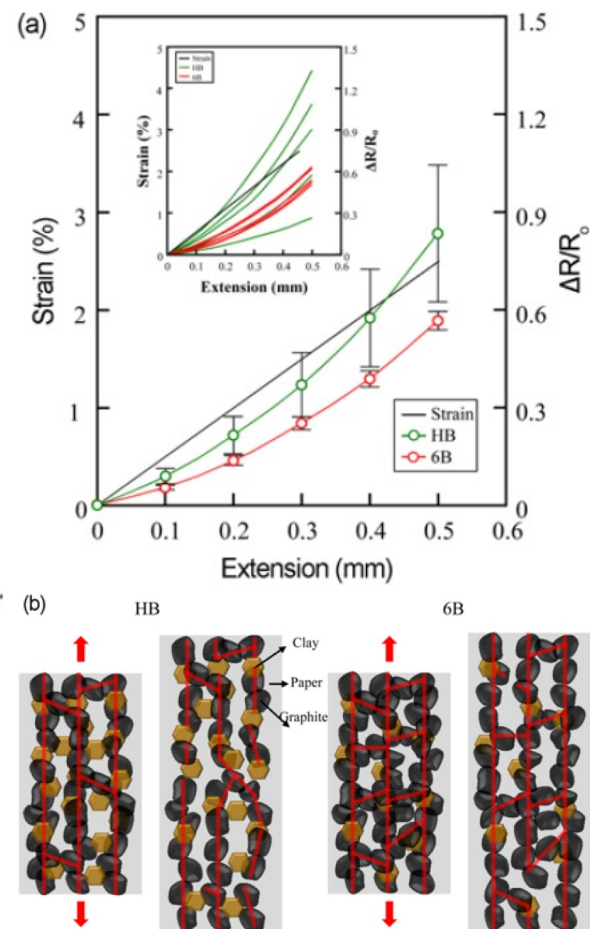
Configuration of different pencil lead types

Hardness	4H	3H	2H	H	F	HB	B	2B	3B	4B	5B	6B	7B	8B		
Graphite (%)	55	58	60	63	66	68	71	74	76	79	82	84	87	90		
Clay (%)	39	36	34	31	25	26	23	20	18	15	10	7	5	2		
Wax (%)	5	5	5	5	5	5	5	5	5	5	5	5	5	5		

Strain sensing of PLDPS with different paper types



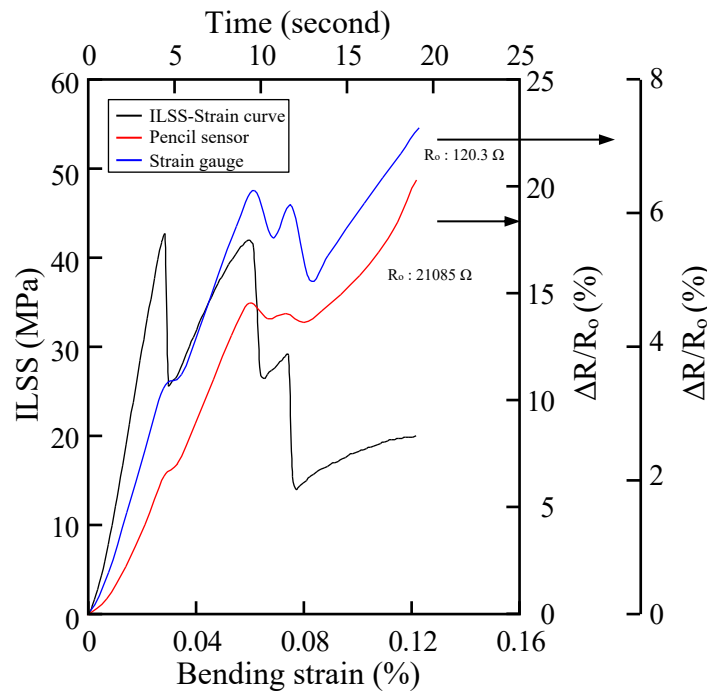
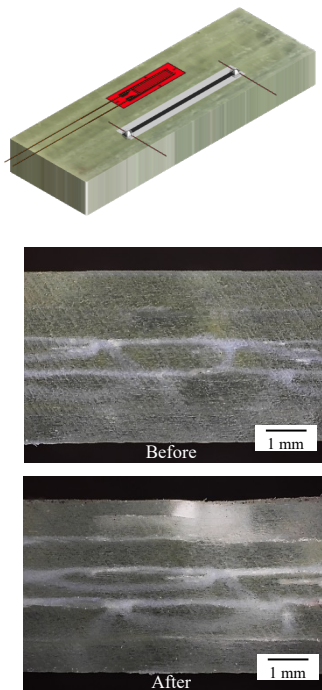
Strain sensing of PLDPS with different pencil types



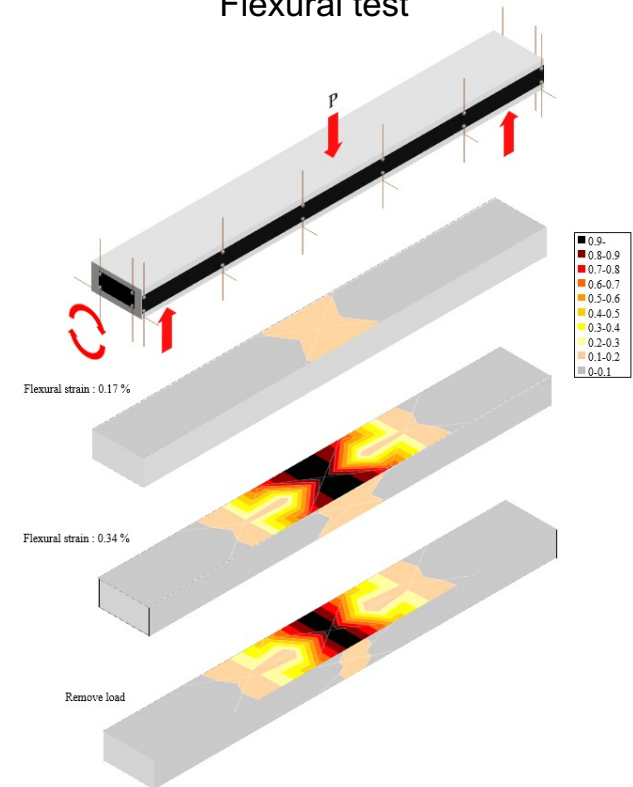
# •Results and Discussion

## Flexural detecting results of FRP using pencil sensor

Short beam test



Flexural test



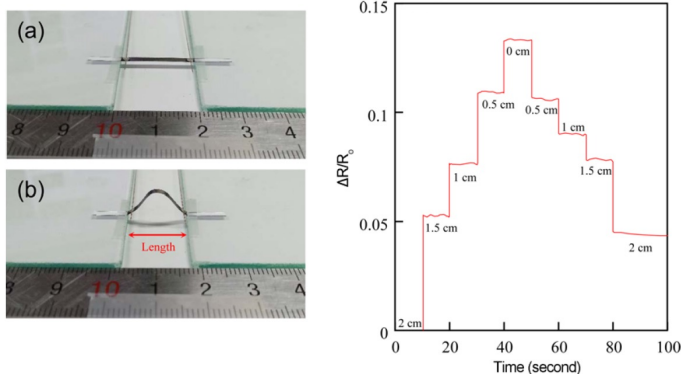
A specimen consisting of a single mass had a larger change in ER due to a stronger deformation at the center than at the edge and at the lower side than at the side.

*Fibers and Polymers* 21, 1566-1572 (2020)

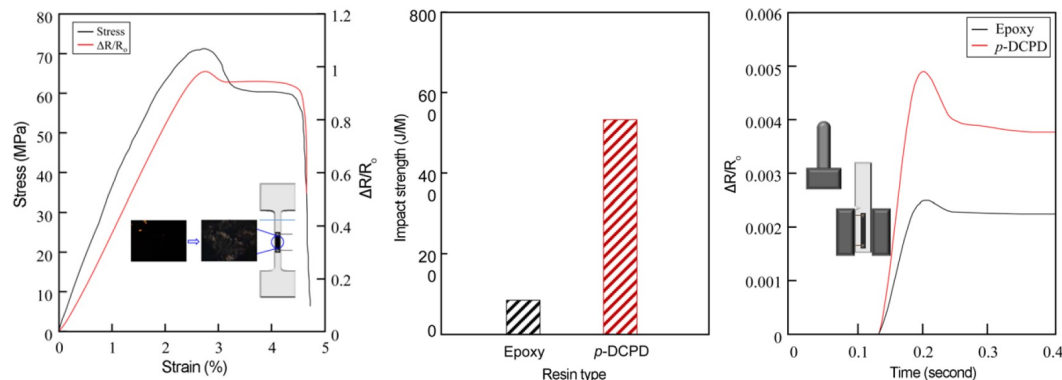
Innovation of Pencil Lead Drawn Paper Sensors (PLDPS) Using Electrical Resistance (ER) Measurement:

II. Load, Micro-Damage, and Thermal Sensing on Composites by PLDPS

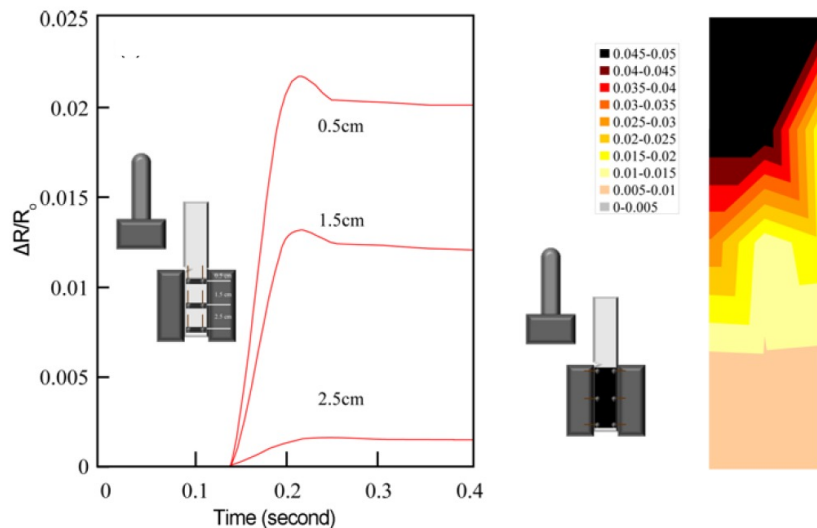
### ER sensing of bending property of PLDPS



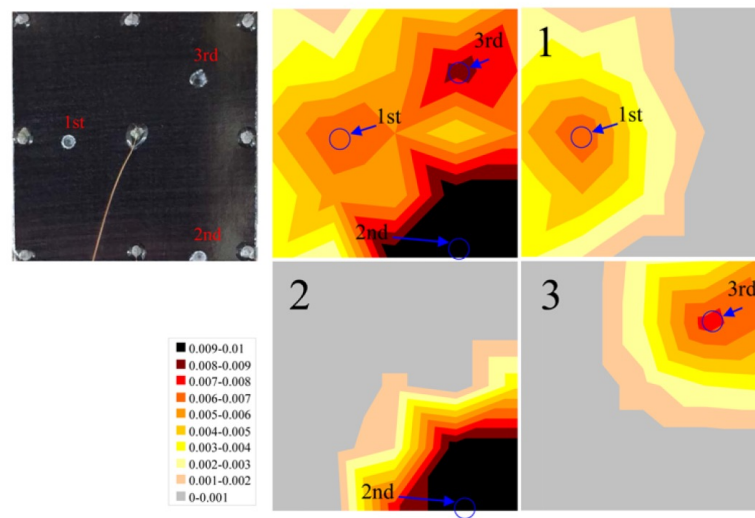
### Mechanical properties sensing of PLDPS



### Damage mapping in impact test *in-situ*



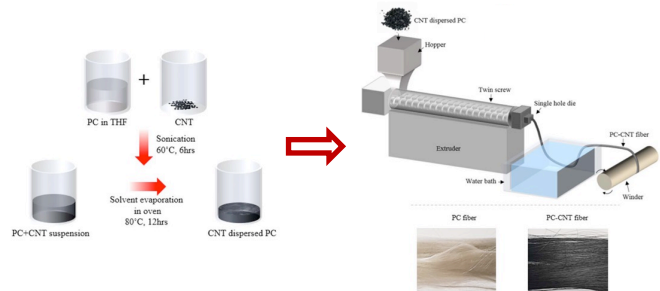
### Damage mapping in hole drilling process *in-situ*



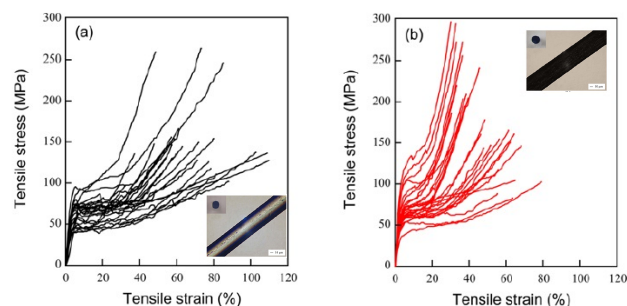
*Fibers and Polymers* 20, 2400-2406 (2019)

## Interfacial and Mechanical Properties of Carbon Fiber Reinforced Polycarbonate (PC) Film and PC Fiber Impregnated Composites

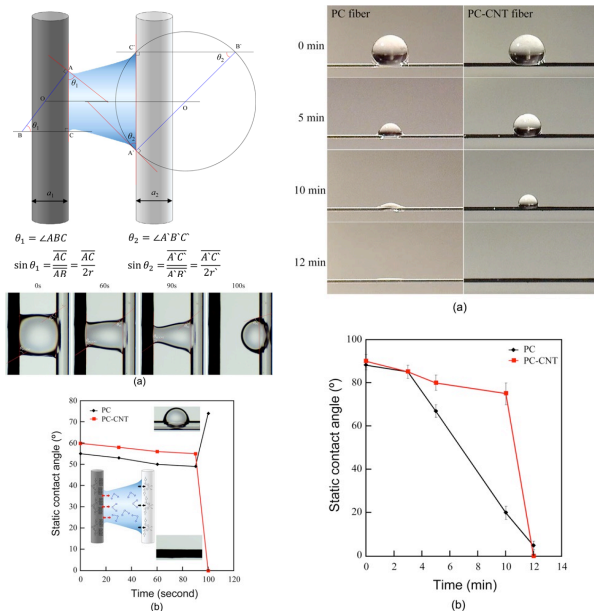
### Scheme of CNT-PC fiber manufacturing process



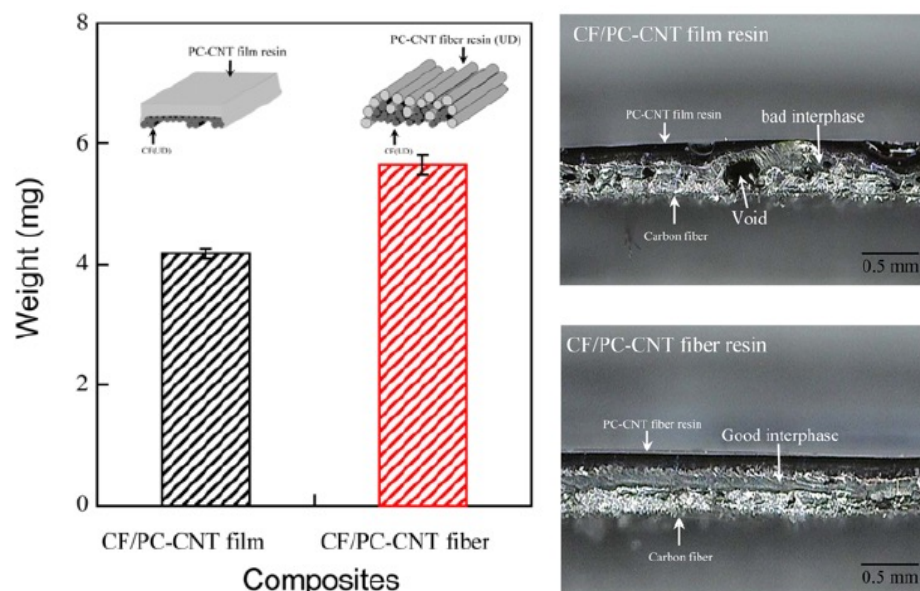
### Tensile strength of PC fiber with CNT containing



### Wettability test of PC and CNT-PC fiber at same time



### Impregnation property of PC fiber with CNT containing by UD carbon fiber



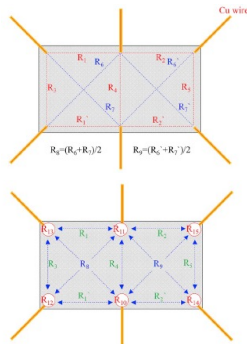
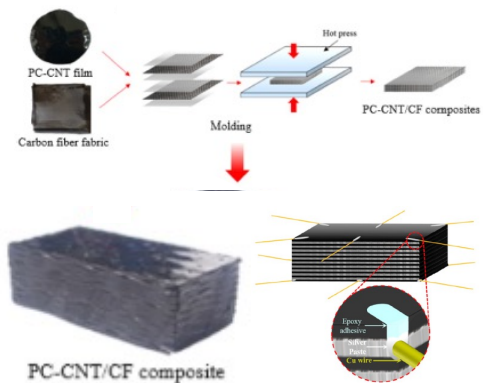


**Cited 12th**

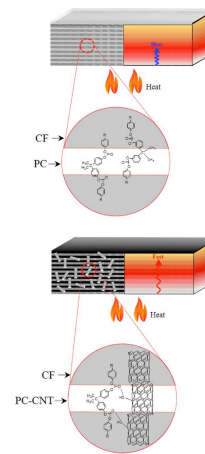
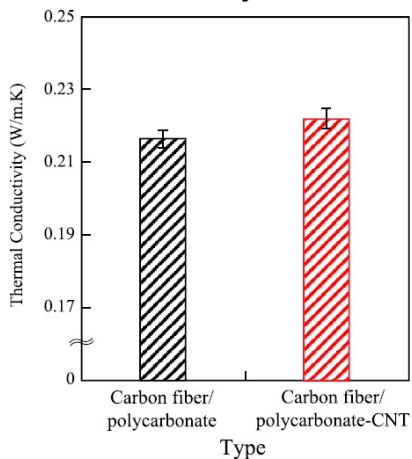
**Polymer Testing** 81, 106247 (2020)

Thermal transfer, interfacial, and mechanical properties of carbon fiber/polycarbonate-CNT composites using infrared thermography

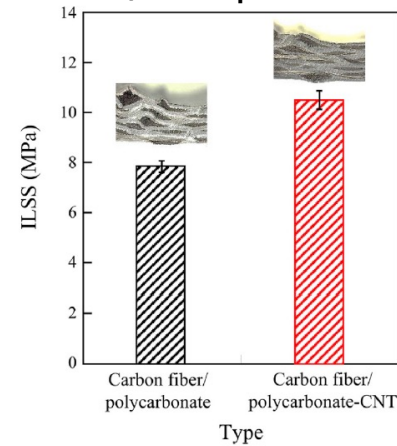
### Scheme of ER measurement of CNT-PC/CF composites



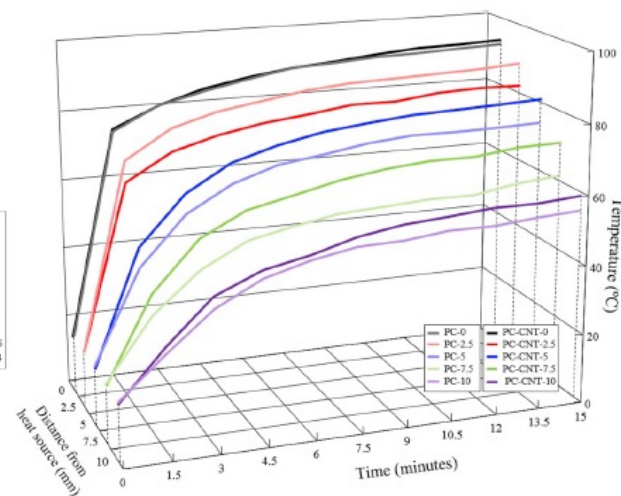
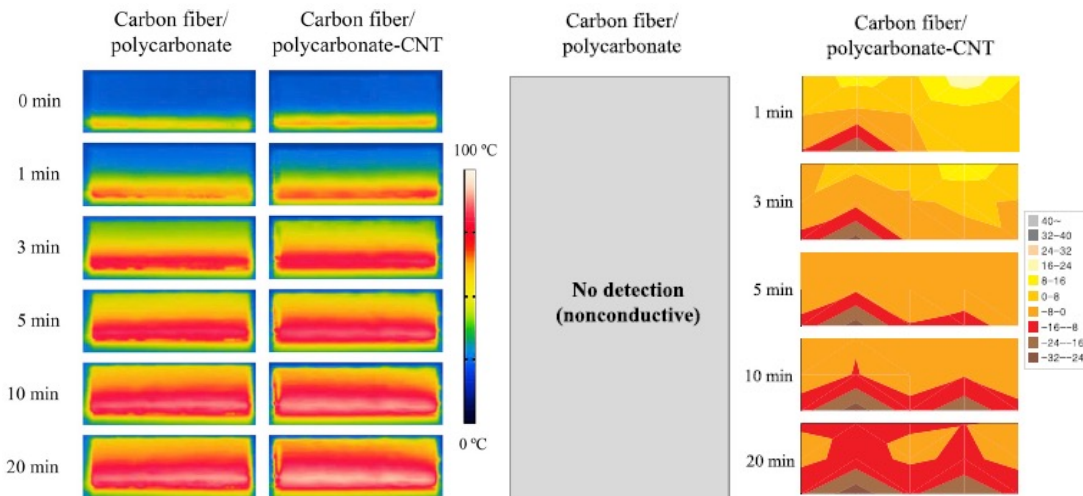
### Thermal conductivity of CNT-PC/CF composites



### Interfacial property of CNT-PC/CF composites



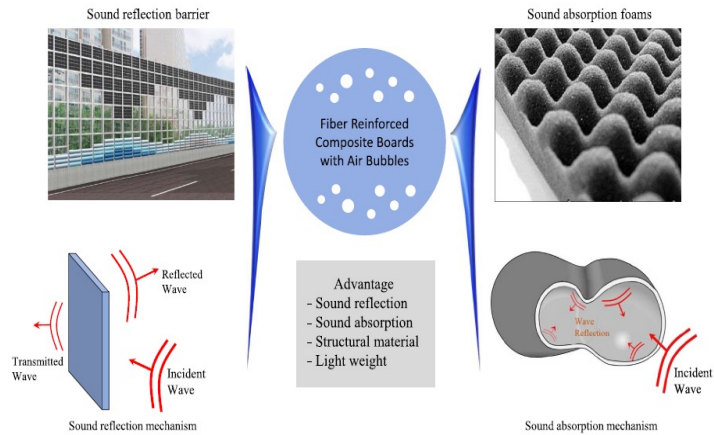
### Thermal observation of CNT-PC/CF composites



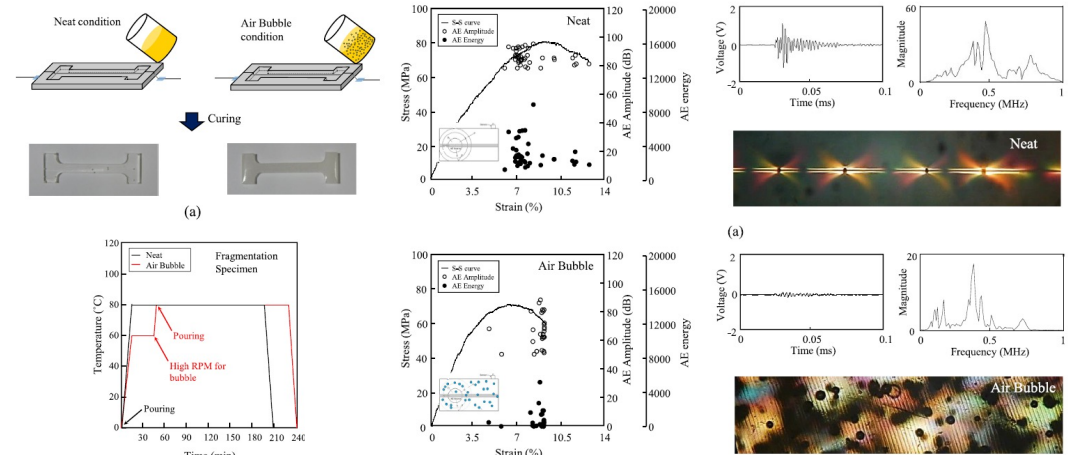
**Cited 5th**

**Composites Science and Technology 194, 108166 (2020)**

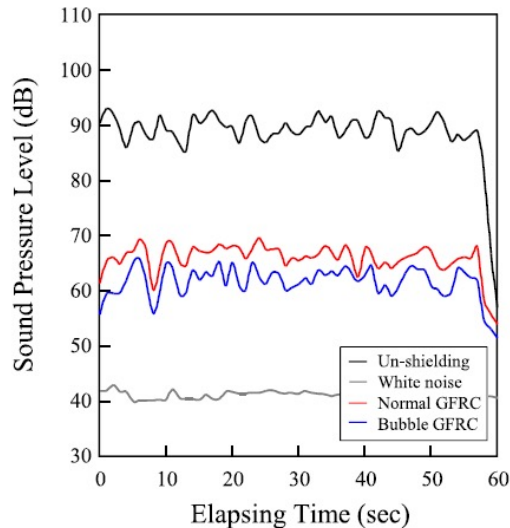
Manufacturing and qualitative properties of glass fiber/epoxy composite boards with added air bubbles for airborne and solid-borne sound insulation



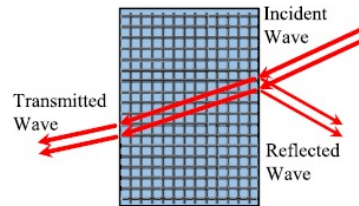
**Fragmentation tests for AE with bubble containing**



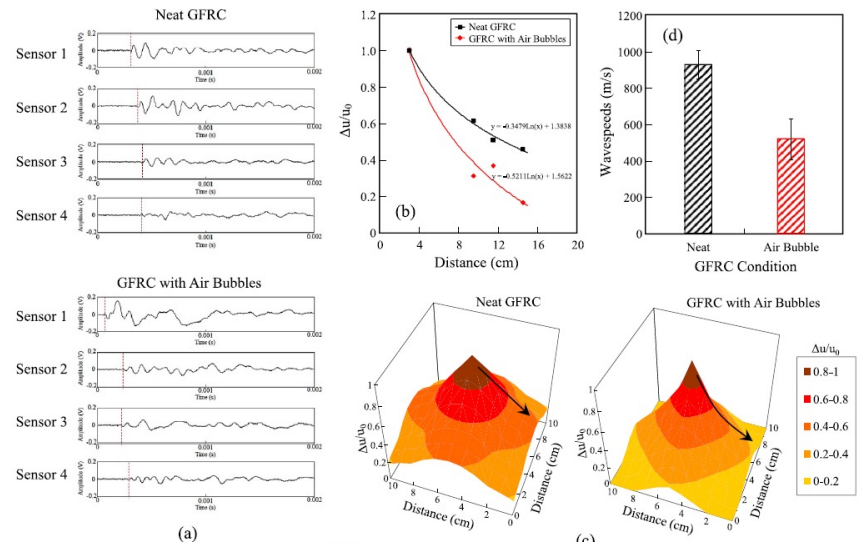
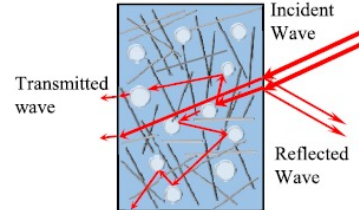
**Sound insulation measurement using AE and decibel meter**



**Fabric Bidirectional GF Mat**

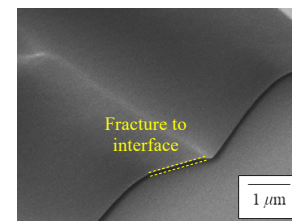
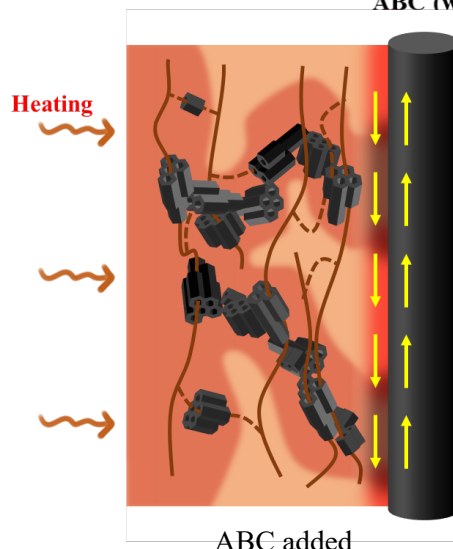
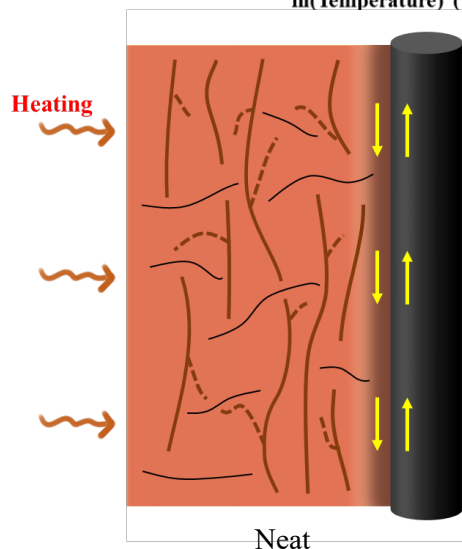
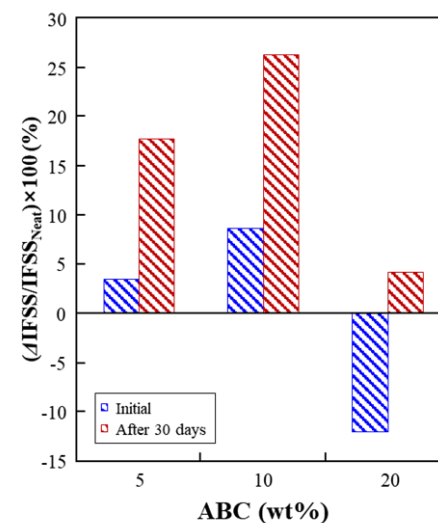
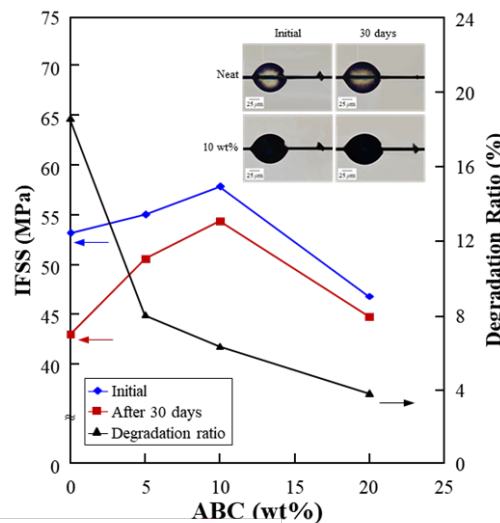
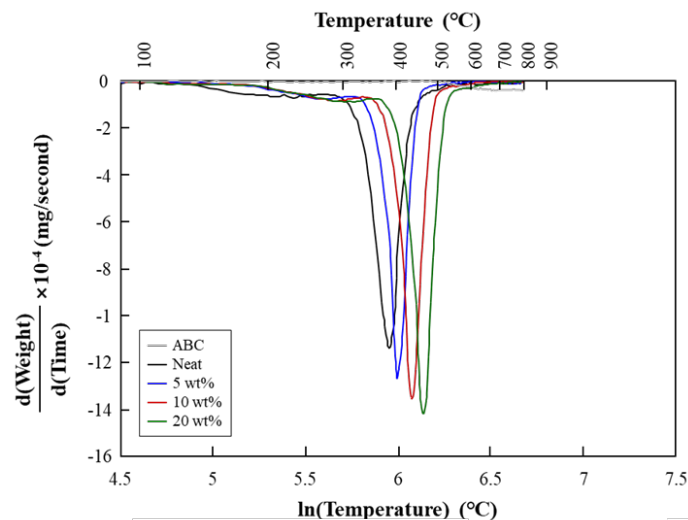


**Randomly-Chopped GF Mat**

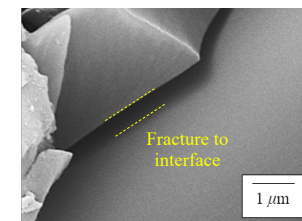


# Composites Part A 151, 106660 (2021)

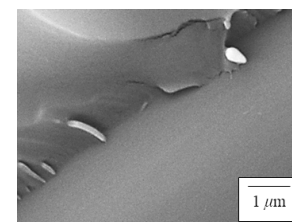
Evaluation of interfacial, dispersion, and thermal properties of carbon Fiber/ABC added epoxy composites manufactured by VARTM and RFI methods



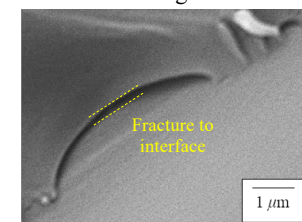
Neat-initial



Neat-degraded



ABC-initial



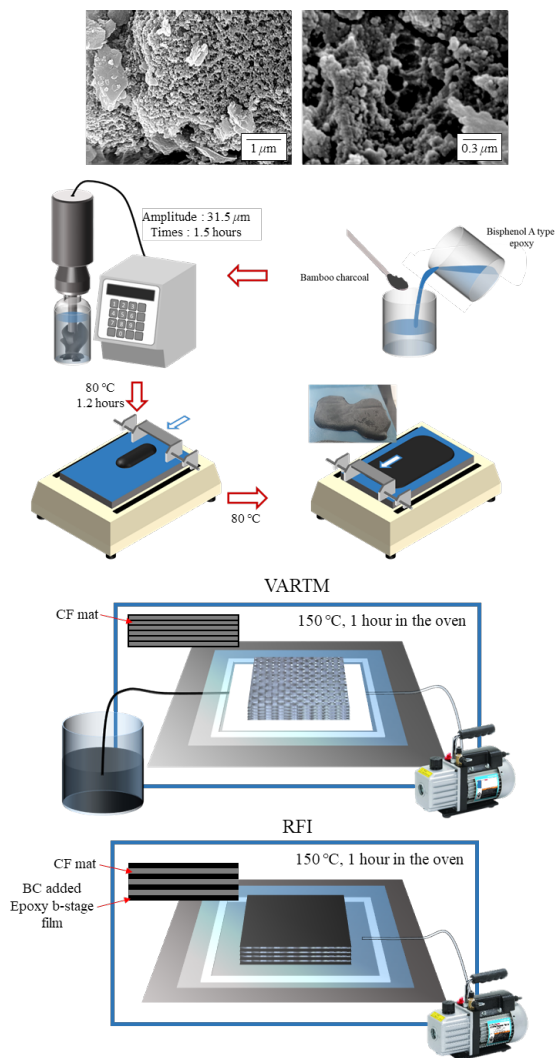
ABC-degraded

- Thermal degradation of epoxy resin could be delayed using ABC addition.

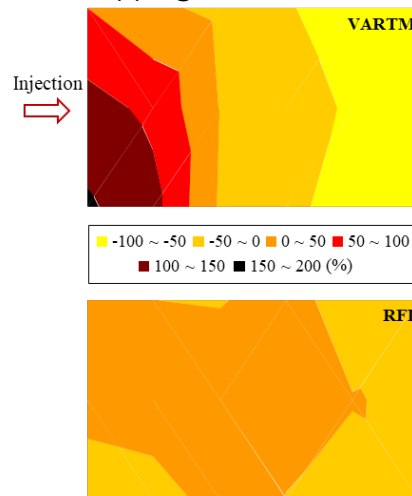


## Composites Part A 151, 106660 (2021)

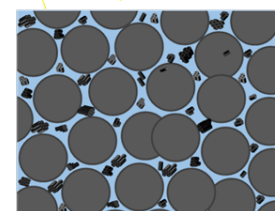
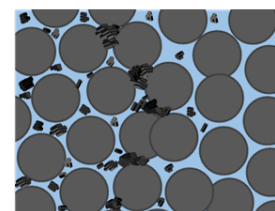
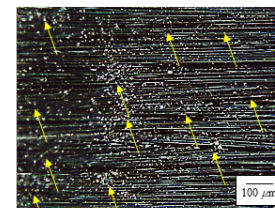
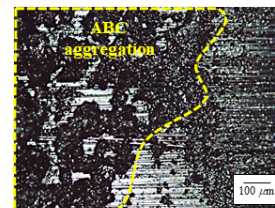
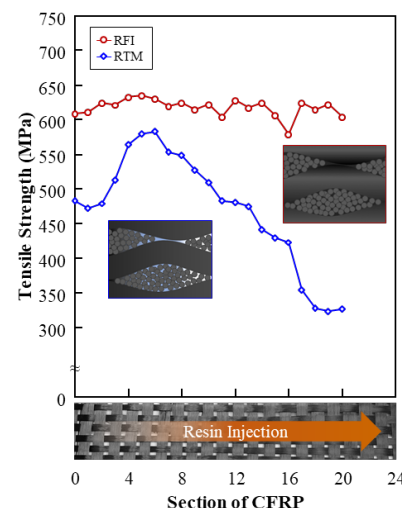
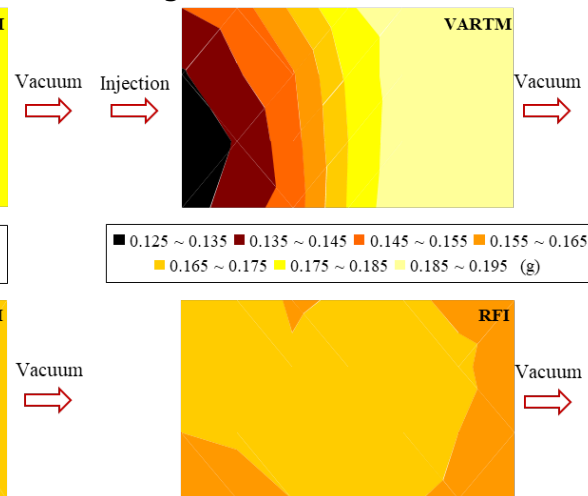
Evaluation of interfacial, dispersion, and thermal properties of carbon Fiber/ABC added epoxy composites manufactured by VARTM and RFI methods



### ER mapping



### Weight



- The ABC dispersion could be improved using resin film injection(RFI) process.



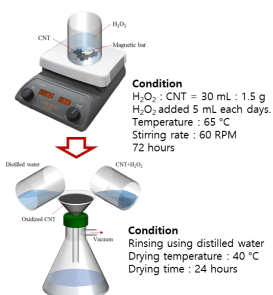
# Topcoat modification for aircraft - Lightning strike protect (LSP) coating

*Progress in Organic Coatings, Vol. 163 in press (2022)*

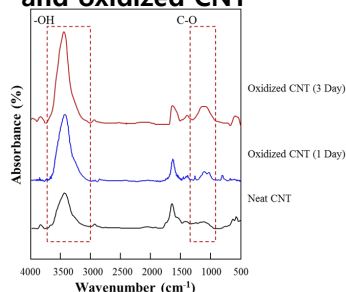
Interfacial, electrical, and mechanical properties of MWCNT in polyurethane nanocomposite coating via 2D electrical resistance mapping for aircraft topcoat



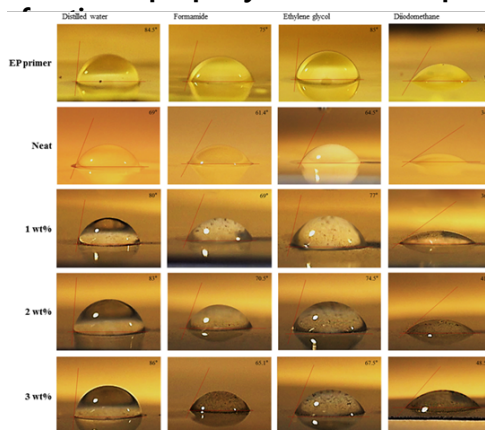
## CNT oxidation method



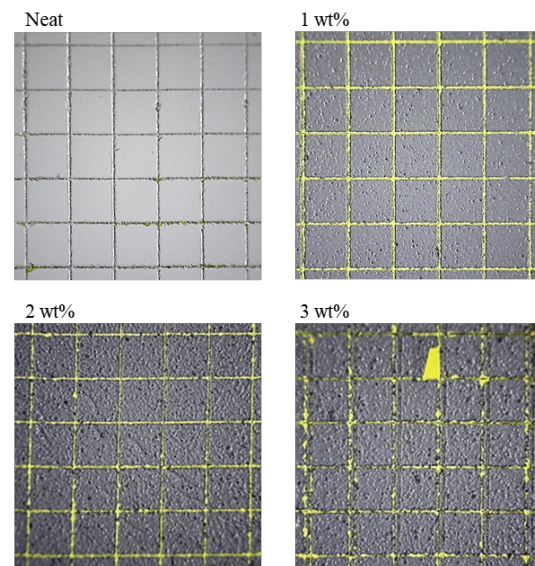
## FT-IR analysis of neat and oxidized CNT



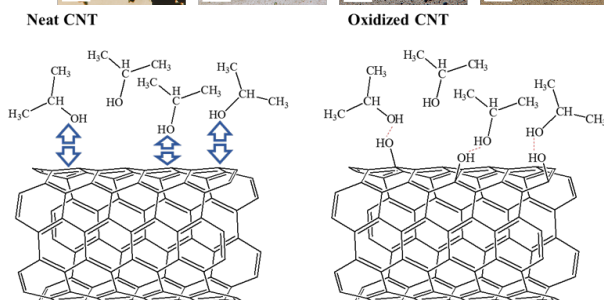
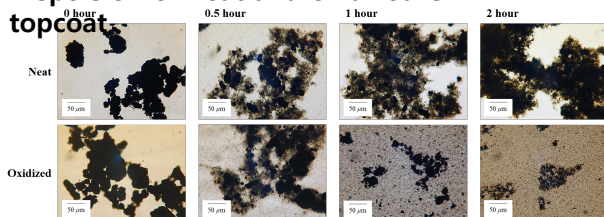
## Adhesion property of CNT/PU topcoat with different CNT weight



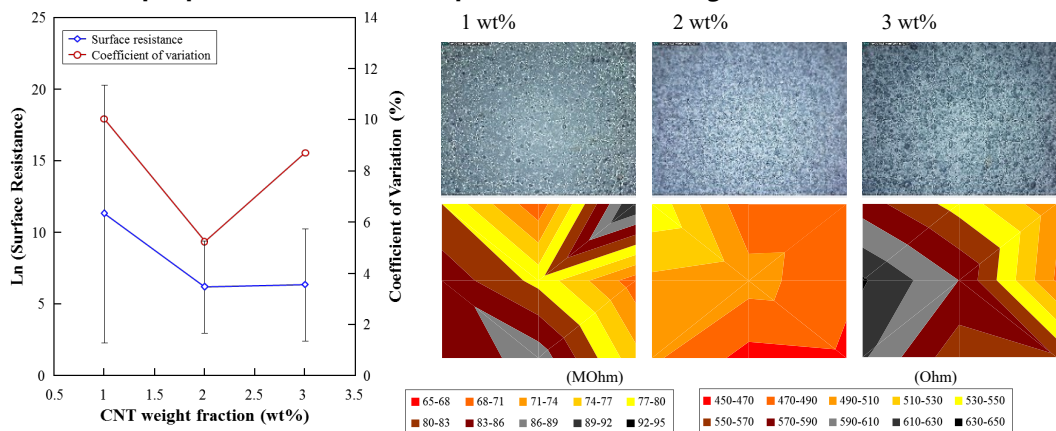
	$\gamma_s$	$\gamma_s^{LW}$	$\gamma_s^{AB}$	$\gamma_s^+$	$\gamma_s^-$	$\gamma^d$	$\gamma^p$	$W_s$
EP primer	30.4	28.9	1.5	4.7	0.1	14.1	9.2	-
Neat	45.5	42.5	3.1	7.0	0.3	21.3	14.3	74.4
1 wt%	41.6	41.6	0.0	4.2	0.0	21.3	8.0	70.8
2 wt%	40.1	39.1	1.0	2.4	0.1	22.0	6.9	69.7
3 wt%	36.4	35.1	1.3	0.2	1.8	24.4	6.2	69.7



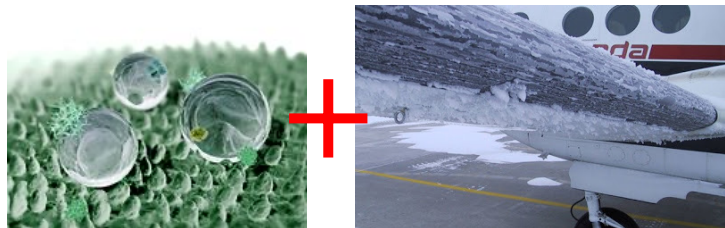
## Dispersion of neat and oxidized CNT in topcoat



## Electrical properties of CNT/PU topcoat with CNT weight fractions

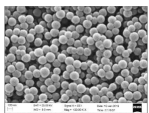


# Topcoat surface modification for aircraft - Anti-icing and de-icing coating

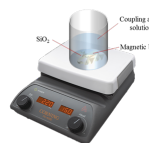


## Materials to improve anti- and de-icing

### Substrate

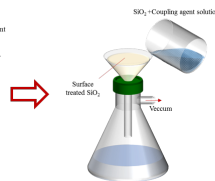
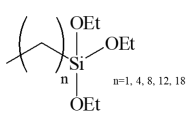


SiO<sub>2</sub> Nanoparticle



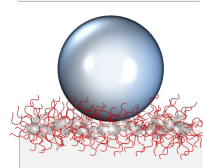
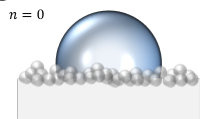
**Condition**  
Coupling agent : 80% Ethanol : 10% Acetic acid : 10% Water  
pH range : 3-4 pH  
Temperature : 160 °C  
Stirring rate : 220 RPM  
Stirring time : 5 minutes

### Coupling agent

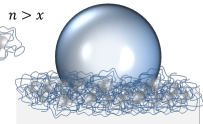


**Condition**  
Rinsing using distilled water  
Drying temperature : 180 °C  
Drying time : 4 hours

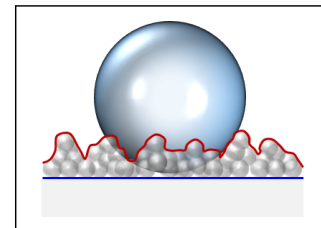
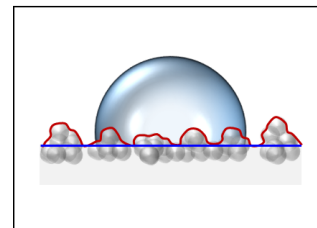
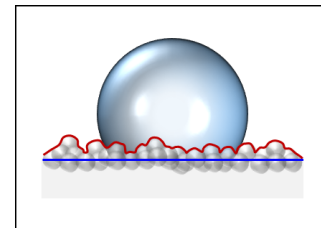
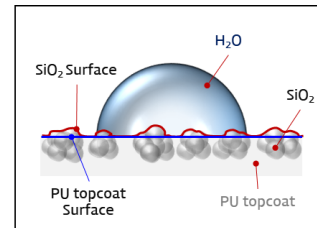
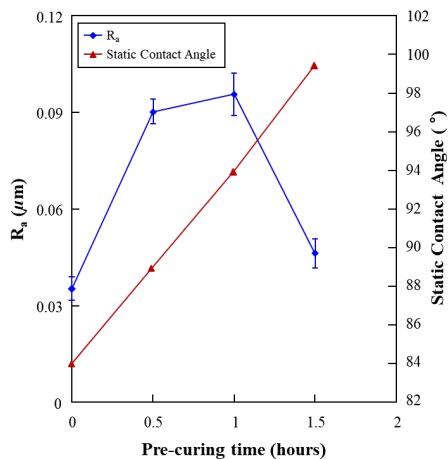
$n = 0$



$n > x$

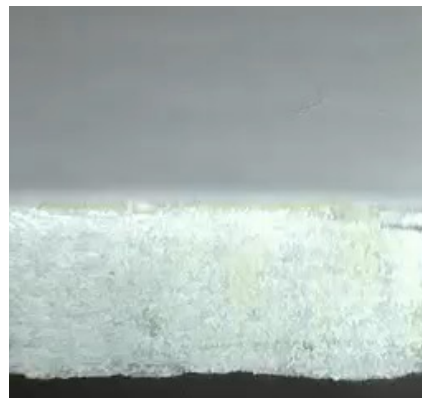


## Surface roughness and hydrophobicity of SiO<sub>2</sub>/PU topcoat

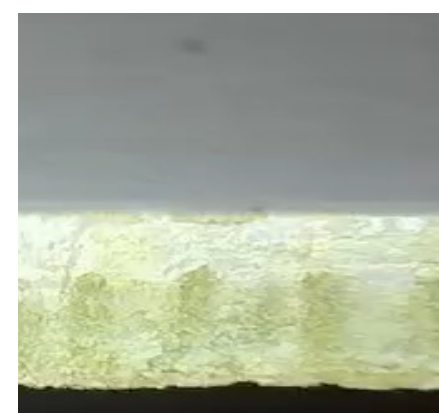


## Frost formation of SiO<sub>2</sub>/PU topcoat

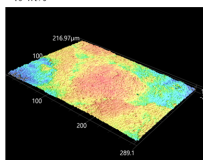
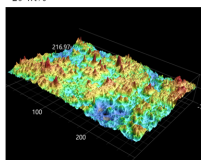
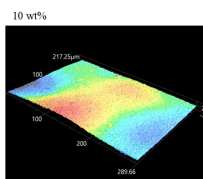
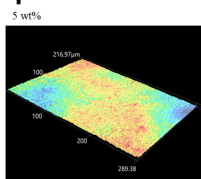
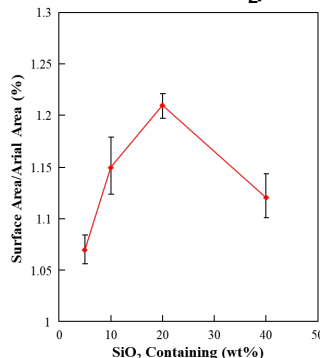
Neat



10 wt% SiO<sub>2</sub> coated



## Surface area of SiO<sub>2</sub>/PU topcoat



- Delayed starting time of the frost for 20 min.

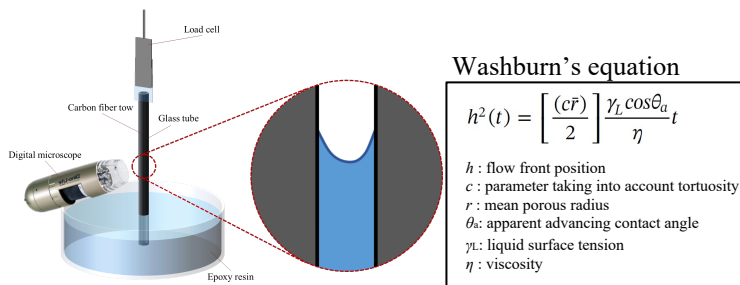


## Micro-impregnation property using capillary test

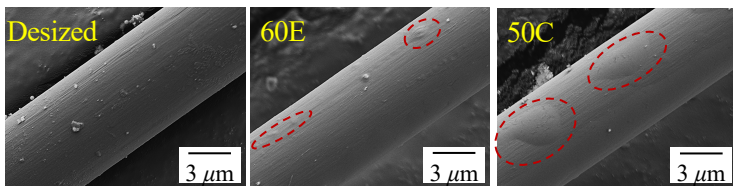
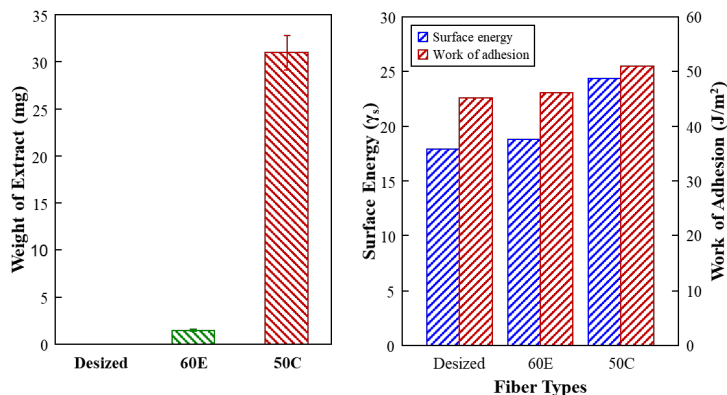
*Composites Science and Technology in press (2022)*

Innovative Wicking and Interfacial Evaluation of Carbon Fiber (CF)/Epoxy Composites by CF tow Capillary Glass Tube Method (TCGTM) with Tripe-CF Fragmentation Test

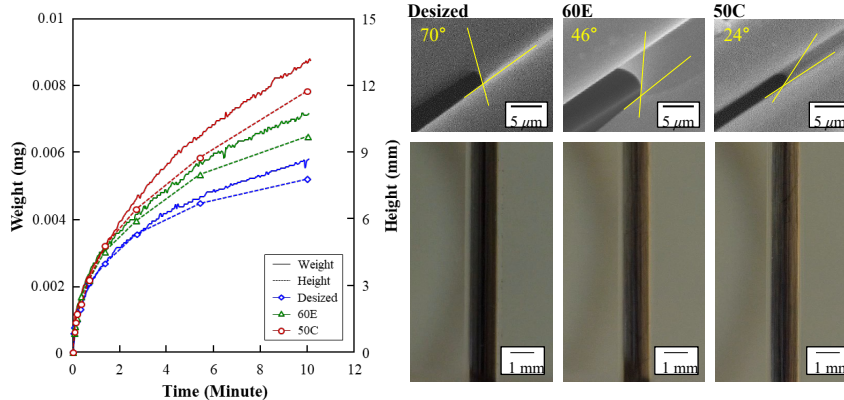
### Capillary test of resin into fiber bundle



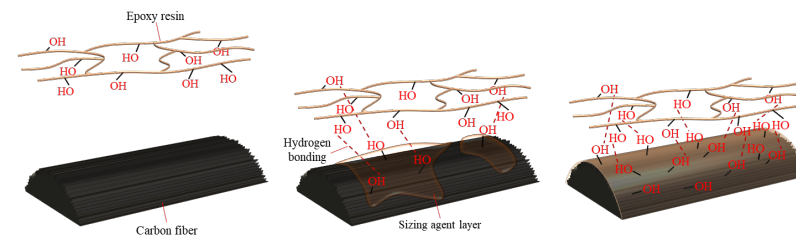
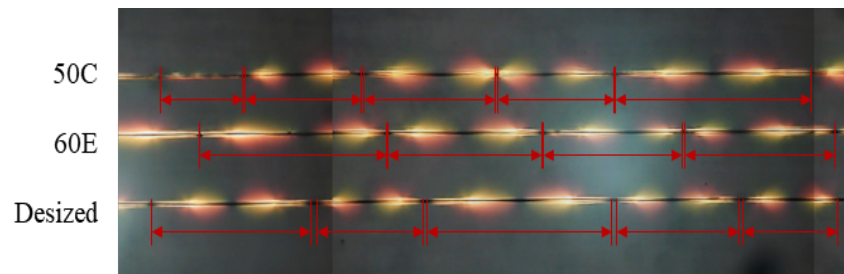
### Wettability with different sizing agent amounts



### Capillary test with different sizing agent amounts



### Triple fiber fragmentation test with different sizing agent amounts



- The weight of capillary specimens was measured to evaluate capillary properties of epoxy resin with different sizing agent.
- The 50C type of carbon fiber was optimized interfacial property and wettability than other fibers.

## Improvement of adhesive property with inserting GFRP

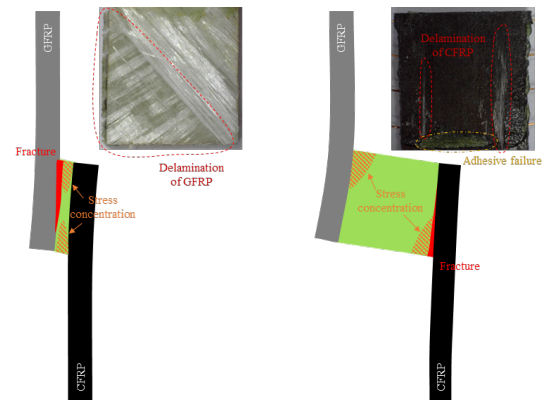
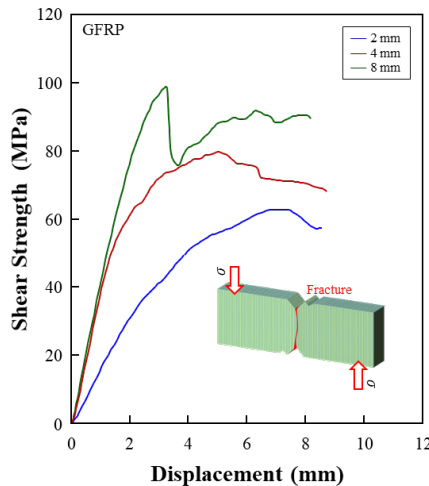
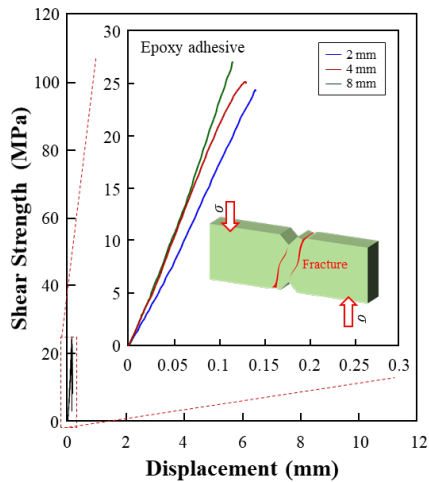
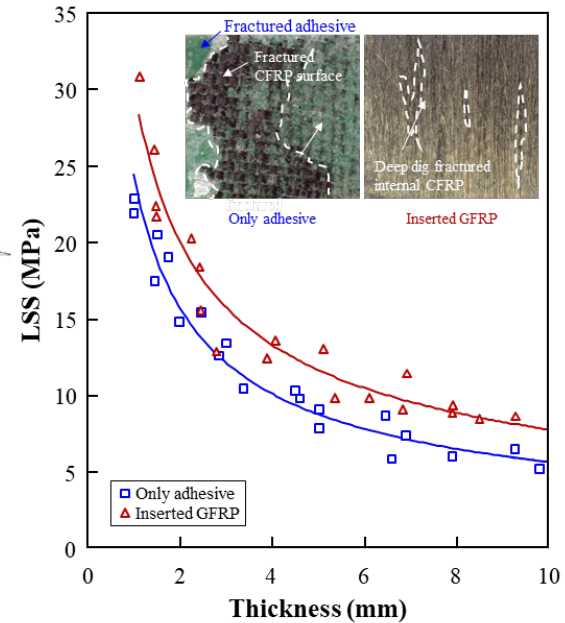
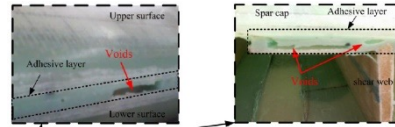
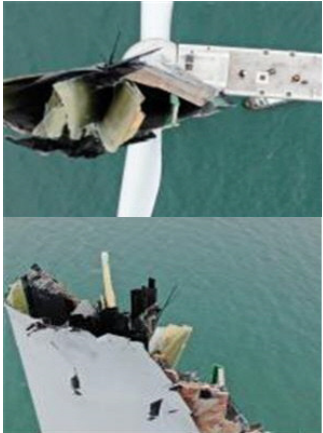
*Composites Part B submitted (2022)*

Innovative Effects on GFRP Inserted Epoxy Adhesives with the Different Thicknesses for Bonding Wind Turbine Blades of Two Parts

영제 2022

부울경 '메가시티' 힘쓰는 문 대통령...울산 해상풍력단지  
36조 투자

출처: 2021-05-06 19:44 수정: 2021-05-06 20:03



- In the case of **GFRP inserted specimen**, the **adhesive part** was more **deformed** significantly than the only epoxy adhesive used case.
- It caused by the **GFRP** exhibited **lower shear modulus** than neat epoxy adhesive.



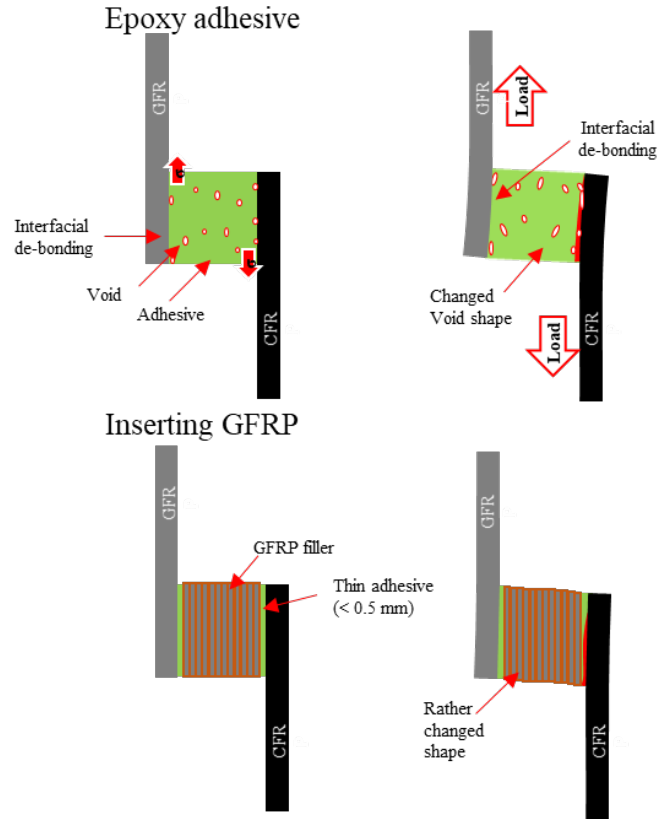
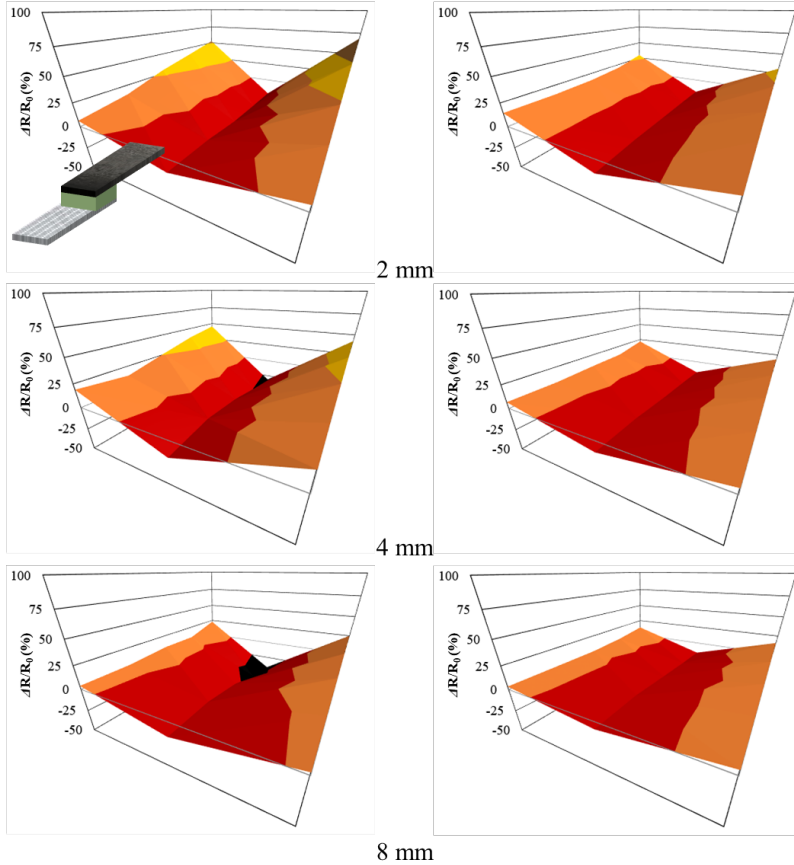
## Improvement of adhesive property with inserting GFRP

*Composites Part B submitted (2022)*

Innovative Effects on GFRP Inserted Epoxy Adhesives with the Different Thicknesses for Bonding Wind Turbine Blades of Two Parts

Only adhesive

Inserted GFRP



- The fracture and shear behaviors could be monitored using ER variation of CFRP substrate.

# General Total Summaries

- **Evaluation of interfacial property** of composite materials is very important issue to control desirable total performance of composite materials under humid, especially extreme (cryogenic) and long term environments.
- **Electro-micromechanical testing methods** can evaluate interfacial properties such **IFSS, microfailure, durability** by combining with electrical resistance (ER) measurements and **2D and 3D mapping**.
- ER can also provide valuable composites information on **micro- & macro-damage sensing, interfacial adhesion, permeability, curing procedure, and durability etc.**
- Practical applications for structural composites with my lab. work can be available for **aerospace (top coating, de-icing), automobile, home appliance, defense, sports, marine, civil etc.**

*Thank you!*  
*Inquires, Comments?*

